CHALMERS
UNIVERSITY OF TECHNOLOGY

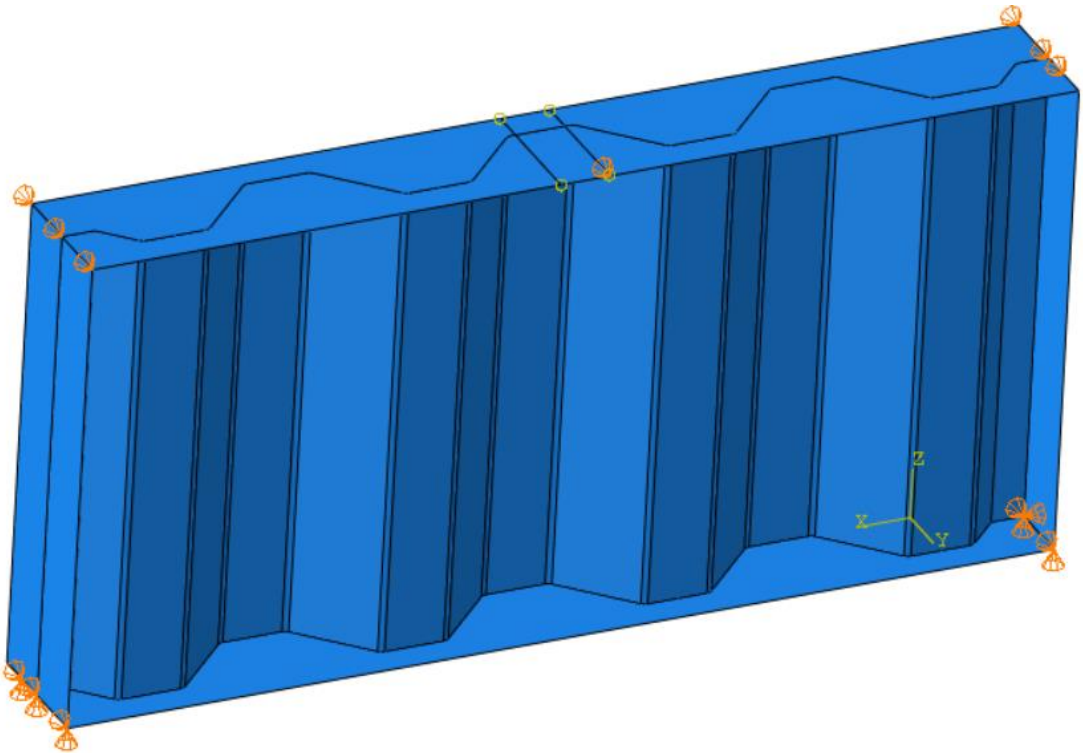

Nonlinear finite element analysis of stainless steel corrugated web girders subjected to patch loading

A parametric study

Master's thesis in the Master Programme Structural Engineering and Building Technology

DANÍEL SÆMUNDSSON
SIGNÝ INGÓLFSDÓTTIR

Department of Architecture and Civil Engineering
Division of Structural Engineering
Lightweight Structures
CHALMERS UNIVERSITY OF TECHNOLOGY
Master's Thesis ACEX30
Gothenburg, Sweden 2021

MASTER'S THESIS ACEX30

Nonlinear finite element analysis of stainless steel corrugated web girders subjected to patch loading

A parametric study

Master's Thesis in the Master Programme Structural Engineering and Building Technology

Daníel Sæmundsson
Signý Ingólfsdóttir

Department of Architecture and Civil Engineering
Division of Structural Engineering
Lightweight Structures
CHALMERS UNIVERSITY OF TECHNOLOGY
Gothenburg, Sweden 2021

Nonlinear finite element analysis of stainless steel corrugated web girders subjected to patch loading
A parametric study

Master's Thesis in the Master's Programme Structural Engineering and Building Technology.

DANÍEL SÆMUNDSSON

SIGNÝ INGÓLFSDÓTTIR

Examensarbete ACEX30
Institutionen för arkitektur och samhällsbyggnadsteknik
Chalmers tekniska högskola, 2021

Master's Thesis 2021
Department of Architecture and Civil Engineering
Division of Structural Engineering
Lightweight Structures
Chalmers University of Technology
SE-412 96 Gothenburg
Sweden
Telephone: + 46 (0)31-772 1000

Cover: Girder examined in the parametric study along with the boundary conditions used.

Department of Architecture and Civil Engineering
Gothenburg, Sweden, 2021

Nonlinear finite element analysis of stainless steel corrugated web girders subjected to patch loading

A parametric study

Master's thesis in the Master's Program Structural Engineering and Building Technology

Daníel Sæmundsson

Signý Ingólfsdóttir

Department of Architecture and Civil Engineering
Division of Structural Engineering
Lightweight Structures
Chalmers University of Technology

ABSTRACT

In recent years, the use of corrugated web girders has been increasing all around the world. The shape of the corrugation can provide increased shear stiffness and sufficient lateral stability in the girder without introducing transverse stiffeners and are thus well suitable for certain types of structures such as bridges. Stainless steel can be a beneficial choice of material for these girders as they are often used in corrosive environment with limited accessibility for maintenance. With the increased strength of stainless steel, compared to carbonated steel, the combination of thin-walled stainless steel and the corrugated shape can provide an optimal solution with respect to the environment, life cycle cost and structural capacity due to being lightweight.

Steel girders are often subjected to patch loading in various locations, for example during transportation, construction phase, operation etc. Limited research has been conducted on the patch loading capacity of trapezoidal corrugated web girders made from stainless steel subjected to patch loading. In this thesis, an extensive finite element (FE) parametric study was performed for analysis of the patch loading resistance of stainless steel girders with trapezoidal corrugated webs as well as an overview of existing theoretical, numerical, and analytical research on the subject.

In the parametric study three different load locations are considered for the patch loading, that is central loading on the longitudinal fold, inclined fold and at the intersection of the folds. The geometrical parameters that have been examined in the study are: number of unit cells, flange width, corrugation angle, depth of the corrugation, flange- and web thickness. The results of this parametric study are compared to four existing design models and the formula from the newest draft of Eurocode 3 to examine its validity and accuracy level for stainless steel corrugated web girders. The results showed that the Eurocode 3 formula was very conservative and none of the other available design models analyzed in this study were conservative enough compared to the FE-analysis. The longitudinal load case showed different behavior for the patch loading resistance compared to the other two load cases. Different failure mechanisms had a large influence on the patch loading resistance.

Key words: Trapezoidal corrugated web, stainless steel, deep girder, patch loading resistance, parametric study, patch load.

Contents

List of Figures

List of Tables

Preface

This master thesis was done at the Division of Structural Engineering, Department of Architecture and Civil Engineering at Chalmers University of Technology, Sweden, from January 2021 to June 2021. Due to Covid-19 situation the circumstances this year were a bit different.

Firstly, we thank our examiner Associate Professor Mohammad al-Emrani for all the help, useful insight and information he has provided us with during this thesis. Then we would also like to thank our supervisor, faculty researcher Rasoul Atashipour, for his contributions and support to our work.

We did not have any experience with Python scripting beforehand so in that regard we would like to thank Mohsen Heshmati, previous Ph.D. student at Chalmers and currently working for WSP, for providing us help in form of showing us one of his Python scripts which was for linear buckling analysis on girder subjected to shear force. That script made us capable of understanding the Python scripting so we could enhance the code for our nonlinear analysis under patch loading.

We would also like to thank Alexandre Mathern a Ph.D. student at Chalmers for his contribution to help with using the Python script to construct the models in the cluster.

Lastly, we thank our opponent group Ellen Johanson and Johan Ahlstrand for their interest in the thesis and good perspective of what could be improved.

Gothenburg June 2021,

Daníel Sæmundsson

Signý Ingólfsdóttir

Notations

Roman upper case letters

E	Youngs modulus.
C_{radius}	Radius of the curved edges between the corrugated folds.
F_R	Patch loading resistance.
L	Length of the girder.
L_{corr}	Length of one unit cell.
M_{cr}	Elastic critical moment.
$M_{pl,f}$	Flange plastic moment capacity.
M_{ult}	Ultimate moment.
P_{fl}	Resistance of the flanges.
P_w	Resistance of the web.
R_{d1}	Reaction force in the web.
R_{d2}	Force due to bending moment in the flange.
R_{d3}	Pressure increase due to normal force in the flange.
W	Total weight of the girder.

Roman lower case letters

h_w	Height of the web.
a_1	Length of the longitudinal fold.
a_2	Length of the inclined fold.
a_3	Depth of the corrugation.
a_4	Width of the inclined fold.
a_i	Length of the loaded fold.
b_f	Width of the flange.
e_0	Initial imperfection factor.
f	Distance from the patch load to the plastic hinge.
f_{y1}	Yield stress lower limit.
f_{y2}	Yield stress upper limit.
f_{yf}	Yield stress of the flange material.
f_{yw}	Yield stress of the web material.
k_0	Correction factor.
k_r	Correction factor.

k_w Correction factor.

k_α Correction factor.

n Factor considering the number of developed plastic hinges.

n_{corr} Number of unit cells.

s_s Loading length.

t_f Thickness of the flange.

t_w Thickness of the web.

Greek lower case letters

α Corrugation angle.

β Ratio between the depth of the corrugation and flange width.

γ_M Material safety factor.

γ_{M1} Material safety factor.

ε_1 Plastic strain lower limit.

ε_2 Plastic strain upper limit.

η Correction factor.

λ_i i-th eigenvalue.

ν Poisson's ratio.

ρ Mass density.

ρ_t Factor dependent on the ratio between flange and web thickness.

σ_f Stress in the flanges.

τ_w Shear stress in the web.

χ Reduction factor.

1 Introduction

1.1 Background

In recent years more focus has been put forward on patch loaded corrugated web girders although research has been limited, main focus has been on shear and bending resistance. Few researchers have presented formulas to predict the patch loading resistance of corrugated web girders, and it is not yet included in standards such as Eurocode, although it is planned to be introduced in the upcoming Eurocode.

The usage of stainless steel can substantially increase the strength and corrosion resistance of a structure, compared to the conventional carbonated steel. Using stainless steel can also be more cost effective as the increased strength allows for the steel plate to be more slender and thus reduces the amount of steel required. The reduced web thickness of a stainless steel girder comes at the expense of susceptibility of buckling and instability, especially for patch loading. An innovative way of constructing the girder with stainless steel is to introduce the corrugated shape for the web. The corrugation shape increases the lateral stability of the girder and increases its shear stiffness and thus greatly reduces the need for transversal stiffeners.

The subject of corrugated web under patch loading has not been studied to a sufficient extent and the same subject with stainless steel has been investigated even less. There is a great deal of benefits in using stainless steel in construction and in addition using it with corrugated web design means that less material is needed and higher resistance is gained which can optimize the ratio between load resistance and weight ratio.

A thorough research on this topic is needed to get an idea and the knowledge to make models which can estimate the patch loading resistance of girders with corrugated web in an efficient way and therefore a parametric study is made. The parametric study investigates how different parameters effect the patch loading resistance of girders subjected to patch loading.

1.2 Aim and objectives

The aim of this thesis is to analyze the structural behavior of stainless steel girders with corrugated web subjected to patch loading and identify the optimal geometrical configuration with regard to the patch loading resistance. Also, the optimal patch loading resistance is considered with respect to total weight of the girder and thus optimizing cost and environmental aspects. Additionally, how valid and accurate existing design models and the model in the latest draft of Eurocode 3 (2020), developed for carbonated steel, are at predicting the failure patch load of stainless steel corrugated web girders. Furthermore, how well do these design models fare for geometry outside of the parametric range they are developed from. To achieve these aims and objectives, a parametric study is performed with varying geometrical parameters.

1.3 Method

To achieve the aim and objectives the following is done:

First, a literature study is performed where the strengths and weaknesses of corrugated web and stainless steel are investigated. An overview of previous research on the topic are presented. Existing design models are introduced which have constructed formulas on how to estimate the patch loading of girders with corrugated web, considering different parameters.

Furthermore, a Python script is developed which establishes finite element (FE) models in the ABAQUS CAE software. These models are verified and validated by using convergence study and reference models.

Then a parametric study is performed based on varying several different geometric parameters in the Python script to develop multiple models and perform the comparative optimization.

Finally, the results of the parametric study are analyzed and compared to the existing design models and the formula presented in the draft of the upcoming Eurocode 3.

1.4 Limitations

- Height of the web and length of the girders are constant in the analysis.
- The self-weight of the girder is neglected.
- Only trapezoidal corrugation shape with curved intersection is used.
- Patch load applied at three locations only and on the top flange.
- Same material used for both flanges and the web.
- One stainless steel material grade is considered.
- One initial imperfection factor considered.
- Patch loading length is constant and narrow.
- Separation traction is not considered for the patch load.
- The results from the parametric study is limited to the parameters varied in the FE-analysis. They will not necessarily correlate to the existing design models considered.

2 Literature study

In this chapter, three sections are addressed. The first section focuses on the stainless steel material in general and its strengths and weaknesses. Next, the corrugated shape of the web is covered and its benefits and disadvantages are addressed. A review of the theoretical, numerical and experimental researches that have provided design models for the patch loading resistance of girders with corrugated webs are presented. Some of these existing design models are further analyzed. Finally, the model which is planned to be included in the upcoming Eurocode 3 for the resistance of corrugated web girders subjected to patch loading is presented.

2.1 Stainless steel

When designers make decisions regarding the type of steel to use in design, they normally consider multiple aspects, e.g., the financial remarks, the strength, and the environmental aspects around the structure. One benefit of choosing stainless steel over carbonated steel is that it has higher strength, however, the initial cost of the material is greater. Other advantages of using stainless steel are that it is resistant to corrosion and can be fully recycled (Henrysson and Yman, 2020) which optimizes its life-cycle cost. In recent years more focus has been put on life-cycle cost compared to the initial cost (Dahlström and Persson, 2018). Therefore, stainless steel is becoming more popular in design, and it has been used in structures for more than hundred years.

Stainless steel is divided into four classes, that are: martensitic, ferritic, austenitic and duplex. One of the deciding factors of what category the stainless steel fits in is the chromium content. The chromium content must be at least 10.5% to be considered as stainless steel (Den Uijl and Carless, 2012). Increasing chromium content causes an increase of the corrosion protection. The development of duplex stainless steel started around 1930 and it is a combination of austenitic and ferritic. Duplex grade is often used in bridge girders since it has high strength and high resistance against corrosion (Karabulut et al, 2021). Austenitic steel grade also has high resistance against corrosion and is often used in bridges, but it has lower strength compared to duplex steel (Baddoo, 2008).

Stainless steel costs more on the market than carbon steel, which is mainly due to uncertainties as well as the price of nickel. Nickel does not have a stable price on the market and therefore the price is fluctuating, in recent years it has been increasing which is not beneficial for the price of stainless steel. Austenitic and duplex stainless steel cost more than ferritic steel since they include nickel. Austenitic contains around 8% nickel while duplex contains 1-6% therefore it influences the cost of austenitic steel more (Baddoo, 2008).

2.2 Corrugated web girders

Corrugated web was released on the market in the 1960s; the concept of corrugated web girder is a Swedish design. Sweden, France, Germany, Japan and Austria are the leading countries in manufacturing and building with corrugated webs (Raviraj, 2009).

Girders with corrugated webs are preferable in some cases compared to girders with flat webs since research and experience has shown that they have higher shear stability

and enhanced design life. In addition, the strength to volume ratio is increased with the use of corrugated web due to thinner webs and therefore they can be more cost-efficient. Transversal stiffeners are often a crucial design part of plane web girders but when corrugated webs are used, the need for transversal stiffeners is greatly reduced since the corrugation provides sufficient stiffening for the web (Inaam and Upadhyay, 2020).

By using corrugated web transversal stiffeners are not needed as much and the web thickness can be reduced since the corrugated web design provides higher resistance around the weak axis (Boutillion et al 2015). Using a corrugated web can also lower the cost of the construction, due to the fact that there is not as much need for extra lifting equipment in the building phase since the weaker axis is more resistant to bending (Raviraj, 2009).

There are different shapes of corrugation design, the most common ones in practice are shown in Figure 1, that is the trapezoidal, the sinusoidal and the zig-zag shape. The most common one in bridges is the trapezoidal shape, that shape provides high shear capacity for thin webs and optimizes the amount of steel required (Karlsson, 2018). The trapezoidal web shape is also the one that has been investigated the furthest out of the three shapes mentioned (Górecki and Śledziewski, 2020). In girders with sinusoidal shaped corrugation the local buckling in the longitudinal part of the corrugation is not relevant while it can occur in the trapezoidal girder, but the manufacturing of sinusoidal shape is more challenging (Raviraj 2009).

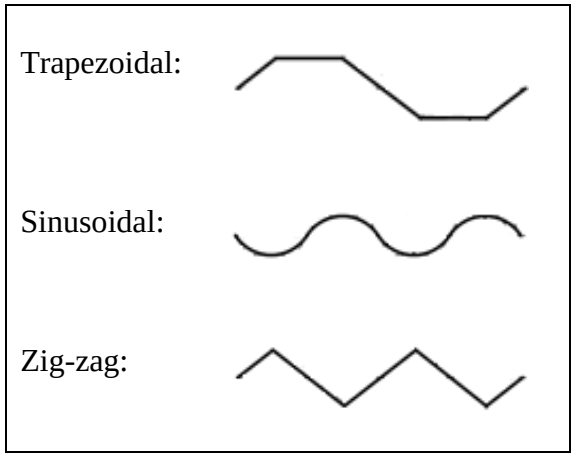

Figure 1. Three different most common corrugation shapes.

The corrugation shape allows web members to be slenderer and therefore can appear more appealing to some extent in terms of aesthetics. The corrugation shape gives the flanges high longitudinal stiffness but lowers the longitudinal web stiffness. Similar to flat web girders, the flanges provide bending resistance (Górecki and Śledziewski, 2020).

In a research carried out in 1984, it was shown that girders with corrugated webs are lighter than flat webs with stiffeners to the extent of 9- 13% in self-weight. The ratio between strength and weight is improved by using corrugated web in the girder since they are stronger and require less material (Hamada et al, 1984).

In Figure 2, geometrical configuration of the corrugated web girder is shown together with different possible locations of applied transverse loads. The notation of each parameter, positions of load cases and overall visual representation of the girders analyzed in this thesis are also presented in the figure.

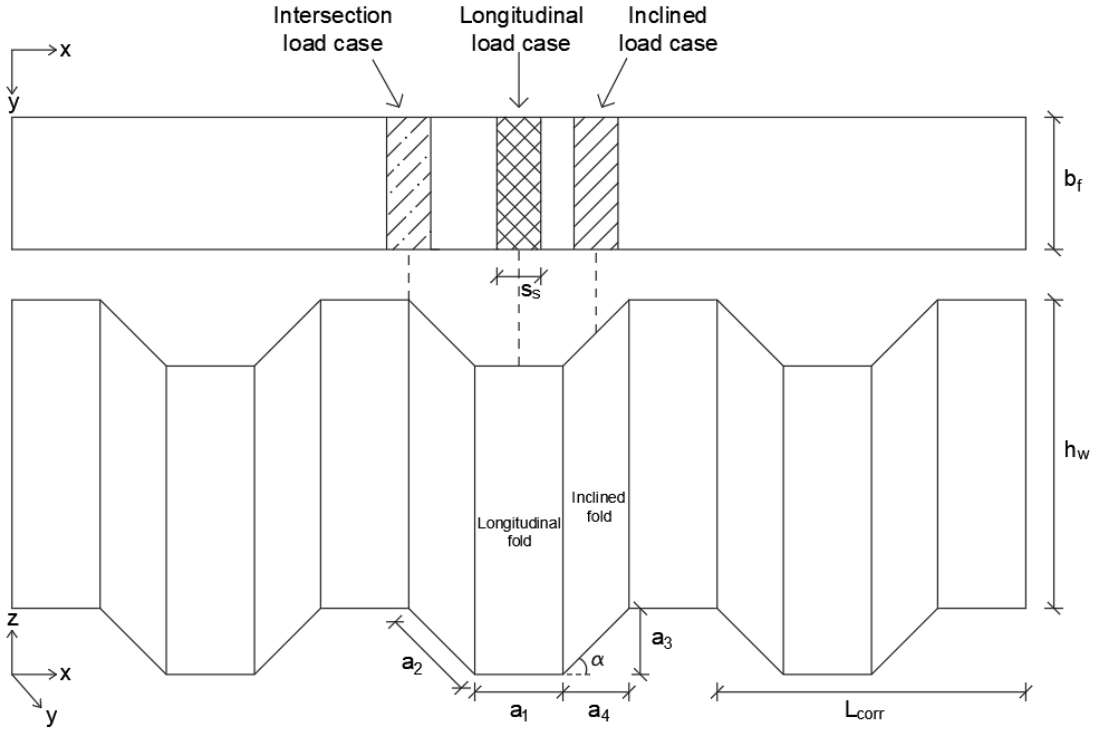

Figure 2. Geometry of the trapezoidal corrugation shape along with notation of parameters.

2.3 Previous research on corrugated web girders subjected to patch loading

As mentioned previously, utilizing a corrugation shape instead of the conventional flat web strengthened with stiffeners will enhance the resistance. Therefore, the amount of steel could be reduced due to the corrugated shape and thinner webs can be used. This will lead to susceptibility of the structural element to the buckling. which is dominantly in the form of local patch buckling or lateral-torsional buckling. These two forms of failure can be postponed by using corrugated shape for the web. However, the extent of improvement by corrugating relatively thinner webs is the topic of research.

Numerical, theoretical and experimental research have been performed for corrugated web girders subjected to patch loading. In this chapter an overview of the previous research on corrugated web girders subjected to patch loading and existing design models are presented. Four of the existing design models are presented in more detail since they will be further analyzed and compared to the results from the parametric study. Note that none of these existing design models considers stainless steel, all of them are based on experiments on girders with carbonated steel.

In 1974 a design model for the patch loading resistance, F_R, was presented by Carling (1974), see equation 1, based on results from experimental studies made at a Swedish consulting firm. In the test two girders were examined and 52 tests were done on them.

$$F_R = 0.04 \cdot E \cdot t_w^2 \qquad (1)$$

Leiva-Aravena performed a test in 1983, in that test three parameters were analyzed that is the web thickness, t_w, loading length, s_s, and load location. Leiva-Aravena and Edlund (1987) analyzed the results from the test and found out that the behavior of girders with corrugated web is very dependent on the web thickness. The patch loading resistance increased 35-40% with increasing the web thickness from 2.0 to 2.5 mm. They also concluded that the patch loading resistance would increase twice by using corrugated shaped web compared to flat web.

Dahlén and Krona (1984) used the results from the test done by Leiva-Aravena and Edlund (1987) and compared the results from that to the obtained patch loading resistance using the model that Bergfelt (1974) constructed, the so called "Three-Hinge-Flange". Dahlén and Krona (1984) assumed that the inclined part of the corrugation shape would act as stiffeners. The results showed that the "Three-Hinge-Flange" model resulted in 20% lower values for the patch loading resistance and girders that were loaded at the inclined fold have around 14% higher resistance then when the load is applied at the longitudinal fold. Changing the height of the web did not influence the resistance of the girder according to Dahlén and Krona (1984).

Rockey and Roberts (1979) introduced a four plastic hinge failure mechanism and based on that they developed a design model for girders with flat webs, see equation 2.

$$F_R = 2 \cdot \sqrt{4 \cdot M_{pl,f} \cdot t_w \cdot f_{yw}} + f_{yw} \cdot t_w \cdot (s_s + f) \qquad (2)$$

In the equation *f* is the distance from the edge of the patch load to the nearest plastic hinge. The plastic moment capacity of the flange, $M_{pl,f}$, is calculated with equation 3. It takes into account the flange width, b_f, the yield stress of the flanges, f_{yf}, and the flange thickness, t_f.

$$M_{pl,f} = \frac{b_f \cdot f_{yf} \cdot t_f^2}{4} \qquad (3)$$

Kähönen (1988) presented in 1988 a design model for girders with corrugated web. The model is based on the four plastic hinge failure mechanism presented by Rockey and Roberts. The model Kähönen developed for the patch loading resistance for girders with corrugated web, see equation 4, considers the interaction between shear force and bending moment, and the increasing pressure due to the normal force in the flange.

$$F_R = (R_{d1} + R_{d2} + R_{d3}) \cdot \frac{k_0 \cdot k_r}{\gamma_M} \qquad (4)$$

Where R_{d1} is the reaction force in the web, R_{d2} is force due to bending moment in the flange, R_{d3} considers the increasing pressure due to normal force in the flange, γ_M

material safety factor, k_0 and k_r are correction factors (Kähönen, 1988). The model by Kähönen can be hard to use in practice since it is dependent on many design factors.

Bergfelt and Lindgren (1974) made a simple model for girders with flat webs. The model is presented in equation 5 and it has proven to underestimate the patch loading resistance.

$$F_R = 13.0 \cdot \rho_t \cdot t_f \cdot t_w \cdot f_{yw} \quad (5)$$

ρ_t is a positive parameter which depends on the ratio between the thickness of the flange and web, t_f/t_w, and f_{yw} is the yield stress of the web. This formula is very conservative and underestimates the resistance if it is used on girders with corrugated web (Bergfelt and Lindgren, 1974).

Luo and Edlund (1996) studied how six different parameters affected the patch loading resistance using nonlinear FE-analysis. The factors considered were strain-hardening models, initial imperfections (both local and global), corner effect, loading position, loading length, and five geometric parameters (α, t_f, t_w, h_w and L). Their results showed that the loading length, s_s, and the corrugation angle, α, had the biggest impact. When the load was applied as uniformly distributed patch load it resulted in higher patch loading resistance compared to a girder subjected to a line load over the width of the flange, the difference in the load capacity was 20-40% so changing the loading had drastic influence. The geometric parameters that influenced the patch loading resistance were α, t_w and t_f. The patch loading resistance increases with increasing all these factors, although when the corrugation angle is between 75 and 90 degrees the resistance is almost equal. The result also showed that the patch loading resistance can increase 8- 12% by using Ramberg-Osgood strain-hardening model instead of elastic-perfectly plastic model and that the patch loading resistance can decrease about 7% due to local initial imperfection in the web. The corner effect does not have much influence on the patch loading resistance. The patch loading resistance is lowest when a line load over the width of the flange is applied on the center of the longitudinal fold of the web but highest at the inclined fold (Luo and Edlund, 1996).

After this study Luo and Edlund (1996) took the formula presented by Bergfelt and Lindgren (1974) for girders with flat web subjected to patch loading and modified it for girder with corrugated web. Luo and Edlund (1996) suggested that the patch loading resistance for girders with corrugated web and with a corrugation angle less or equal to 75 degrees can be estimated with equation 6.

$$F_R = \gamma \cdot t_f \cdot t_w \cdot f_{yw} \quad (6)$$

That means that the patch loading resistance is influenced by the web thickness, t_w, flange thickness, t_f, the yield stress of the web, f_{yw}, and a factor γ which is determined by equation 7, that is one constant along with two factors γ_α and γ_c (Luo and Edlund, 1996).

$$\gamma = 10.4 \cdot \gamma_\alpha \cdot \gamma_c \quad (7)$$

At first the constant 10.4 was presented as 15.6 but was reduced afterwards to 10.4 which has been used since, according to Ljungström and Karlberg (2010). The first factor γ_α considers the corrugation of the web. It is also affected by the ratio between

the thickness of the flange and the web. If the ratio is less than 3.82 then this factor is 1 but if it more or equal to 3.82 than this factor is calculated with equation 8 (Luo and Edlund, 1996). The equation in the original article published by Luo and Edlund (1996) had a misprint according to Ljungström and Karlberg (2010) who had Bo Edlund as their supervisor, hence the equation from the published article was changed in accordance.

$$\gamma_\alpha = \frac{a_1+a_2}{a_1+a_2 \cdot cos(\alpha)} \text{ for } \frac{t_f}{t_w} \geq 3.82 \tag{8}$$

The factor, γ_α, is dependent on the corrugation angle, α, length of the inclined fold, a_2, and the length of the longitudinal fold, a_1. The second factor γ_c accounts for how the load is distributed, it is calculated with equation 9.

$$\gamma_c = 1 + \eta \cdot s_s \tag{9}$$

It is dependent on the loading length, s_s, and correction coefficient, η, given as 1/240 (Luo and Edlund, 1996).

Elgaaly and Seshadri (1997) performed a parametric study with three different load locations, on the longitudinal fold, inclined fold and intersection. The load length was narrow in the study. The varying parameters considered were the web thickness, flange thickness, yield stress, corrugation profile and width of the patch plate. Based on the result of this parametric study they presented a design model to calculate the patch loading resistance. The results showed that there were two different failure modes when the girder was subjected to patch loading. The failure modes were web crippling and web yielding, the one that yields lower value determines the capacity. The patch loading resistance for web crippling failure is calculated with equation 10.

$$F_R = P_{fl} + P_w \tag{10}$$

The patch loading resistance for web crippling is calculated with the sum of the resistance from the web, P_w, and the resistance of the flanges, P_{fl}. The patch loading resistance of the web, P_w, is calculated with equation 11.

$$P_w = \left(E \cdot f_{yw}\right)^{0.5} t_w^2 \tag{11}$$

The capacity of the web depends on the Young's modulus, E, the yield stress of the web, f_{yw}, and the thickness of the web, t_w.

The patch loading resistance of the flanges, P_{fl}, is calculated with equation 12.

$$P_{fl} = \frac{4 \cdot M_{pl,f}}{a - \frac{s_s}{4}} \tag{12}$$

The patch loading resistance of the flanges depends on the flange plastic moment capacity, $M_{pl,f}$, which is calculated with equation 3. The capacity of the flanges is also influenced by the loading length, s_s, and the distance between the plastic hinges at the

positive and negative bending moment location, a, or it can be calculated with equation 13.

$$a = \left(\frac{f_{yf} \cdot b_f \cdot t_f^2}{2 \cdot f_{yw} \cdot t_w}\right)^{0.5} + \frac{s_s}{4} \quad (13)$$

The second failure is web yielding, the patch loading resistance for that failure is calculated with equation 14. This failure is not considered for the longitudinal load case.

$$F_R = (b + b_a) \cdot t_w \cdot f_{yw} \quad (14)$$

Where b is the length of the inclined fold, a_2 or determined by equation 15. This equation is only considered in the FE-analysis for the value, b, since it is only applicable for the inclined load case, however it is also used for the intersection load case.

$$b = \frac{a_4 + a_1}{2} \quad (15)$$

b_a is calculated with equation 16.

$$b_a = \alpha_b \cdot t_f \cdot \left(\frac{f_{yf}}{f_{yw}}\right)^{0.5} \quad (16)$$

where the α_b factor is determined by equation 17.

$$\alpha_b = 14 + 3.5\beta - 37\beta^2 \geq 5.5 \quad (17)$$

Where β is defined as the ratio between the depth of the corrugation and flange width, a_3/b_f (Elgaaly and Seshadri, 1997).

In 2007, Kuchta (2007) used finite element analysis to research how different web thickness and different loading length effects the patch loading resistance of girders with sinusoidally corrugated web. The results showed that with increasing the loading length the patch loading resistance increased. In the results it was also observed that for wide loading lengths, and thicker webs the patch loading resistance was more affected compared to thinner webs.

Kuhlmann and Braun (2008) developed a design model which is based on the design model presented by Kähönen in 1988, see equation 2. To develop the formula further they used results from parametric study done by Kövesdi (2010). The parameters considered in the study by Kövesdi (2010) were the loading length, corrugation angle, flange width, flange thickness, web slenderness ratio, h_w/t_w, and fold slenderness ratio, a_i/t_w. According to the parametric study made in the research the design model is valid for corrugation angle of 15 to 65°, a_i/t_w between 12.5 and 116.7, b_f between 150 and 500mm, t_f between 20 and 100mm, the ratio of s_s/h_w between 0.4 and 0.8 and web slenderness ratio h_w/t_w between 200 and 500 (Kövesdi, 2010). The formula presented by Kuhlmann and Braun (2008) to determine the patch loading resistance can be seen in equation 18.

$$F_R = \left(k_\alpha \cdot F_{R,w} + F_{R,fl}\right) \cdot k_0 \quad (18)$$

The design method is applicable for girders with a fold length that fulfills the criteria in equation 19.

$$a_i \geq \left(\frac{h_w}{t_w} + 260\right) \cdot \frac{t_w}{11.5} \tag{19}$$

The equation considers contribution from the flange, $F_{R,fl}$, and the web $F_{R,w}$. Along with two modification factors k_a and k_0. The first one is due to the corrugation angle, see equation 20, and the second one due to influence of shear and bending interaction, see equation 21.

$$k_a = \frac{a_1 + a_2}{a_1 + a_4} \tag{20}$$

$$k_0 = \begin{cases} 1.0, & \frac{\sigma_f}{f_{yf}} \cdot \frac{\tau_w \cdot \sqrt{3}}{f_{yw}} \geq 0.23 \\ 1.63 \cdot \frac{\sigma_f}{f_{yf}} \cdot \frac{\tau_w \cdot \sqrt{3}}{f_{yw}} + 0.63, & \frac{\sigma_f}{f_{yf}} \cdot \frac{\tau_w \cdot \sqrt{3}}{f_{yw}} < 0.23 \end{cases} \tag{21}$$

The first part of equation 18 which considers the contribution from the web, $F_{R,w}$, is determined by equation 22.

$$F_{R,w} = \chi \cdot t_w \cdot f_{yw} \cdot s_s \cdot k_w \tag{22}$$

In the equation there is one modification factor, k_w, which considers the interaction between shear and the transverse force, see equation 23.

$$k_w = \sqrt{1 - \left(\frac{\tau_w}{0.5 \cdot f_{yw}}\right)^2} \tag{23}$$

The reduction factor in equation 22, χ, is due to the corrugation angle, calculated with equation 24 and it is dependent on $\bar{\lambda}_p$ which is shown in equation 25.

$$\chi = \begin{cases} 1.0, & \bar{\lambda}_p \leq 1.273 \\ \frac{1.9}{\bar{\lambda}_p} - \frac{0.798}{\bar{\lambda}_p^2}, & \bar{\lambda}_p > 1.273 \end{cases} \tag{24}$$

$$\bar{\lambda}_p = \sqrt{\frac{f_{yw}}{\sigma_{cr}}} \tag{25}$$

Where the critical stress is calculated with equation 26.

$$\sigma_{cr} = \frac{k_\sigma \cdot \pi^2 \cdot E}{12(1 - v^2)} \cdot \left(\frac{t_w}{a_i}\right)^2 \tag{26}$$

Where k_σ is a constant set to 1.11 and a_i is the loaded fold length or the maximum fold length if there are more than one fold loaded.

The second part of equation 18 considers the contribution from the flanges which is shown in equation 27.

$$F_{R,fl} = 2 \cdot \sqrt{4 \cdot M_{plf} \cdot t_w \cdot \chi \cdot f_{yw} \cdot k_f \cdot k_w} - 0.07 \cdot \sigma_f \cdot b_f \cdot t_f \quad (27)$$

The plastic moment capacity of the flanges is like before determined by equation 3 and the reduction factor is determined from equation 24. There are two modification factors considered in the contribution from the flanges and that is k_w and k_f. The first one is calculated with equation 23 and the later one is due to bending interaction, see equation 28 (Kuhlmann and Braun, 2008).

$$k_w = 1 - \left(\frac{\sigma_f}{f_{yf}}\right)^2 \quad (28)$$

In 2010 Kövesdi et al (2010) presented an enhanced design model to calculate the patch loading resistance for girders with corrugated web, see equation 29. The equation presented by Kövesdi et al is based on the parametric study done by Kövesdi which is the same as the parametric study the model by Kuhlmann and Braun is based on. It is not known without a doubt if the design model fits for parameters outside of the previously described range. The results showed that the patch loading resistance increases almost proportionally to the increase of the loading length. The patch loading resistance also increases with increased corrugation angle but decreases with high web and fold ratios (Kövesdi et al, 2010).

$$F_R = 2 \cdot \sqrt{4 \cdot M_{plf} \cdot t_w \cdot \chi \cdot f_{yw}} + \chi \cdot t_w \cdot f_{yw} \cdot s_s \cdot k_\alpha \quad (29)$$

The first part of the formula considers the contribution from the flanges and the second one considers contribution from the web. The contribution from the flange is influenced by the plastic moment capacity, thickness of the web, yield stress and a reduction factor, χ. The reduction factor is due to the corrugation angle, calculated with equation 30 and it is dependent on the factor $\bar{\lambda}_p$ which is shown in equation 25 (Kövesdi et al., 2010).

$$\chi = \begin{cases} 1.0, & \bar{\lambda}_p \leq 1.273 \\ \dfrac{1.9}{\bar{\lambda}_p} - \dfrac{0.8}{\bar{\lambda}_p^2}, & \bar{\lambda}_p > 1.273 \end{cases} \quad (30)$$

The contribution from the web is influenced by the reduction factor, thickness of the web, yield stress of the web, loading length and modification factor, k_α, due to the corrugation angle, see equation 20 (Kövesdi et al, 2010).

In 2010 Kövsedi (2010) published his PhD dissertation which included an even more enhanced design model, see equation 31.

$$F_R = 2 \cdot \sqrt{n \cdot M_{plf} \cdot t_w \cdot \chi \cdot f_{yw}} + \chi \cdot t_w \cdot f_{yw} \cdot s_s \cdot k_\alpha \quad (31)$$

This equation is the same as equation 29 except that now the constant 4 in the contribution from the flange has been enhanced to a factor n. This factor considers the ratio between thickness of the flange and the web and according to Kövesdi it should be determined with equation 32. This factor considers how many plastic hinges can develop in the flange.

$$n = \begin{cases} 4, & \frac{t_f}{t_w} < 4 \\ 3, & 4 \leq \frac{t_f}{t_w} \leq 7 \\ 2, & \frac{t_f}{t_w} > 7 \end{cases} \tag{32}$$

In 2011, Kövesdi and Dunai (2011) tested 12 girders and examined how the patch loading resistance is influenced by the location of the load, loading length, span and flange thickness. In addition, they investigated what effect the loading eccentricity has. The results showed that the post-buckling behavior for the deflection was different, the difference was due to the imperfection size. The EN 1993-1-5 (2006) Annex C lacks information on how the imperfection factor should be determined. Therefore, the imperfection shapes were further researched and from those results they proposed scaling factors. The scaling factor proposed for the imperfection was to divide the fold length by 200 (Kövesdi and Dunai, 2011).

All of the previously mentioned researches are directed at simply supported girders, but a recent research by Inaam and Upadhay (2020) analyses other static forms such as simply supported girders with overhang, continuous girders and cantilever girders. The results showed that for cantilever spans the patch loading resistance formulas are unconservative, so they suggested a formula for that, see equation 33.

$$F_R = \chi_M \cdot t_w \cdot s_s \cdot f_{yw} \tag{33}$$

Where χ_M is a modification factor, see equation 34, which considers the effect that the change in static form has on the capacity (Inaam and Upadhyay, 2020).

$$\chi_M = 0.4718 \cdot \left[\frac{s_s}{2 \cdot (a_1 + a_4)}\right]^{-0.786} \tag{34}$$

Regarding loading positions all of the studies agree that the highest resistance of the girder is obtained when the load is applied at the inclined fold. Although there is not an agreement of if the lowest value is obtained when it is applied at the intersection or on the longitudinal fold. According to Lieva-Aravena and Edlund (1987), and Elgaaly and Seshadri (1997) applying the load at the intersection yields the lowest resistance but according to Luo and Edlund (1996) the lowest resistance is obtained by applying the load at the longitudinal fold.

2.4 Eurocode 3

In the current Eurocode there is not a formula that addresses patch loading resistance of girders with corrugated web. EN 1993-1-5 (2006) Annex D addresses members with corrugated web and as it is now there is no formula provided to estimate the patch loading resistance. The newest draft for EN 1993-1-5 (2020) includes a formula for the problem. The formula that is provided in the draft of Eurocode to estimate the design resistance of a trapezoidal corrugated web under patch loading is presented in equation 35.

$$F_R = \frac{\chi \cdot k_a \cdot s_s \cdot t_w \cdot f_{yw}}{1.20 \cdot \gamma_{M1}} \tag{35}$$

The modification factor due to corrugation angle, k_a, is the same as the one presented by Kuhlmann and Braun (2008), calculated with equation 20. The reduction factor, χ, is due to the corrugation angle is calculated with equation 36.

$$\chi = \begin{cases} 1.0, & \bar{\lambda}_p \leq 1.27 \\ \dfrac{1.9}{\bar{\lambda}_p} - \dfrac{0.8}{\bar{\lambda}_p^2}, & \bar{\lambda}_p > 1.27 \end{cases} \tag{36}$$

Where $\bar{\lambda}_p$ and σ_{cr} are determined like in equations 25 and 26. The design method is applicable for girders with a fold length that fulfills the criteria in equation 19, that is the same as was presented by Kuhlmann and Braun (2008).

This formula is similar to the one suggested by Kövesdi et al (2010) and Kövesdi (2010), that is the part in the formulas that considers the contribution from the web. Although this formula has some improvements and it includes the material safety factor unlike the Kövesdi et al (2010) and Kövesdi (2010) model.

3 Finite element analysis

In this chapter, finite element (FE) analysis of stainless steel girders with corrugated webs under patch loading is developed and checked. Multiple FE models are established and evaluated. The models are established by running a Python script in the FE program ABAQUS CAE. The models have varying geometry, but same material properties, boundary conditions, loading length and mesh size. All the models are analyzed by running a linear eigen-buckling analysis as well as non-linear post-buckling analysis. Also, a linear static analysis is used in a mesh convergence study. The model is verified and validated in comparison with two reference models.

3.1 Geometry and material properties

All of the girders studied here have corrugated web with a shape that is shown in Figure 2. The intersections between the longitudinal and inclined folds are curved. In Table 1 the fixed variables and parametric ranges are presented. The length of all the girders is set to 3 meters to have the length more than two times the height of the girder.

Table 1. Geometrical parameters of the girder.

Variable	Value	Unit
Length of girder, L	3000	mm
Height of web, h_w	1450	mm
Thickness of web, t_w	4-8	mm
Width of flanges, b_f	250-500	mm
Thickness of flanges, t_f	20-40	mm
Loading length, s_s	150	mm
Initial imperfection, e_0	7.25	mm
Length of the longitudinal fold, a_1	Varies	mm
Corrugation angle, α	30-70	°
Depth of the corrugation, a_3	100-400	mm
Radius at the intersection, C_{radius}	25	mm
Number of unit cells, n_{corr}	2-4	-

Each girder is developed in ABAQUS CAE in a way that makes the results for each girder more comparable to other girders. For each variation of the number of unit cells an additional quarter of a unit cell (one half of the longitudinal fold and one half of the inclined fold)is added at each end of the girder, as well as a 100 mm long plate centered at the flange width. This way of constructing the girder makes it symmetric around the weak axis at the middle of the girder. Additionally, 20 mm thick transversal stiffeners are included at each end of the girder to provide further lateral stability at the supports.

The length of one unit cell, L_{corr}, is kept constant for each number of unit cells, $n_{corr,}$ that means that when the depth of the corrugation, a_3, and the corrugation angle, α, are changed then the length of the longitudinal fold, a_1, changes accordingly so that the length of one unit cell, L_{corr}, does not change.

The material properties for the stainless steel grade is taken from Table 2.1 in EN 1993-1-4 (2006) for 1.4462 hot rolled plate and can be seen in Table 2. This stainless steel is a duplex steel grade which is frequently used in bridges due to its corrosion resistance.

Table 2. Material properties of the stainless steel constituent for the girders.

Stainless steel 1.4462	**Value**	**Unit**
Mass density, ρ	7800	kg/m^3
Young's modulus, E	200	GPa
Poisson's ratio, v	0.3	-
Yield stress lower limit, f_{y1}	460	MPa
Plastic strain lower limit, ε_1	0	-
Yield stress upper limit, f_{y2}	640	MPa
Plastic strain upper limit, ε_2	0.09	-

3.2 Loading and boundary condition

Boundary conditions are applied on the flanges. On both sides the edges of the bottom flange are constrained in y- and z direction and the edges of the top flange are locked in y-direction. To increase lateral stability, one point is fixed in the patch plate in y-direction. Additionally, one rigid point is applied at the middle of the bottom flange. The boundary conditions applied are displayed in Figure 3.

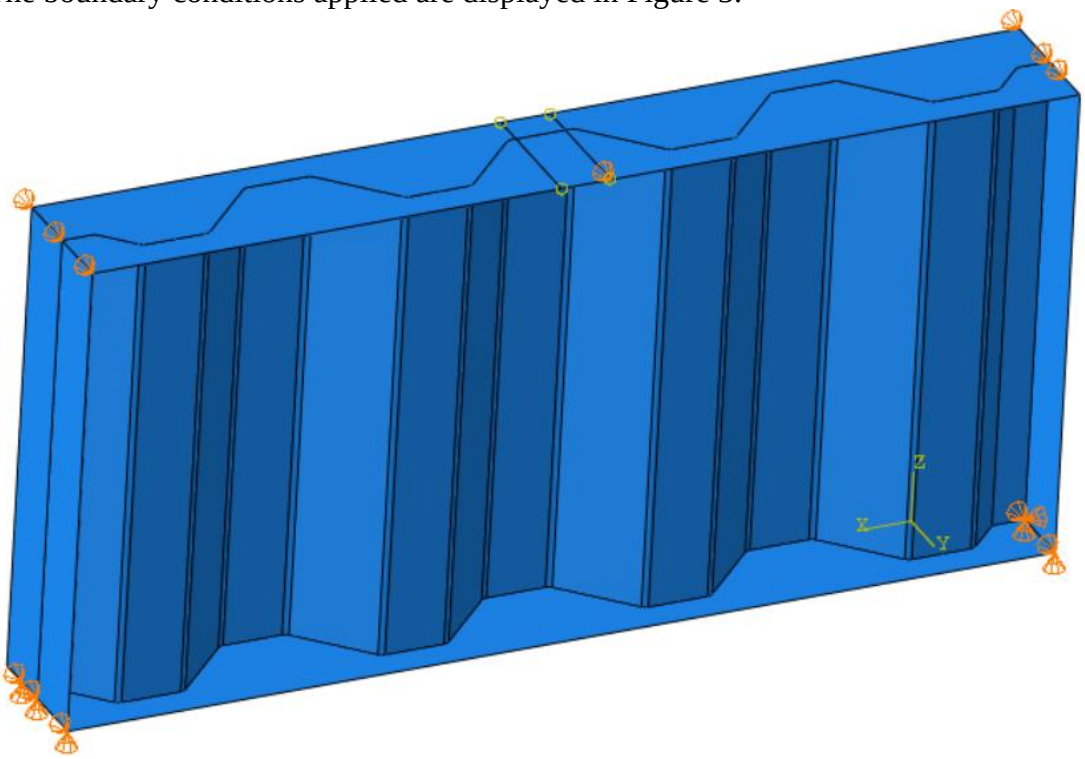

Figure 3. The boundary condition applied.

Patch loading is applied on the girder by making a partition on the flange to mimic a patch plate. The area of the patch plate is the flange width multiplied by the loading length and on it a pressure load is applied. The load is applied at three different places that is on the longitudinal fold, inclined fold and the intersection between the two, see Figure 4.

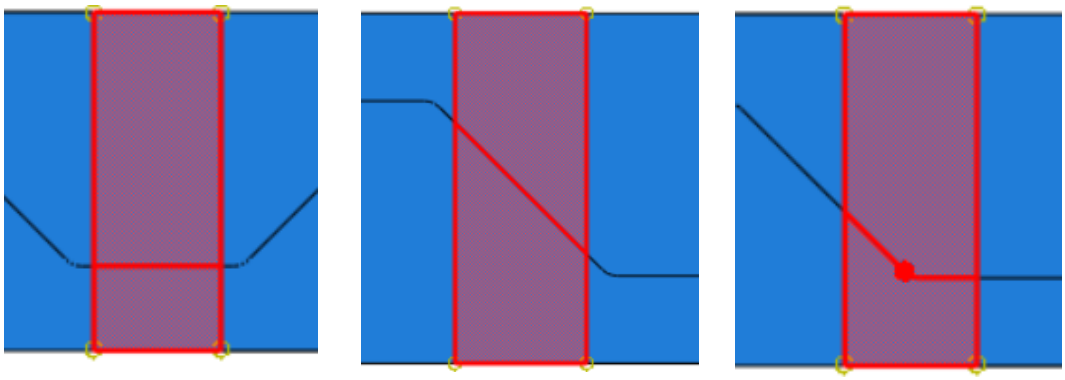

Figure 4. The three loading locations of the girder. The one on the left is the longitudinal fold, middle one is the inclined fold and the one on the right is the intersection.

The load is applied at these three locations to see how the loading position effects the patch loading capacity of the girder. These three locations should present crucial types of behavior in the girder.

3.3 Mesh and analysis

Same mesh density is used over the whole girder. Element type of S8R is used which is an eight-node shell element. The reason why element type of S8R is used instead of the general type of S4R is that S8R has more nodes and when comparing the convergence rate for the two, S8R is a lot faster to convergence. That means that with the same element size, S8R exhibits better results. The mesh size used in the analysis is a mesh with element size of 20 mm which can be seen in Figure 5.

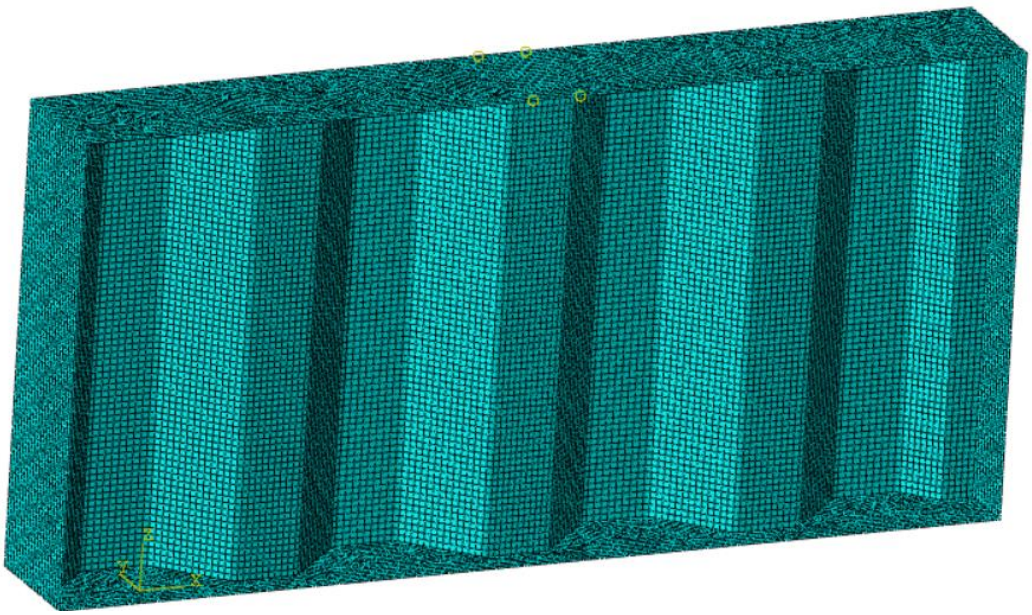

Figure 5. Mesh used in the analysis.

The linear static analysis is only used for the convergence study of the mesh and will not be used further on in the study. The analyses that are used further are a buckling analysis to get the eigenvalue for the girder which is then used in the second analysis which is a non-linear analysis.

In the eigen-buckling analysis the eigen solver used is Lanczos and the minimum eigenvalue derived is set to 0.0 that means that no negative eigenvalues are extracted.

The linear buckling load capacity is estimated by using linear eigen-buckling analysis. The buckling load capacity is estimated by multiplying the eigenvalue with the reference load.

In the non-linear analysis the general static Riks method is used. The Riks method is an arc-length based incremental method, the initial arc increment was set to 0.01 and the maximum number of increments is set as 75. For most of the girders 75 is too much but since it is a large parametric study the number of increments must be sufficient for majority of the girders.

3.4 Verification and validation

The model is examined from different perspectives to validate and verify it. To verify the model a mesh convergence study is performed. Next, the effect of the initial imperfection and size of the patch plate are checked. Lastly, the model is verified and validated by comparing it to two known reference models.

3.4.1 Mesh sensitivity and convergence study

To decide the size of elements in the mesh, three different mesh convergence studies are performed. One for each analysis, that is, for linear static -, buckling - and nonlinear analysis.

The convergence study for the linear static analysis considers the maximum vertical deflection of the girder. The results are shown in Table 3. There the element size in the mesh is shown along with the number of elements and the corresponding maximum vertical deflection of the girder. The last column shows the difference between each value, that is the previous value compared to the current value, see equation 37.

$$\delta = \frac{U_{max,i-1} - U_{max,i}}{\left(\frac{U_{max,i-1} + U_{max,i}}{2}\right)} \tag{37}$$

Table 3. Results from mesh convergence study for linear static analysis.

Element size [mm]	Number of elements	Maximum vertical displacement [mm]	Difference
75	2086	-9.152	-
60	2604	-9.375	2.41%
50	3379	-9.775	4.18%
40	5587	-9.793	0.18%
30	8545	-9.908	1.17%
20	19142	-9.982	0.74%
10	74419	-10.000	0.18%

The convergence rate is shown in Figure 6, the maximum vertical deflection is plotted against number of elements. In the figure it is observed that the model converges to a sufficient extent.

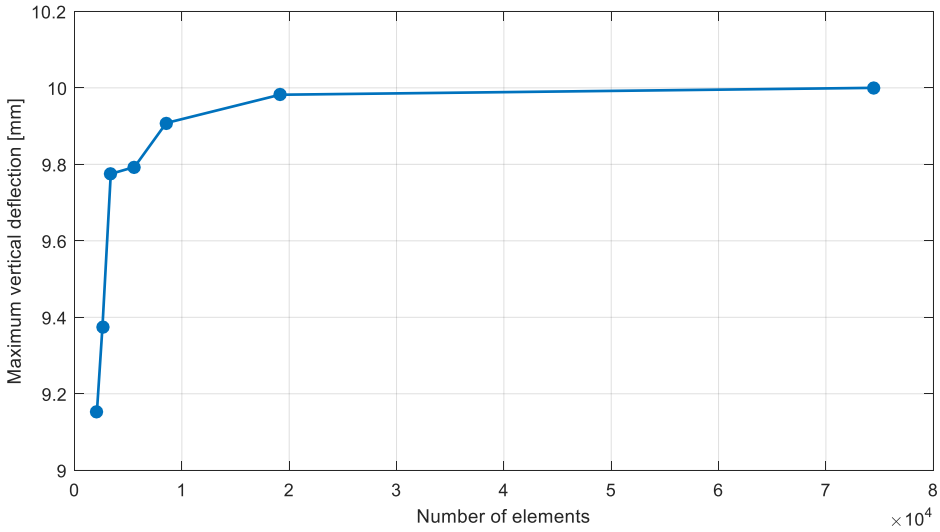

Figure 6. Mesh convergence study for the maximum deflection.

The mesh size that is deemed sufficient from this convergence study is a mesh with element size of 30 mm.

The convergence study for the linear eigen-buckling analysis considers the first five eigenvalues of the girder. Table 4 presents how the first five eigenvalues change with decreasing the element size in the mesh.

Table 4. Results from mesh convergence study for eigen-buckling analysis.

Element size [mm]	**Number of elements**	λ_1	λ_2	λ_3	λ_4	λ_5
75	2086	2.6804	2.9400	3.3323	3.7172	4.1319
60	2604	2.5367	2.6470	3.1547	3.3097	3.7794
50	3379	2.2001	2.3794	2.8516	2.9900	3.4545
40	5587	2.1371	2.3324	2.7804	2.9248	3.3572
30	8545	2.1061	2.3053	2.7445	2.8869	3.3017
20	19142	2.0971	2.2966	2.7338	2.8743	3.2841
10	74419	2.0935	2.2932	2.7300	2.8702	3.2789

The convergence rate is shown in Figure 7, the maximum vertical deflection is plotted against number of elements, all eigenvalues converge to a sufficient extent.

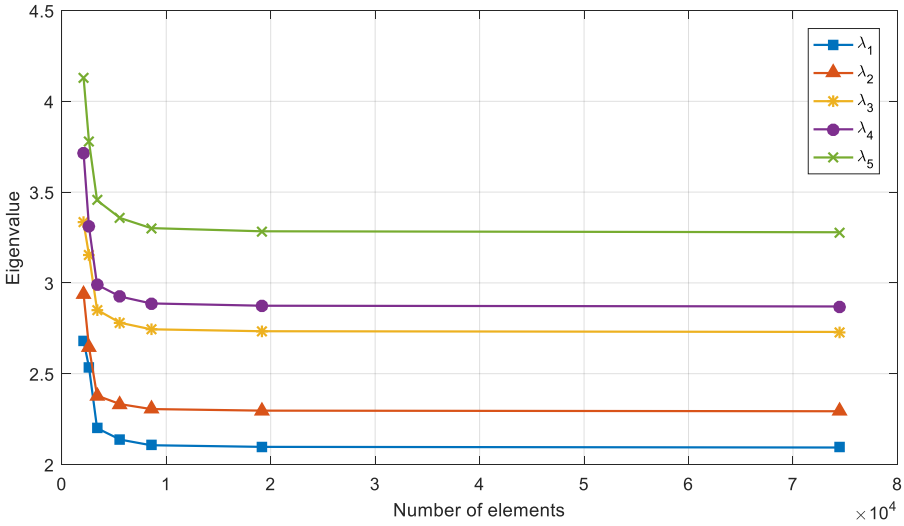

Figure 7. Mesh convergence study for the eigen-buckling analysis.

Eigenvalue 1 is examined further, see Table 5, since that is the eigenvalue extracted in the FE-analysis. The eigenvalue does not change much after a element size of 30 mm, therefore the element size that is deemed sufficient for the mesh from this convergence study is element size of 30 mm.

Table 5. Results from mesh convergence study for eigenvalue 1.

Element size [mm]	Number of elements	λ_1	Difference
75	2086	2.6804	-
60	2604	2.5367	5.51%
50	3379	2.2001	14.21%
40	5587	2.1371	2.91%
30	8545	2.1061	1.46%
20	19142	2.0971	0.43%
10	74419	2.0935	0.17%

The convergence study for the non-linear analysis considers the patch loading resistance of the girder and the results are presented in Table 6 and Figure 8. The mesh that is deemed sufficient from this convergence study is a mesh with element size of 20 mm since when changing it to 10 mm it changed less than 1% with drastically increased computational time.

Table 6. Mesh convergence study for nonlinear analysis.

Mesh size	Number of elements	F_R [kN]	Difference
75	2086	916.72	-
60	2604	943.67	2.90%
50	3379	892.04	5.63%
40	5587	845.26	5.39%
30	8545	817.43	3.35%
20	19142	797.79	2.43%
10	74419	791.13	0.84%

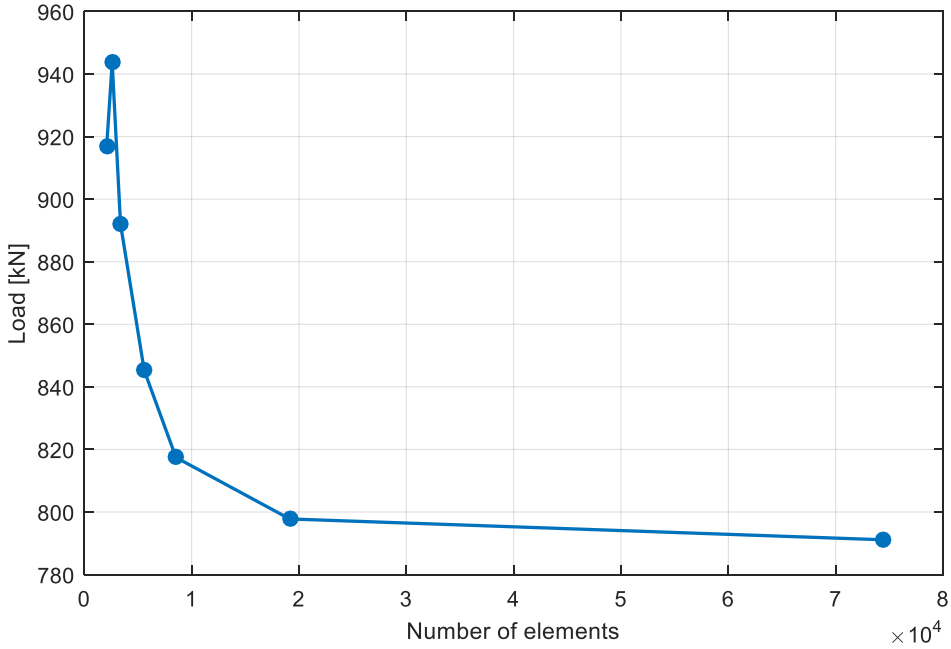

Figure 8. Mesh convergence study for the patch loading resistance.

Therefore, from these three mesh convergence studies at different analysis type a mesh with element size of 20 mm is chosen and is used for the rest of this study.

3.4.2 Effect of initial imperfection

The initial imperfection of the girder is accounted for with guidelines from EN 1993-1-5 (2006) Annex C. There it is suggested to relate the imperfection factor to the depth of the web that means that the initial imperfection can be calculated with equation 38. The initial imperfection can also be related to the length of the loaded fold which was suggested by Kövesdi and Dunai (2011). In this study the initial imperfection is related to the height of the web since those results were more conservative and yielded higher imperfection.

$$e_0 = \frac{h_w}{200} \tag{38}$$

Different imperfection factors are analyzed for a reference girder, the geometry of the girder is presented in Table 15. The girder was loaded at three different locations and the results for that are shown in Figure 9. The figure shows the results for all three load cases with six different values for the initial imperfection factor. From this figure it is observed that the intersection and inclined load cases are more sensitive to changed imperfection factor while for the longitudinal load case the difference in patch loading resistance is very small.

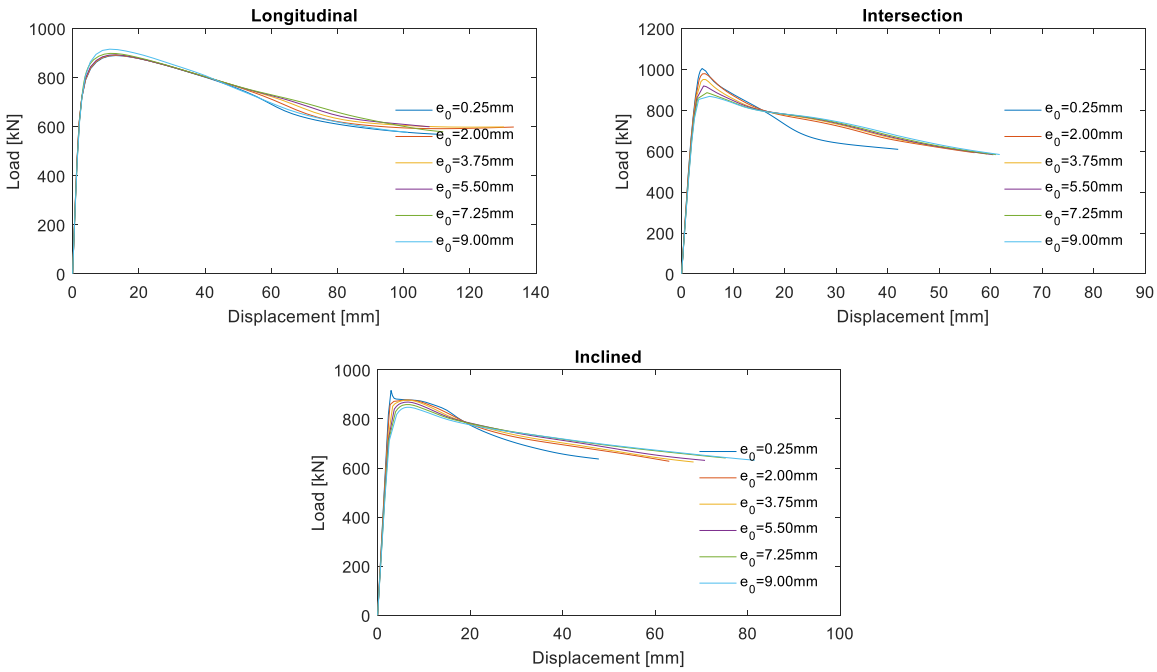

Figure 9. Load-displacement curves for different initial imperfection factors for all load cases.

3.4.3 Effect of the size of patch plate

Different ways of loading the girder are analyzed to see if the patch load should be applied over the whole width of the flange or with a width less than the flange which gives a square or rectangular area on the flange like is shown in Figure 10.

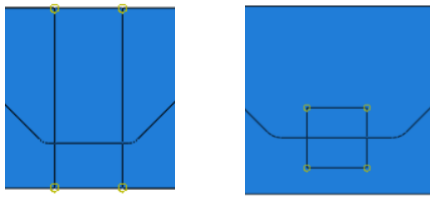

Figure 10. The two different shapes of the patch plate analysed. On the left is over the whole witdh of the flange and the one on the right is with an square or rectangular shape.

The results from these two different loading ways are shown in Figure 11. The patch loading resistance increases with increasing the loading length which matches previous studies. The curves show that for the FE-model at hand, it is more conservative to apply the load over the whole width of the flange which is also consistent to previous studies that is for example Kövesdi et al (2010), and Ljungström and Karlberg (2010). Applying the load over the whole width makes the resistance more influenced by the bending of the flanges and therefore it yields a lower value.

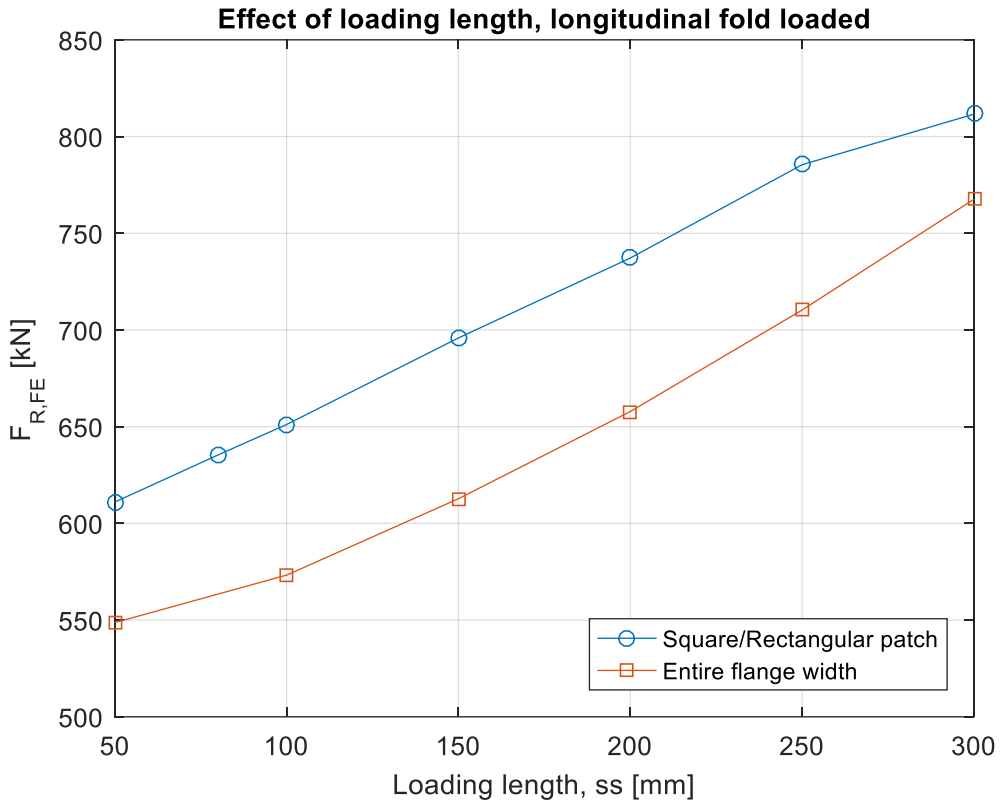

Figure 11. Visual representation on how the loading length and the shape of the patch plate influences the patch loading resistance.

Since loading the entire flange width is more conservative, a decision is made to apply the load over the whole width of the flange and also since that is more comparable to previous studies. In ABAQUS CAE, the load is applied on the flange as pressure so applying the load over the entire width of the flange causes more bending and deformations than it would in reality. The material applying the load would have to deform as much as the flange to make this way of applying the load realistic.

3.4.4 Comparison with known FE results

Here two reference models are compared to results from the FE-analysis to further validate the model.

3.4.4.1 Reference model 1 (al-Emrani, 2020)

This reference model examines one girder with corrugated web made from carbonated steel, with steel grade of S355. In the reference model lateral torsional buckling is to be analyzed so it is different from the task in this thesis, but it can despite that verify if the Python script is working correctly in terms of for example the non-linear analysis. The Python script is changed so it correlates to the reference model. That is different load, boundary condition and geometry. The results are then compared and checked if they correlate together. The geometry of the reference model is shown in Table 7 and Figure 12. There is a small difference between the geometry of the models. The Python script creates a small curve in the corrugation which can affect the results.

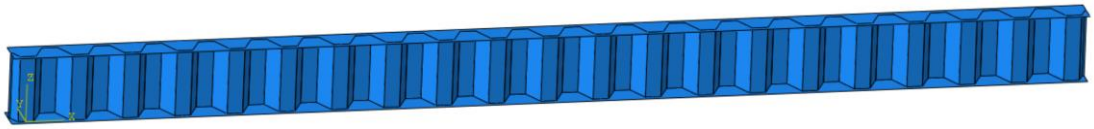

Figure 12. Girder examined in reference model 1.

Table 7. Geometrical parameters for reference model 1.

Variable	Value	Unit
Length of girder, L	4800	mm
Height of web, h_w	300	mm
Thickness of web, t_w	6	mm
Width of flanges, b_f	150	mm
Thickness of flanges, t_f	10	mm
Initial imperfection, e_0	12, 16 and 24	mm
Length of the longitudinal fold, a_1	70	mm
Corrugation angle, α	65	°
Depth of the corrugation, a_3	100	mm
Radius at the intersection, C_{radius}	0	mm

The load acting on the girder is a moment, M, of 100 kNm which is simulated by applying an evenly distributed edge load on the flanges of the girder, applied on both top and bottom flanges. To calculate the shell edge loading, equation 39 is used.

$$F_{shell\_edge} = \frac{M}{b_f \cdot (h_w + t_f)} \tag{39}$$

The boundary conditions used is equivalent to fork supports. The web on both sides is restrained to displace in the lateral direction. Then on one end a point is restrained at the middle of the web in x-, y- and z-direction and also to rotate about the x-axis that is the longitudinal axis. On the other side a point is restrained at the middle of the web height in y- and z-direction and to rotate about the x-axis.

The analytical calculations are shown in Appendix A.1. In Table 8 the results are presented and compared to the results from the FE-analysis. The ultimate moment capacity is presented for three different buckling curves (b, c and d). The difference is highest 28.85% which is rather high, but it was expected since the analytical values are more conservative than the values extracted from the FE-analysis.

Table 8. Results from analytical calculations and FE-analysis.

	Analytical	FE-analysis	Difference [%]
M_{cr} [kNm]	150.89	162.00	7.10
M_{ult} [kNm]			
Curve b	92.51	110.94	18.11
Curve c	83.65	105.38	22.99
Curve d	72.34	96.73	28.85

Then the FE-analysis is compared to the FE-analysis values from the reference model, those values are presented in Table 9. The values correlate well to each other and the highest difference is 3.12% which is reasonable.

Table 9. Results from the reference model compared to FE-analysis.

	Reference model	FE-analysis	Difference [%]
Eigenvalue	1.60	1.62	1.27
M_{cr} [kNm]	159.96	162.00	1.27
M_{ult} [kNm]			
Curve b	108.92	110.94	1.83
Curve c	102.94	105.38	2.34
Curve d	93.76	96.73	3.12

The difference between the two values can be explained in some part since the reference model has sharp edges at the intersections between the inclined fold and longitudinal fold while the other has a curved shape. Load displacement graphs are extracted for all three curves. In Figure 13 curve b is presented which correlates to initial imperfection of 12 mm. The other two curves are shown in Appendix A.2.1 and A.2.2. All of the curves correlate well together and have the same trend. This verifies that the nonlinear analysis of the code is working correctly compared to the reference model.

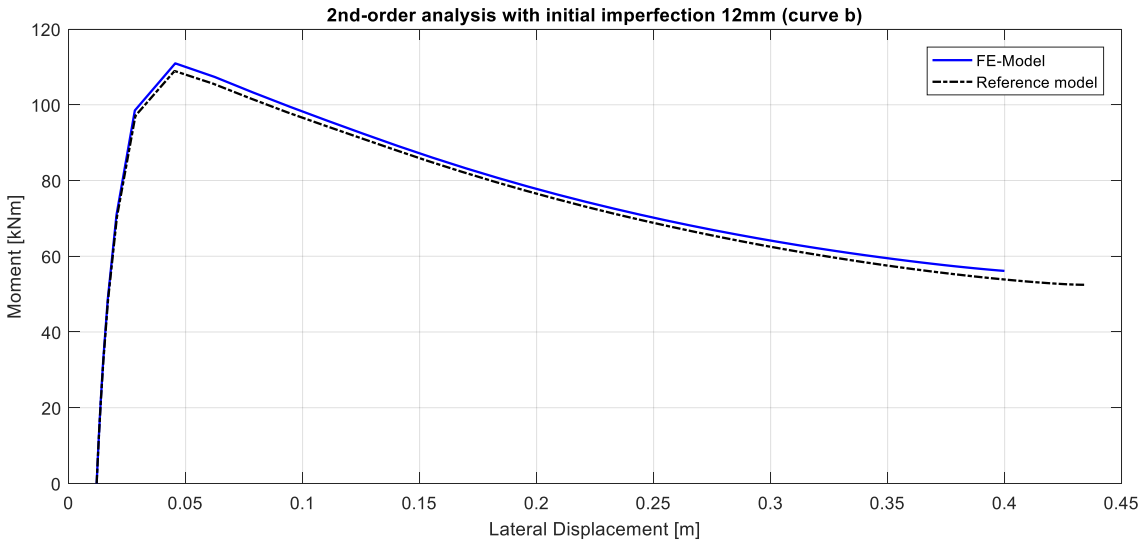

Figure 13. Moment-displacement graph for both analyses.

3.4.4.2 Reference model 2 (Ljungström and Karlberg, 2010)

For this reference model corrugated web girders made with material grade of S355 are examined. The material parameters used for the S355 steel are shown in Table 10.

Table 10. Material parameters used in the FE-analysis.

S355	**Value**	**Unit**
Mass density, ρ	7800	kg/m^3
Young's modulus, E	193	MPa
Poisson's ratio, ν	0.3	-
Yield stress lower limit, f_{y1}	357	MPa
Plastic strain lower limit, ε_1	0	-
Yield stress upper limit, f_{y2}	491	MPa
Plastic strain upper limit, ε_2	0.0601	-

A parametric study is made where a few variables are varied. The geometric values of the girders are shown in Table 11. The corrugation shape of the girders is fixed in this parametric study and there are three parameters varied that is the initial imperfection factor, thickness of the flanges and the web.

Table 11. Geometrical properties of reference model 2.

Variable	**Value**	**Unit**
Length of girder, L	3000	mm
Height of web, h_w	600	mm
Thickness of web, t_w	2-4	mm
Width of flanges, b_f	160	mm
Thickness of flanges, t_f	10-20	mm
Loading length, s_s	50	mm
Initial imperfection, e_0	0-5	mm
Length of the longitudinal fold, a_1	140	mm
Corrugation angle, α	45	°
Depth of the corrugation, a_3	50	mm
Radius at the intersection, C_{radius}	30	mm

The load is applied around 1 meter away from the support and at three different load locations on the girder. The three different locations are the following:

- Inclined fold
- Intersection
- Longitudinal fold

For each load case there are 10 different girders examined and therefore in total 30 girders are examined. The 10 different combinations of girders that are examined are shown in Table 12. Where X represents each load case, for example X equal to 3 means that the girder is loaded on the longitudinal fold.

Table 12. The 10 different girders examined and their respective parameters.

	t_f				t_w			e_0				
[mm]	**10**	**12**	**16**	**20**	**2**	**3**	**4**	**0**	**0.5**	**1**	**2**	**5**
X00		●				●			●			
X01	●					●			●			
X02			●			●			●			
X03				●		●			●			
X04		●			●				●			
X05		●					●		●			
X06		●				●		●				
X07		●				●				●		
X08		●				●					●	
X09		●				●						●

The boundary conditions that are applied on the girder are shown in Figure 14 along with Table 13.

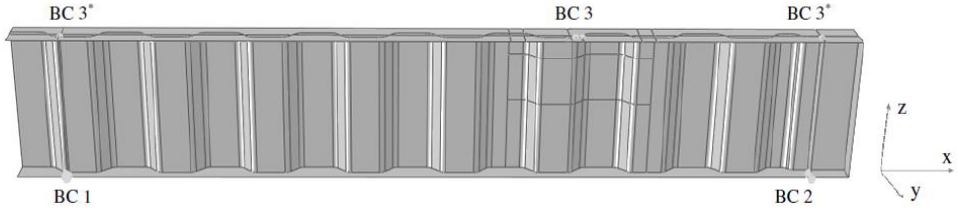

Figure 14. Boundary conditions used in the reference model (Ljungström and Karlberg 2010).

Table 13. Boundary conditions (Ljungström and Karlberg 2010).

	x	y	z
BC 1	Locked	Locked	Locked
BC 2	Free	Locked	Locked
BC 3	Free	Locked	Free
Note:	* Locked just in one node		

The patch loading resistance from the reference model are compared to the results from the FE-analysis along with the trend in the load-displacement graphs. Table 14 shows the results from both methods and how they correlate with each other. The largest difference in percentage is 5.28% which is rather small. The reason for the difference could be explained by the fact that in the parametric study made by Ljungström and Karlberg (2010) different material parameters were used for the flange and the web, however in the FE-model same material parameters are used. The weaker material parameters are chosen to be on the conservative side so it should yield lower value although that is not always the case.

Table 14. Comparison of the results from the reference model and the FE-analysis.

Girder	Reference [kNm]	FE-analysis [kNm]	Diff [%]
100	210.4	211.5	-0.53
101	183.1	187.6	-2.45
102	248.4	247.3	0.43
103	282.8	274.7	2.91
104	123.8	127.6	3.05
105	270.2	271.2	0.36
106	213.6	219.4	2.66
107	206.6	208.7	-0.99
108	190.3	200.6	-5.28
109	189.8	180.5	5.01
301	131.3	131.3	0.0
302	246.4	237.9	3.5
303	285.6	276.3	3.3
304	129.6	132.3	-2.1
305	202.4	194.8	3.8
306	170.5	166.5	2.4
307	174.7	168.3	3.7
308	173.3	168.4	2.9
309	170.8	168.2	1.5

4 Parametric studies

In the parametric study models are developed in the FE-software ABAQUS CAE using a Python script. More than a thousand models are developed so three conditions are considered to reduce computational time and to neglect most models that are not realistic for practice. The three conditions produced are the following:

1. $a_3 \geq 0.3 \cdot b_f$
2. $a_1 \geq 0.2 \cdot L_{corr}$
3. $a_3 \leq b_f - 100\ mm$

The first condition is made since the girders analyzed are with corrugated web and when a certain ratio between the depth of the corrugation, a_3, and the width of the flanges, b_f, is reached the girders starts to behave like an I-beam. That means that the stiffening benefit of having the web corrugated is limited which is not preferred.

The second condition is due to the fact that the script is written in a way that the length of one unit cell, L_{corr}, is constant for each number of unit cells, $n_{corr,}$ this means that the length of the longitudinal fold, a_1, is dependent or changes with change in parameters of the depth of the corrugation, a_3, and the corrugation angle, α. This condition is made to avoid unrealistic values for the length of the longitudinal fold, a_1, that is to take out negative values or small values.

The third condition makes sure that flange width, b_f, is always larger than the depth of the corrugation, a_3, and restricts the ratio of corrugation depth to flange width to a certain extent.

To further investigate the effect of certain parameters, four small parametric studies are made to analyze the influence they have on the patch loading resistance. These studies were done for a reference girder, the parameters of the reference girder are shown in Table 15.

Table 15. Geometrical parameters of the reference girder used.

Variable	Value	Unit
Length of girder, L	3000	mm
Height of web, h_w	1450	mm
Thickness of web, t_w	6	mm
Width of flanges, b_f	400	mm
Thickness of flanges, t_f	20	mm
Loading length, s_s	150	mm
Initial imperfection, e_0	7.25	mm
Length of the longitudinal fold, a_1	200	mm
Corrugation angle, α	45	°
Depth of the corrugation, a_3	200	mm
Radius at the intersection, C_{radius}	25	mm
Number of unit cells, n_{corr}	3	-

Different parameters are varied in the reference girder to do preliminary studies. In these preliminary studies, the range for variation of the parameters are chosen to be wider than a normal range to get a better overview of how each parameter affects the patch loading resistance. The parameters that are varied in each preliminary study are as follows:

1. Thickness of the web and the corrugation angle.

In this preliminary parametric study, the influence of the thickness of the web and the corrugation angle is analyzed. There are five parameters considered for the thickness of the web that are 2, 4, 6, 8 and 10 mm and seven parameters for the corrugation angle that are 30, 35, 40, 45, 50, 60 and 70°. This yields in 35 models but due to the limits previously described only 25 models are constructed and corrugation angle of 30 and 35 does not meet the criteria for this specific girder so no girder is constructed with the two smallest angles.

2. Thickness of the web and width of the flange.

In this preliminary parametric study, the influence of the thickness of the web and the corrugation angle is analyzed. There are five parameters considered for the thickness of the web that are 2, 4, 6, 8 and 10 mm and five parameters for the width of the flange that are 250, 300, 350, 400 and 500. This yields in 25 models but due to the limits previously described only 20 models are constructed and flange width of 250 does not meet the criteria.

3. Thickness of the web and thickness of the flange.

In this preliminary parametric study, the influence of the thickness of the web and the thickness of the flange is analyzed. There are five parameters considered for the thickness of the web that are 2, 4, 6, 8 and 10 mm and five parameters for the thickness of the flange, that are 20, 25, 30, 35 and 40. These yields in 25 models which are all constructed and meet the criteria previously described.

4. Thickness of the web and depth of the corrugation.

In this preliminary parametric study, the influence of the thickness of the web and the depth of the corrugation are analyzed. There are five parameters considered for the thickness of the web that is 2, 4, 6, 8 and 10 mm and for the corrugation depth the parameters considered are 100, 150, 200, 250, 300 and 350 mm. Due to the three conditions only 10 models are developed and only a corrugation depth of 150 and 200 mm are considered. Since there are only two different depths of corrugation, the geometry of the reference girder is adjusted to a girder that gives more variations for the depth of the corrugation. The change can be seen in Table 16 compared to the initial reference girder, the difference is that the new reference girder has higher corrugation angle and wider flange.

Table 16. The geometrical parameters for the initial reference girder and the new reference girder.

Variable	Initial reference girder	New reference girder	Unit
Length of girder, L	3000	3000	mm
Height of web, h_w	1450	1450	mm
Thickness of web, t_w	6	6	mm
Width of flanges, b_f	400	**500**	mm
Thickness of flanges, t_f	20	20	mm
Loading length, s_s	150	150	mm
Initial imperfection, e_0	7.25	7.25	mm
Length of the longitudinal fold, a_1	200	200	mm
Corrugation angle, α	45	**70**	°
Depth of the corrugation, a_3	200	200	mm
Radius at the intersection, C_{radius}	25	25	mm
Number of unit cells, n_{corr}	3	3	-

In addition to these preliminary studies, a extensive parametric study is executed using the verified model. The parameters which are varied between the models are presented in Table 17. In total there are six parameters varied, although the length of the longitudinal fold, a_1, changes as well since it is dependent on the corrugation angle, α, number of unit cells, n_{corr}, and corrugation depth, a_3.

Table 17. The geometrical parameters that are varied in the parametric study.

Variable	Values	Unit
Thickness of web, t_w	4-6-8	mm
Width of flanges, b_f	250-300-400-500	mm
Thickness of flanges, t_f	20-30-40	mm
Number of unit cells, n_{corr}	2-3-4	-
Corrugation angle, α	30-45-60-70	°
Corrugation depth, a_3	100-200-300-350	mm

This results in 1728 models in total. Due to the three conditions set, not all 1728 models are evaluated and extracted, that means that the models that do not fulfill all of the previously described conditions are neglected from the analysis. Therefore, the total number of analyzed models is reduced from 1728 models to 603 models for each load case. Note, that due to time constraint and allocated computing time the last 7 models are not produced for the intersection load case, in addition the loss of these 7 models is deemed to only affect the results in a minor way. When all load cases are considered, the total number of developed models are 1802.

Note that since this parametric study is developed for girder dimensions applicable for stainless steel, thus the flange-web thickness ratios are considerably higher than for carbonated steel girders.

5 Preliminary results and discussion

In the preliminary studies all three loading locations are considered, and the reference girder shown in Table 15 is used. In each preliminary parametric study, there are two geometrical parameters varied in the reference girder. In this chapter the results from each study are analyzed and discussed. Finally, the results are summarized.

5.1 Thickness of the web and the corrugation angle

The change in the patch loading resistance with varying corrugation angle can be seen in Figure 15 for all load locations. It is interesting to notice that for thin web of 2 mm all the loading locations have almost constant behavior with varying the corrugation angle. From that it can be assumed that for very thin web girders the corrugation angle has little to no influence on the patch loading resistance. The highest patch loading resistance for all load cases is for the thickest web considered and the lowest resistance for the thinnest web considered.

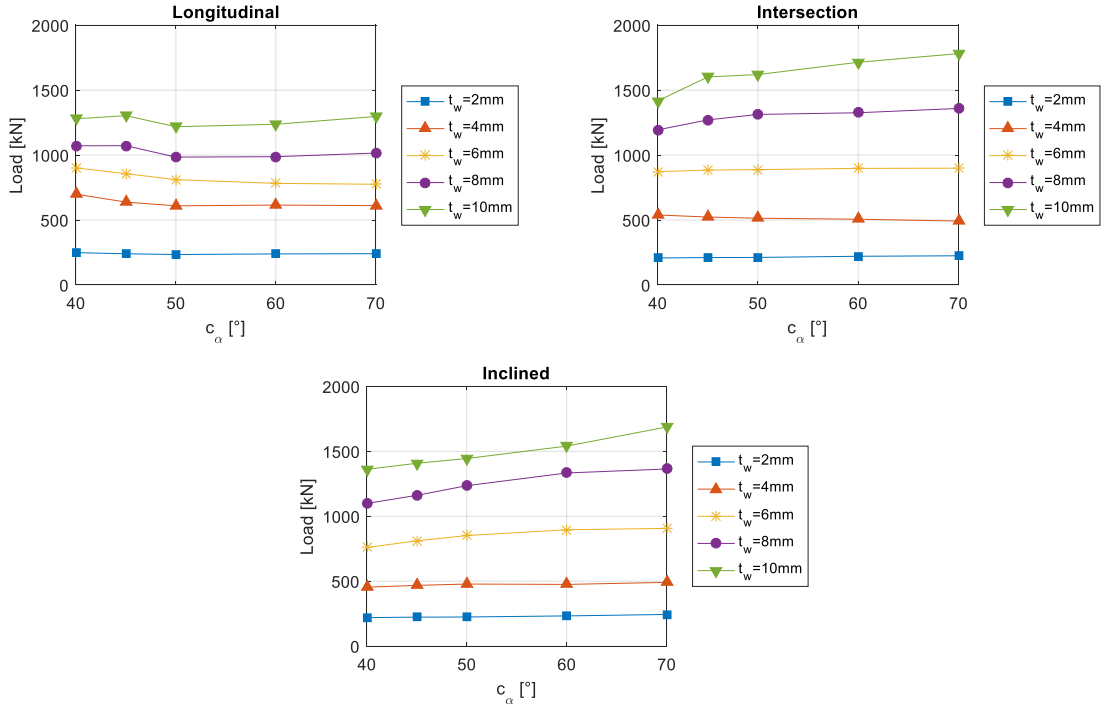

Figure 15. Influence on the patch loading resistance for varying corrugation angle.

The curves for the longitudinal fold have some fluctuating behavior for the lower angles, after that it remains almost constant although there are some increases and decreases in the curves. For lower angles of 40 to 50 degrees the patch loading resistance seems to be decreasing but after that for web thickness of more than 8 mm the patch loading resistance increases slowly. For thinner webs it continues to decrease but with less rate. These changes in patch loading resistance are so minor that they could be neglected but since the results are only for a specific girder, the behavior could be different for other types of girders. For the inclined fold the trend seems to be that with increasing the angle the patch loading resistance increases that is for web thickness of 6 mm and larger and a constant behavior can be observed for the thinner webs. The patch loading resistance has a similar trend for the intersection that is increases for web thickness of 8 mm and more but constant or slow decrease for thinner webs.

For the longitudinal load case, global buckling behavior is observed for girders with small corrugation angle, and local behavior is seen for the larger corrugation angle. In girders loaded at the intersection there is a different behavior for the smallest corrugation angle and the thickest web compared to the other angles, this is due to global buckling behavior in the girder while the other girders show local patch buckling.

Figure 16 shows how changing the web thickness of the girder influences the resistance of the girder for all load cases. There is different trend for each load case which shows that it is important to distinguish between where the load is applied at least for a narrow loading length. For all the load cases the patch loading resistance increases with increased web thickness.

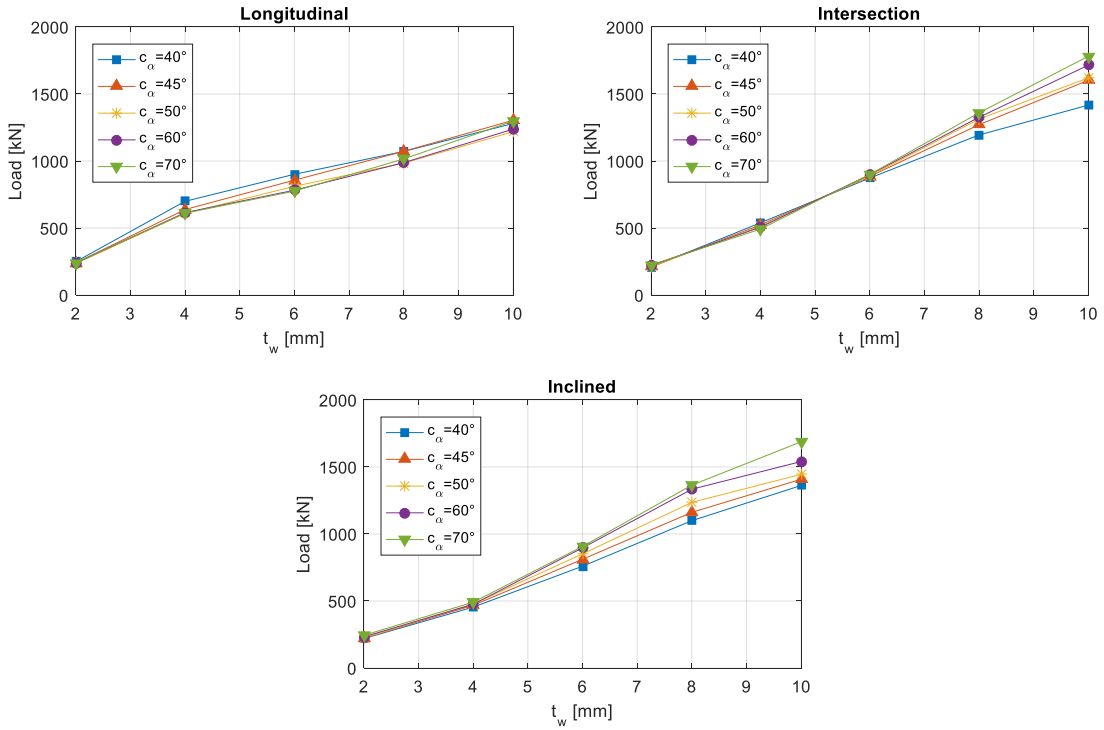

Figure 16. Influence of the web thickness on the patch loading resistance, with different corrugation angles.

For the longitudinal loading location, the patch loading resistance increases linearly for web thickness of 2 to 4 mm. After that, the curves change slope and increase with less intensity from 4 to 10 mm and the effect from the corrugation angle starts to be noticeable. This means that the web thickness from 2 to 4 mm influences patch loading resistance more than from 4 to 10 mm, but the corrugation angle has the opposite effect. Although this change in slope is not drastic this might need to be considered in the design models for corrugated web girders with thin webs. It is interesting to observe that the highest patch loading resistance yields for web thickness from 2 to 8 mm for corrugation angle of 40° but for the stockiest girder, with web thickness of 10 mm, the patch loading resistance is highest for a corrugation angle of 45°. Looking at the corrugation angle of 70°, these girders have the lowest load capacity for a web thickness 2 to 6 mm, but changes slope from 6 to 10 mm and increases the resistance at a faster rate than other angles. It is worth to note that even if different behavior can be observed, that for each angle the change in capacity for the same web thickness the trend is close to identical. The inclined fold load location has similar trend as the longitudinal fold

load location, that is the slope changes at web thickness of 4 mm although after 4 mm the patch loading resistance increases at higher rate than before unlike the longitudinal fold. When the load is applied at the intersection the patch loading resistance increases almost linearly for web thickness from 2 to 6 mm and then increases with higher rate from 6 to 10 mm for all angles expect for angles of lower degree. It is interesting to notice that for the longitudinal fold load case the patch loading resistance is highest for corrugation angle of 40 degrees while it is the other way around for the other two where an angle of 70 degrees yields the highest patch loading resistance. Similar trends are observed when changing the corrugation angle for the inclined and intersection load cases. That is for lower thicknesses the capacity is close to identical for each angle and for thicker webs the corrugation angle influences the capacity, however the behavior is slightly different for the longitudinal load case. This might be due to the flow of forces between the folds, for the longitudinal load case it seems to benefit the girder to have smaller corrugation angle.

Different fold slenderness ratio, that is the ratio between the length of the loaded fold and the thickness of the web, for varying corrugation angle is examined and how it influences the patch loading resistance, the results are shown in Figure 17. It can be observed from the curves that the patch loading resistance is lowest when the load is applied at the longitudinal fold for small fold slenderness ratio but with increased fold slenderness ratio the longitudinal fold yields higher value than the intersection and inclined load cases. Notice that for the longitudinal load case, the highest corrugation angle leads to the highest slenderness ratio but vice versa for the inclined and intersection load cases. This is due to a change in the loaded fold from a_1 to a_2 for the inclined and intersection load cases and with an increased corrugation angle, the fold length of a_1 increases but the length a_2 decreases.

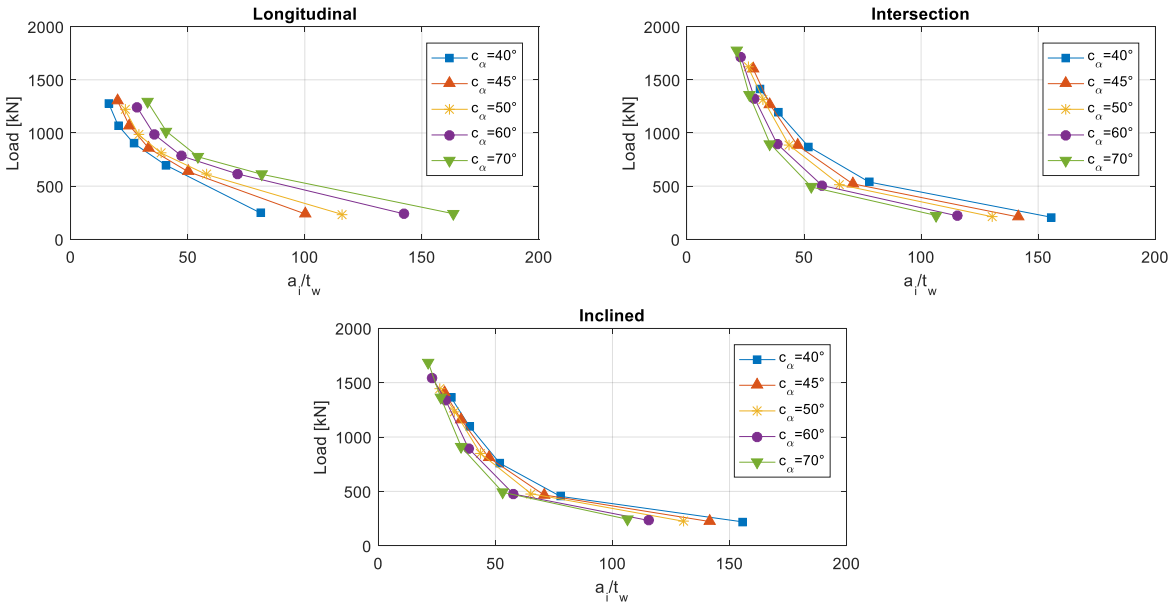

Figure 17. Influence of the fold slenderness ratio on the patch loading resistance for all three loading locations.

When comparing this figure to the figure Inaam and Upadhyay (2020) presented in their research the curves have the same trend. The patch loading resistance derived by Inaam and Upadhyay yields in a slightly higher value than in Figure 17. The reason for this is

that the reference girder used is not the same and there are more parameters influencing the patch loading resistance than the thickness of the web and the corrugation angle.

5.2 Thickness of the web and width of the flange

The effect of changing the width of the flanges on the patch loading resistance can be seen in Figure 18 for all load cases. For the longitudinal loading position, the patch loading resistance increases almost in linear proportion to increasing the flange width. It is interesting that for all three load cases the patch loading resistance is almost constant for thin webs of 2 mm. For the intersection and inclined load cases, the web thickness of 4 mm has also nearly constant behavior. These two also do not have as linear behavior as the longitudinal loading for thicker webs. The 10 mm web thickness for the inclined load location increases from flange width of 300 to 450 mm but for 500 mm it decreases. This indicates that the patch loading resistance is not necessarily enhanced with increasing the flange width if the loading position is on the inclined fold, although from these results it is enhanced with applying the load on the other two locations, that is the longitudinal fold and the intersection. According to this study the highest patch loading resistance is achieved by using the thickest web, hence increasing the thickness of the web enhances the patch loading resistance.

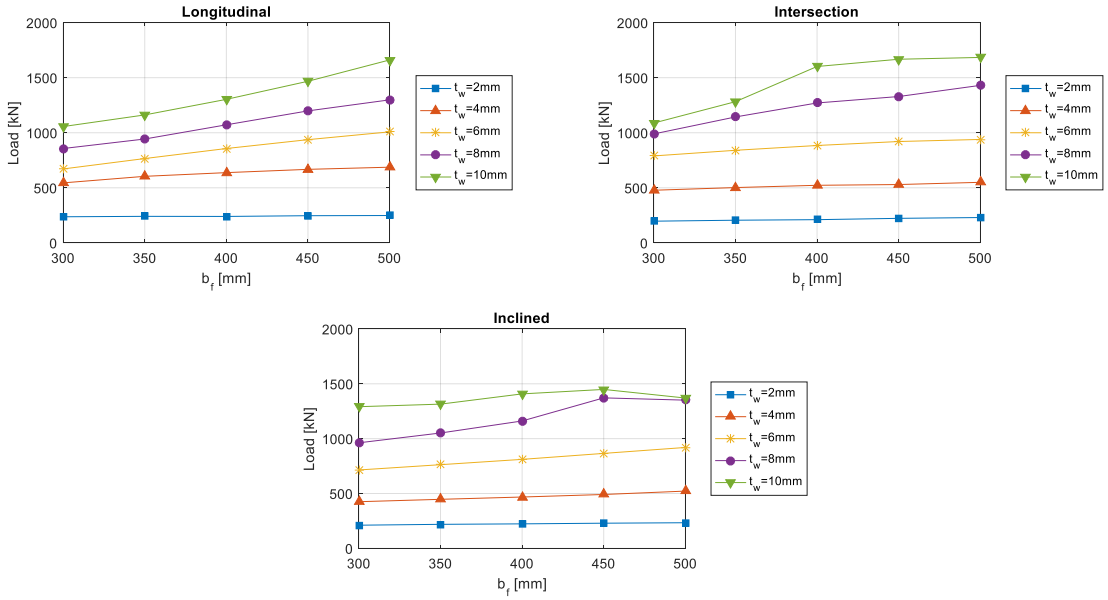

Figure 18. The influence of changing the flange width on the patch loading resistance with different web thickness.

Note that when the buckling shapes are examined for girders with applied load at the inclined fold with 8 mm web thickness and flange width of 400 and 450 mm it is observed that the buckling mode is shifting from a local patch buckling into flange torsional buckling, since the web has become thick enough to change buckling mode. This is the reason for the increase in patch loading resistance between these girders in Figure 18. The difference in failure mechanism for these two girders along with the load-displacement curves are shown in Figure 19, the top two figures are only presented to show the deformed shape of the flange so the scale of the contour can be ignored.

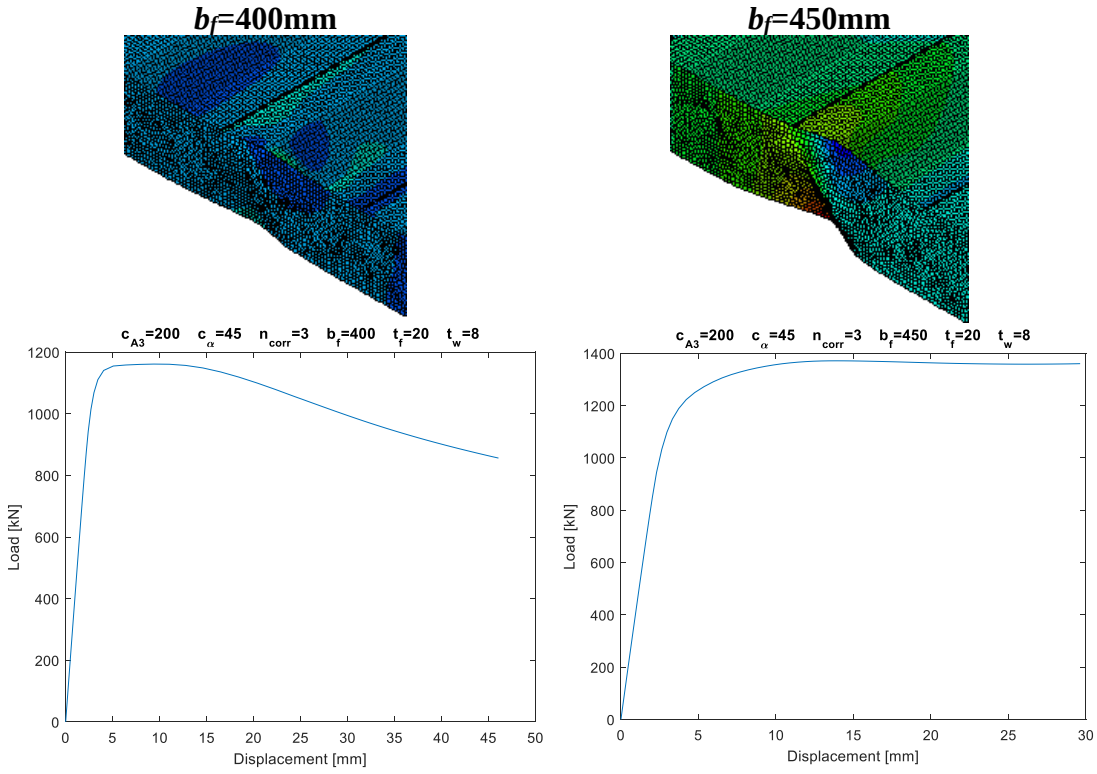

Figure 19. Failure mechanism and load-displacement curves for two girders loaded at the inclined fold.

When observing Figure 18 there is also a difference in behavior between the three load cases for girders with thick web. This difference in behavior is due to the girders not having the same failure mechanism for each load case like can be seen in Figure 20. The scale of the contour in Figure 20 is irrelevant. The buckling occurs in the flange for the inclined load case for girders with web thickness of 8 mm, a flange width of 450 and 500 mm and all girders with a web thickness of 10 mm. For the intersection load case this occurs for girders with web thickness of 10 mm and a flange width of 400 mm or larger. In the longitudinal load case the flange failure mechanism only occurs for the largest girder, that is a flange width of 500 mm and a web thickness of 10 mm.

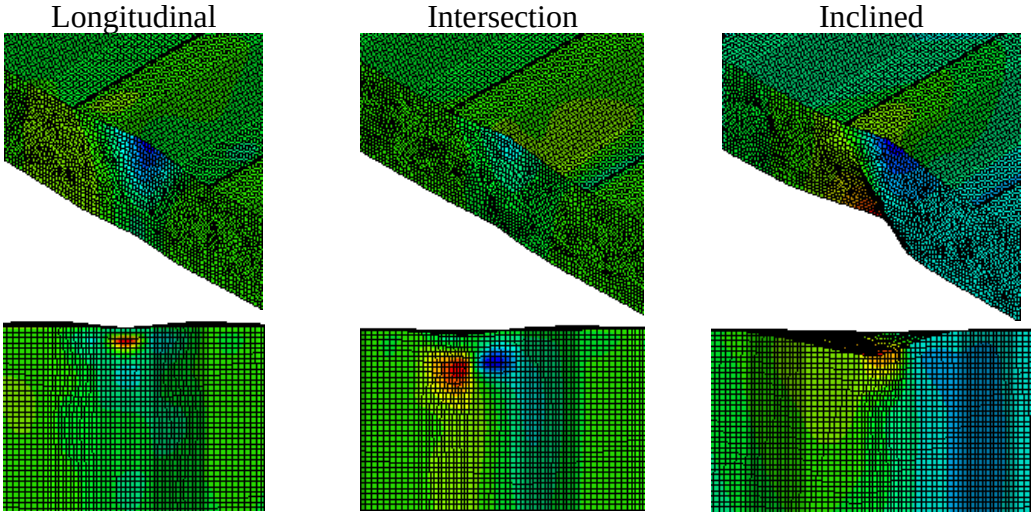

Figure 20. Different failure mechanism for each load case of girders with t_w=8 mm and b_f=450 mm.

The effect of changing the web thickness is again examined and can be seen in Figure 21. For the longitudinal loading position, the patch loading resistance increases almost linearly. It increases with faster rate for web thickness of 2 and 4 mm, which verifies the conclusion made in chapter 5.1 and that is that the web thickness has more influence on the patch loading resistance for thinner webs, although it still increases almost linearly for thicker webs. For the other two loading positions the patch loading resistance increases almost linearly from 2 to 6 mm and then it changes the slope. For the inclined loading position, the values of the patch loading resistance yield similar values for all flange widths and for web thickness of 2, 4 and 10 mm but varying for 6 and 8 mm. It is the same for the intersection besides for web thickness of 10 mm, then it is similar values for flange width of 400 to 500 mm, but yields lower patch loading resistance for flange width of 300 and 350 mm.

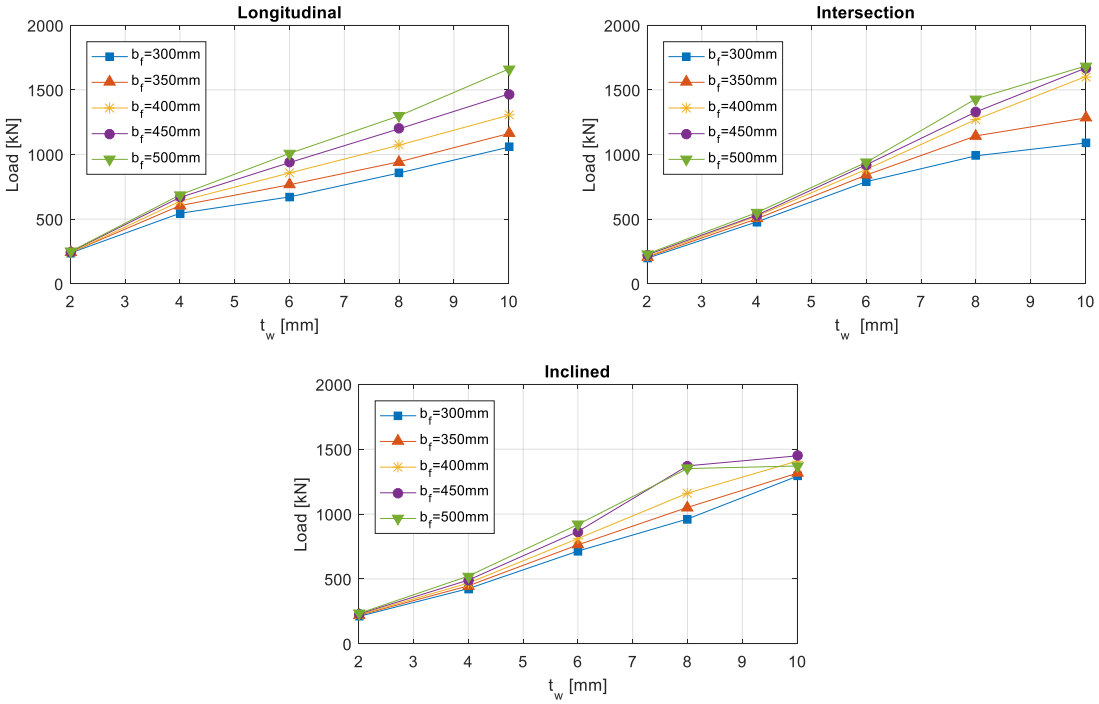

Figure 21. The influence on the patch loading resistance of varying the web thickness with different flange widths.

5.3 Thickness of the web and thickness of the flange

The effect of changing the thickness of the flange is shown in Figure 22 for all load cases. From the figure it can be concluded that patch loading resistance increases linearly with increased flange thickness although for small web thickness of 2 mm the patch loading resistance is less affected and shows nearly constant behavior. The trend for each load case is similar and it also appears that increasing the web thickness increases the slope of the curves. This means that increasing the web and flange thicknesses both enhances the patch loading resistance.

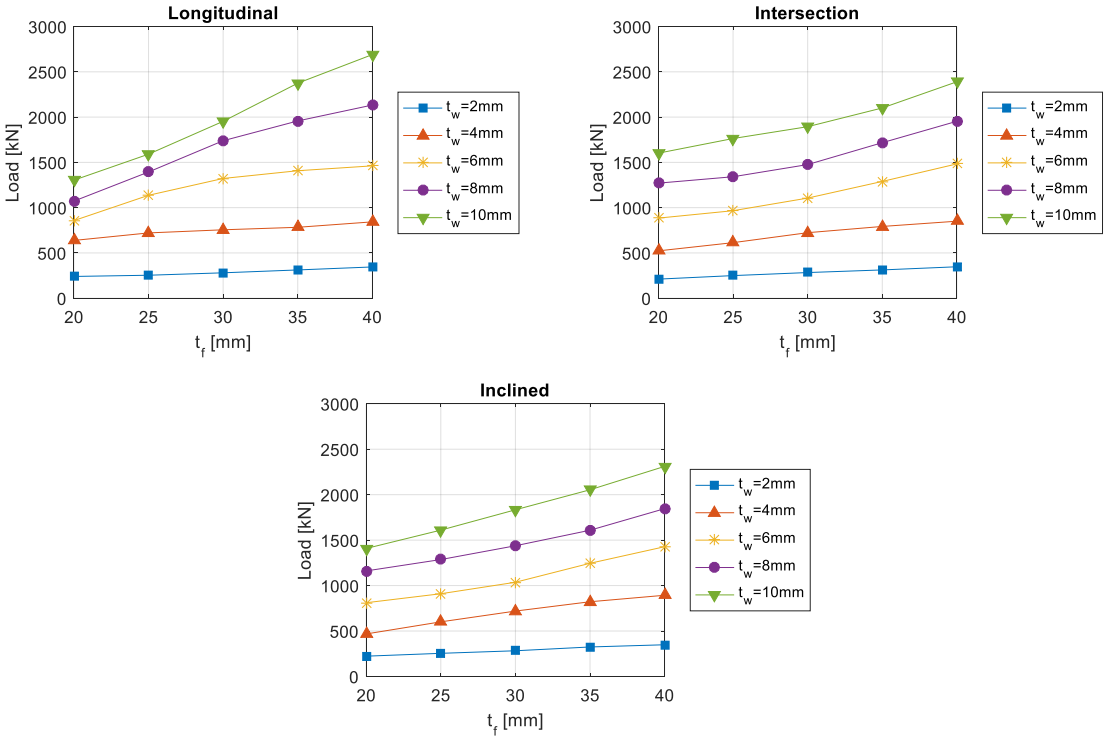

Figure 22. Effect on the patch loading resistance with varying flange thickness and different web thickness.

It is observed that the stockiness of the girder seems to be more beneficial when it is loaded on the longitudinal fold compared to the other two load cases. Since for the longitudinal load case, the girder with web thickness of 10 mm shows an increase in patch loading resistance of more than 1000 kN from flange thickness of 20 to 40 mm while for the other two load cases there is less increase in patch loading resistance.

The change in web thickness and its effect on the patch loading resistance for different flange thicknesses can be seen in Figure 23. For all three load cases the increase in resistance is almost linear, however the slope seems to change for thin webs of 2 to 4 mm. The patch loading resistance seems to be approximately the same for all flange thicknesses when the web thickness is 2 mm, although there is about 100 kN difference between the largest and smallest flange thickness. Increasing either the flange thickness or the web thickness increases the patch loading resistance, like was mentioned before. It can be observed that for the intersection and inclined load cases for a flange thickness of 20 mm that the slope is slightly reduced from 8 to 10 mm web thickness, this minor reduction in slope is due to a change to flange buckling for the 10 mm thick web. When the highest patch loading resistance for all three load cases is compared it is noticed that the longitudinal load case yields the highest resistance of 2690 kN while the

inclined and intersection are below 2500 kN. What is interesting is that the longitudinal fold has the highest resistance compared to the other two for the thickest flange but the lowest resistance for the thinnest flange. The results for the longitudinal loading case are more spread out than the other two.

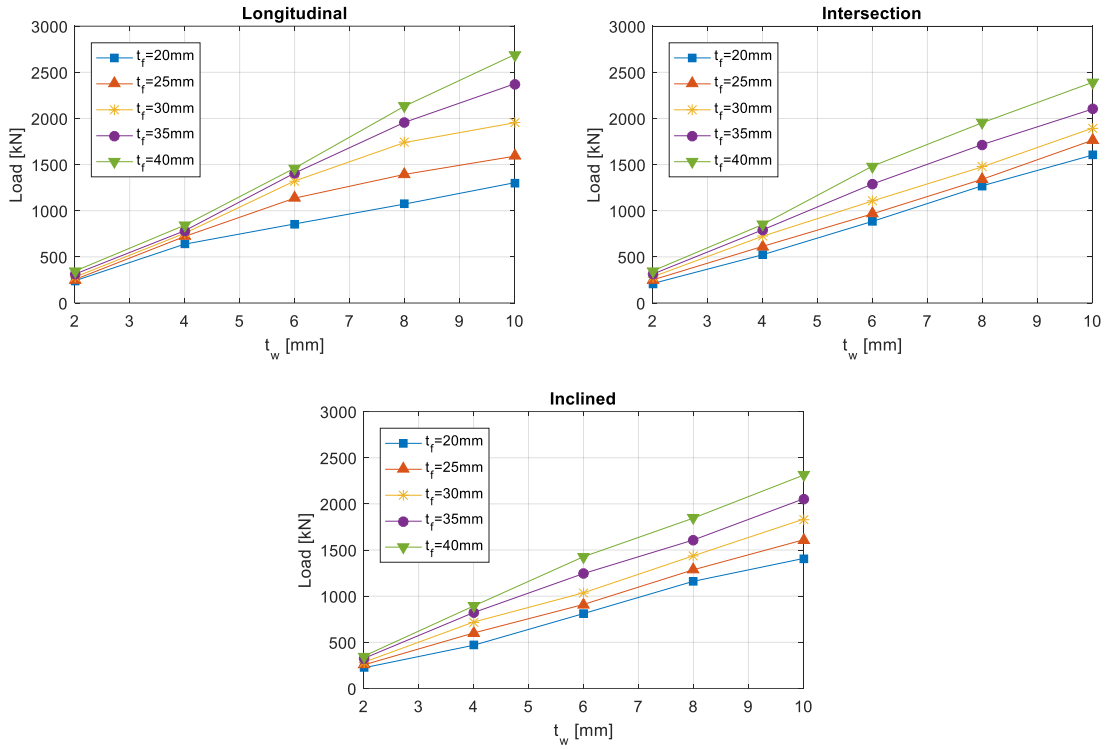

Figure 23. The influence on the patch loading resistance with varying web thickness and different flange thickness.

5.4 Thickness of the web and depth of the corrugation

For the depth of the corrugation, only two different values of the corrugation depth, a_3, fulfil the conditions described in chapter 4 for the reference girder, the results for varying web thickness and these two corrugation depths can be seen in Figure 24. The trend for all loading locations is that with increasing the web thickness the resistance increases. The results show that for both the longitudinal and intersection load case a corrugation depth of 200 mm yields higher patch loading resistance then the 150 mm but the other way around for the inclined load case. For the longitudinal load case the slope changes at a web thickness of 4 mm and has almost the same slope for web thickness of 4 to 10 mm. When the load is applied at the intersection the patch loading resistance increases almost with the same slope for all varying web thicknesses. The inclined load case has some abnormal behavior compared to the other two. Almost the same value is derived for both corrugation depths for web thickness of 2 to 6 mm but at 8 mm web thickness the girder with corrugation depth of 150 mm spikes to a value about 200 kN higher than the girder with corrugation depth of 200 mm.

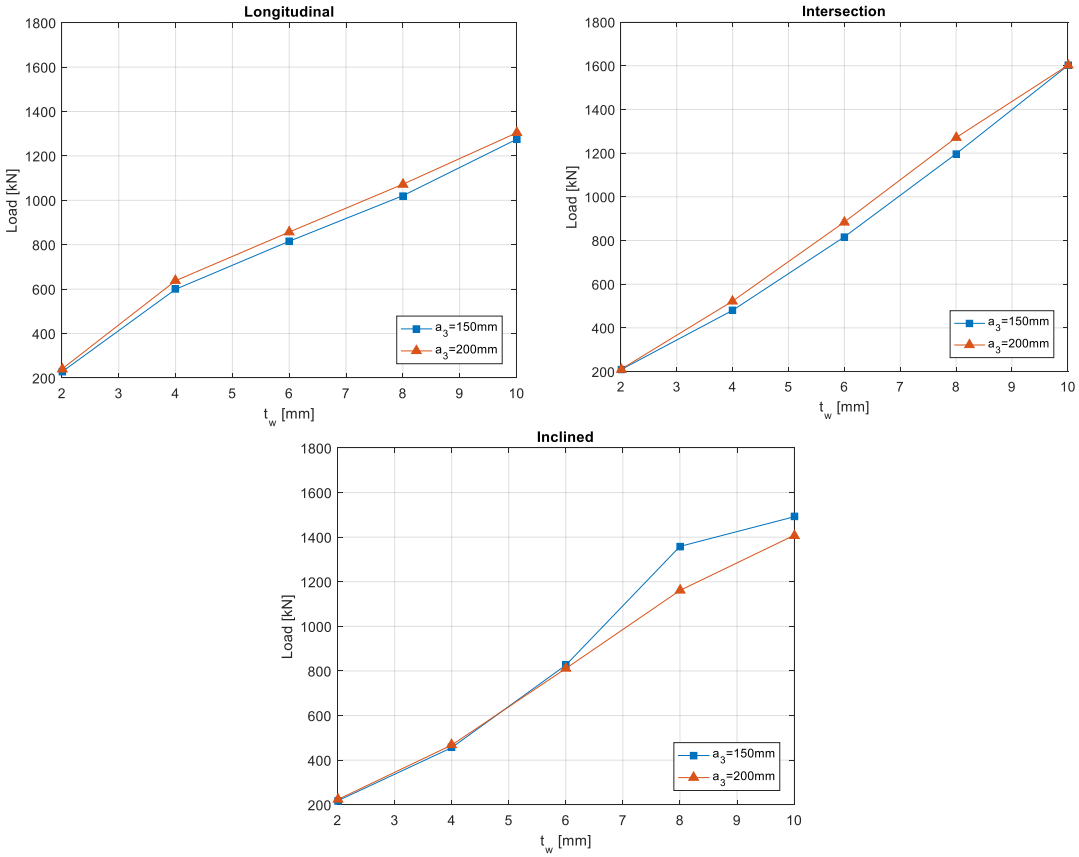

Figure 24. Influence on the patch loading resistance of varying the web thickness for different corrugation depths.

The reason for the abnormal behavior for the inclined load case with corrugation depth of 150 mm and web thickness of 8 mm is due to different buckling behavior compared to the corrugation depth of 200 mm like can be seen in Figure 25. In the figure, the scale of the contour is irrelevant. The larger corrugation depth seems to prevent the buckling mode to switch into flange buckling for the 8 mm web.

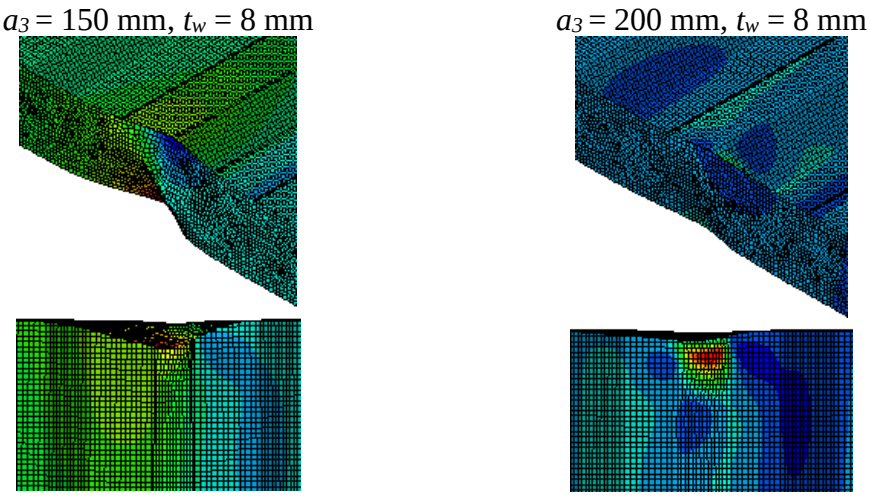

Figure 25. Difference in buckling modes for different corrugation depths and same web thickness, loaded at the inclined fold.

When comparing the different load cases for the girder with 8 mm web thickness and 150 mm corrugation depth, it can be observed that when this specific girder is loaded at the inclined fold the buckling mode is torsional flange buckling but local patch buckling for the other two load cases which can be seen in Figure 26. In the figure, the scale of the contour is irrelevant.

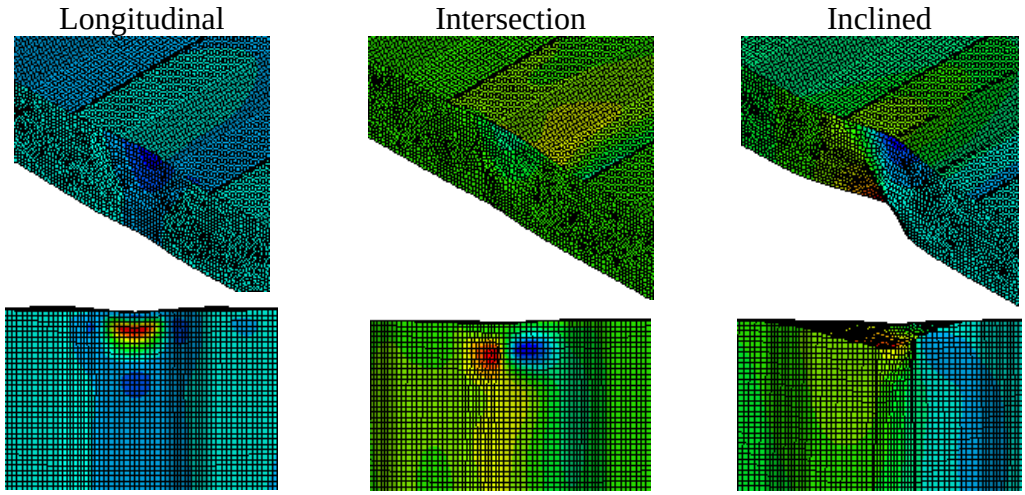

Figure 26. Different buckling modes for the same girder loaded in different positions, web thickness of 8 mm and corrugation depth of 150 mm.

Different fold slenderness ratio, that is the ratio between the length of the loaded fold and the thickness of the web, for varying corrugation depth is examined and how it influences the patch loading resistance, the results are shown in Figure 27. It can be observed from the curves that the patch loading resistance is lowest when the load is applied at the longitudinal fold for small fold slenderness ratio (<50) but with increased fold slenderness ratio the longitudinal fold yields higher value than the intersection and inclined loading locations, this is the same trend as was observed in Figure 17.

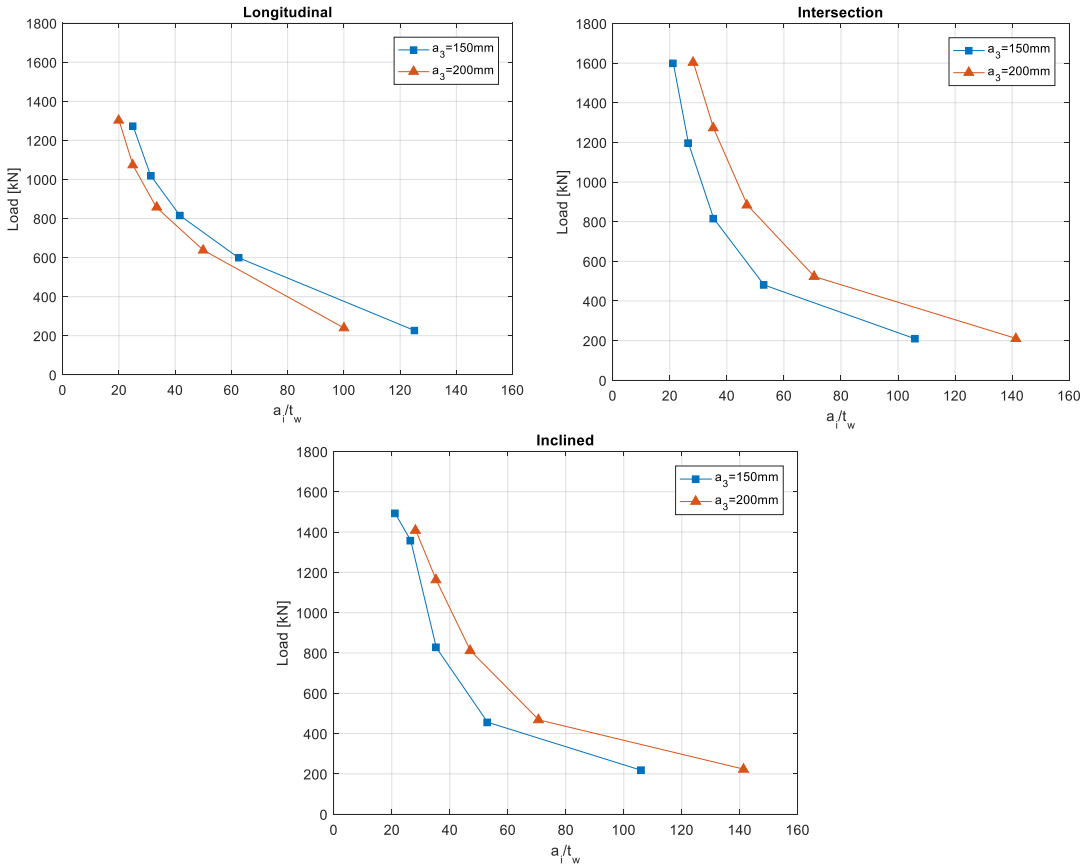

Figure 27. Influence of the fold slenderness ratio on the patch loading resistance for all three loading locations.

Since there are only two different depths of corrugation, the geometry of the reference girder is adjusted to a girder that gives more variations for the depth of the corrugation, see Table 16. The results for the new reference girder with varying the depth of the corrugation can be seen in Figure 28. From the results it is observed that increase in the corrugation depth can enhance and diminish the patch loading resistance of the girder. The trend for all three load cases is that for 4 mm web the resistance is enhanced with increased corrugation depth while for 8 mm web the resistance is diminished except for the intersection load case. The 6 mm web has different behavior depending on where the load is applied. For the longitudinal load location the resistance is almost constant, but for the other two load locations the resistance increases from 200 to 300 mm and then decreases when the depth is increased to 350 mm.

For the intersection load case the smallest corrugation depth shows local buckling mostly in the adjoining longitudinal fold, then with increased corrugation depth the failure is observed first in both folds and then mainly in the inclined fold. This explains the increasing and decreasing behavior for this load case. When girders are loaded at the inclined fold for the smallest corrugation depth and the thickest web, the girder fails in the flanges while in all other cases local patch buckling is observed. For small corrugation depth the failure is mostly seen in the two adjoining longitudinal folds and with increased depth the failure moves more into the inclined fold. The behavior is more linear when the girder is loaded at the longitudinal fold, this is due to the failure always occurring in the longitudinal fold. These results give an idea that the influence of the corrugation depth is very complex and is dependent on other parameters.

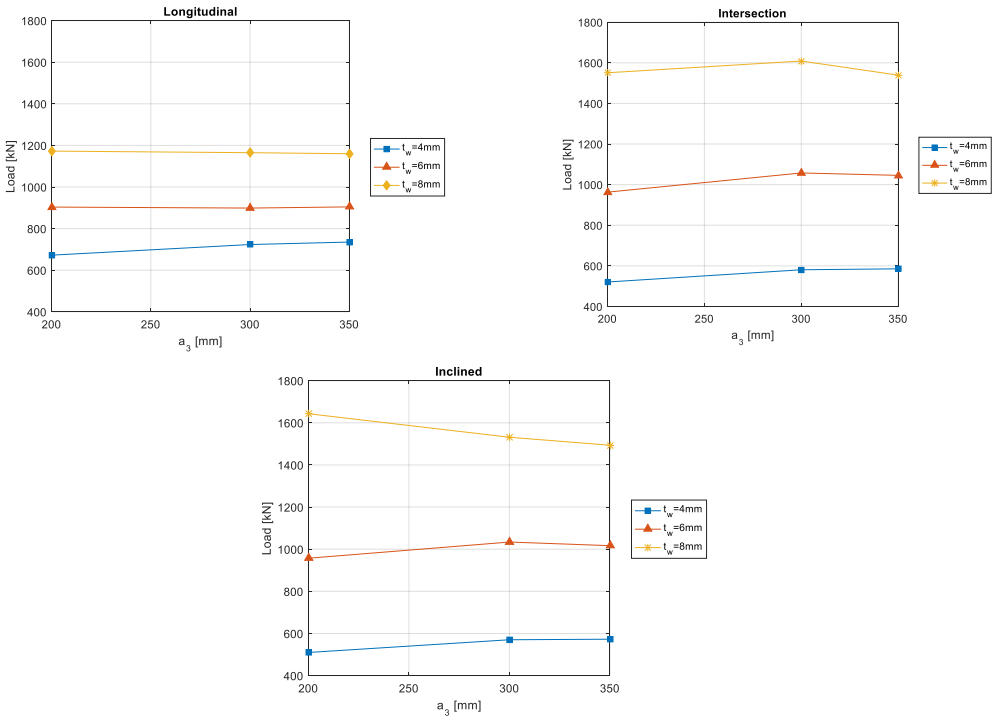

Figure 28. Influence on the patch loading resistance of varying the corrugation depth for different web thickness.

The results for varying the web thickness for the three corrugation depths considered is shown in Figure 29. The trend of all load cases is that with increase in web thickness the patch loading resistance increases.

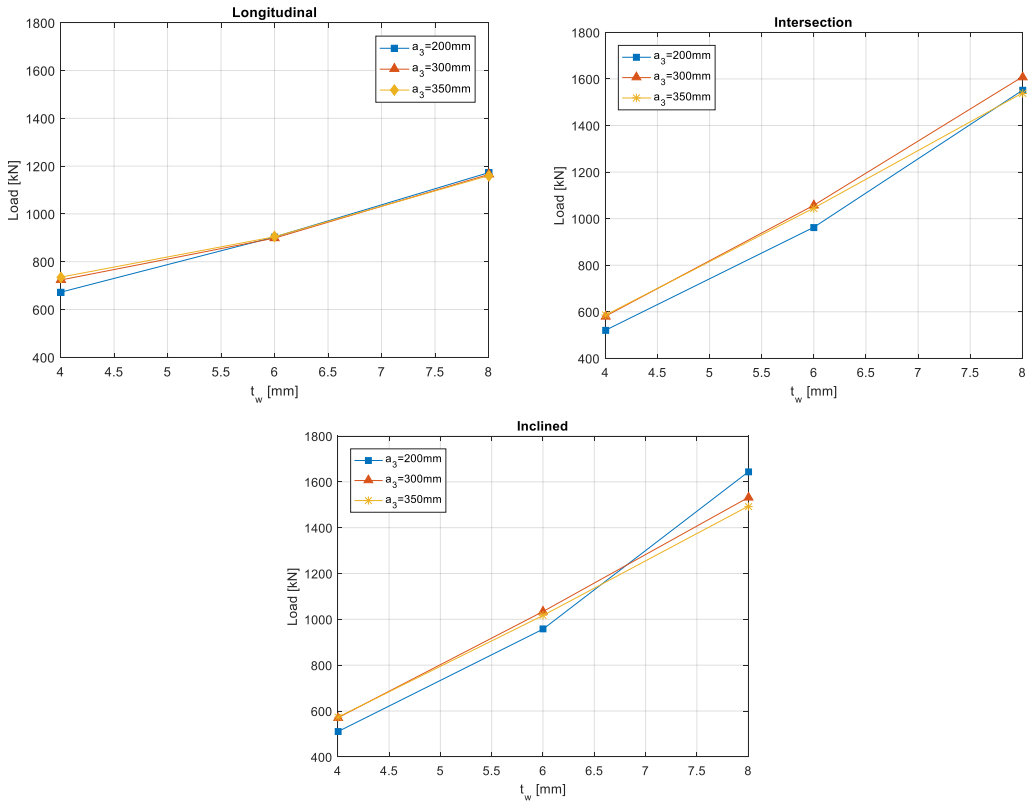

Figure 29. Influence on the patch loading resistance of varying the web thickness for different corrugation depths.

It is interesting to see that for the longitudinal load case the change in patch loading resistance is the smallest or around 500 kN for web thickness from 4 to 8 mm while for the other two it is around 1000 kN. When the load is applied at the longitudinal fold there are similar values derived at web thickness of 6 and 8 mm for all corrugation depth but for web thickness of 4 mm the corrugation depth of 200 mm yields lower value then the other two depths. It is observed that in the inclined load case corrugation depth of 300 and 350 has the same trend but corrugation depth of 200 mm has different behavior. Corrugation depth of 200 mm yields the lowest resistance for web thickness of both 4 and 6 mm but for 8 mm web thickness, it increases at a faster rate than the other two depths and yields the highest resistance. For web thickness of 8 mm the lowest resistance is for corrugation depth of 350 mm. For the intersection load case the smallest corrugation depth yields lower resistance than the other two for web thickness of 4 to 6 mm, and at a web thickness of 8 mm the corrugation depth of 200 to 350 mm is approximately the same. What is interesting to mention here is that for all load cases, the highest load capacity does neither follow the maximum or minimum corrugation depth for all web thicknesses, however the difference in patch loading resistance for the same web thickness and different corrugation depth is very minimal in all cases.

Varying fold slenderness ratios with different corrugation depths for the new reference girder are examined, see Figure 30. The patch loading resistance is lowest when the load is applied at the longitudinal fold for small fold slenderness ratio (<60) but with increased fold slenderness ratio the longitudinal fold yields higher resistance than the intersection and inclined loading locations, similar trend is observed in Figure 17 and 27.

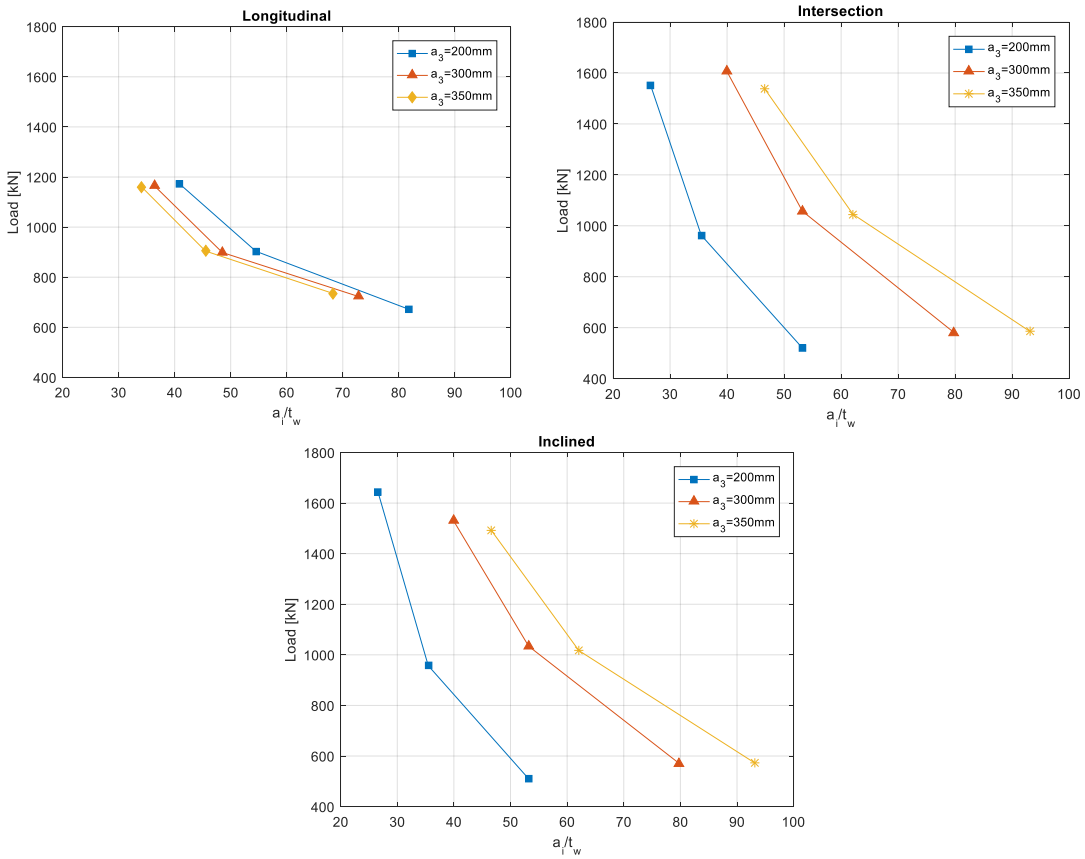

Figure 30. Influence of the fold slenderness ratio on the patch loading resistance for all three loading locations.

It is worth to note that since only three different patch loading resistances are calculated for each varying parameter, it is difficult to conclude anything for the effect of corrugation depth, however clear trends are observed. This subject could use further investigation.

5.5 Summary

The results show that the web thickness has a large influence on the patch loading resistance. Increasing the web thickness increases the patch loading resistance. This matches results from previous research for example research done by Luo and Edlund (1996), and Leiva-Aravena and Edlund (1987) which also showed that the load capacity increased 35-40% with increasing the web thickness from 2 to 2.5 mm. In the preliminary studies, the load capacity increases at a range of 80 to 200% with the average around 100% for increased web thickness from 2 to 4 mm. Proportionally, the preliminary studies show a slightly less increase in capacity compared to the previous researches.

When comparing Figure 23 to Figures 16, 21, 24 and 29 which all show the effect of changing the web thickness along with one other parameter, it seems that varying the flange thickness and web thickness yields more homogeneous results than the other three. This is due to only changing thicknesses in the model and no other geometrical parameters. These results would indicate that the flange thickness has the least complex influence on the patch loading resistance out of the four parameters studied.

The fold slenderness ratio was examined and it was observed that the patch loading resistance decreases with increase in fold slenderness ratios. This verifies the conclusion made by Kövesdi (2010) that the capacity decreases with high web and fold ratios.

The results for the corrugation angle show that for increased corrugation angle the patch loading resistance is close to constant or slightly decreasing for girders with thin webs. For girders with thicker webs the increase in corrugation angle shows that the patch loading resistance increases approximately linearly. Luo and Edlund (1996) and Kövesdi (2010) concluded that the patch loading resistance increases with increasing the corrugation angle. Luo and Edlund (1996) also noticed that when the corrugation angle was between 75 and 90 degrees patch loading resistance was almost equal.

The patch loading resistance increases slightly or is approximately constant with increased flange width for girders with thin web. Girders with thicker webs, that fail with local patch buckling, show linear increase in capacity with increased flange width. When the failure mechanism changes the patch loading resistance increases with less rate.

Varying the flange thickness shows linear increase in patch loading capacity with increased flange thickness and that the slope increases with increased web thickness. This matches the results from Luo and Edlund (1996) that increasing the flange thickness increases the patch loading resistance.

Increasing the corrugation depth shows no clear trend in either increase or decrease of the patch loading resistance, however for all loading positions it seems like there is a slight increase in the capacity for thin webs. The controlling factor on the patch loading resistance for the varied corrugation depth appears to be where, and how the girder fails. Too few variations of girders are analyzed to draw any clear conclusion.

When load is applied at the longitudinal fold, the patch loading resistance is in most cases lower than the resistance for the other load cases, however, the longitudinal load case has slightly higher resistance for girders with high flange-web thickness ratios. Loading of the inclined fold is more sensitive to changing buckling mode from local patch buckling compared to the other two load cases. According to Dahlén and Krona (1984), girders loaded at the inclined fold result in approximately 14% higher patch loading resistance than girders loaded at the longitudinal fold, this conclusion reflects results from some of the preliminary studies but does not seem universal. Since the preliminary studies show both higher and lower resistance for the inclined loading position, and when the resistance is higher it is not necessarily 14% higher, this conclusion is not valid when the parameters above are considered. Research done by Luo and Edlund (1996) also showed that higher capacity was achieved when the load was applied at the inclined fold which is not always the case in the FE-analysis.

6 Extensive parametric study results and discussion

In this chapter the results are presented from the extensive parametric study based on a large number of FE analyses performed using the parallel processing cluster computational tools for all three load cases. The chapter is divided after the loading locations and comparison between them. For each loading location a girder with the optimal load-to-weight ratio is presented for cost efficiency, since stainless steel is more expensive than carbonated steel. In addition, trends for the top 10% most optimal girders with respect to weight are discussed. The patch loading resistance from the three different loading locations are compared to each other. The results are discussed in each subchapter and summarized at the end. In this chapter, the results are often presented with respect to iteration, an algorithmic flow chart is presented in Appendix B.3 to better explain how the iterations are connected to different geometrical parameters.

6.1 Longitudinal fold

The results from the parametric study for the longitudinal load case are shown in Figure 31. The figure shows the patch loading resistance for all 603 girders, each iteration represents one girder from the FE-analysis. The patch loading resistance increases with increasing the geometrical parameters, so the stockiest girder yields the highest patch loading resistance and the thinnest girders give the lowest value.

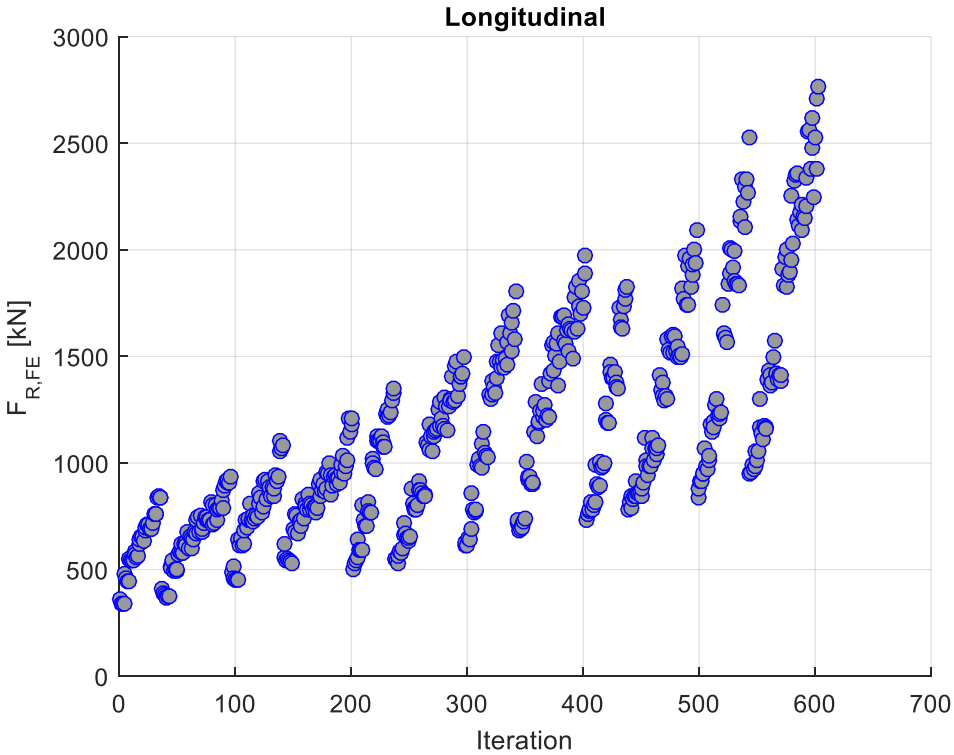

Figure 31. Patch loading resistance for each girder examined for the longitudinal load case.

If the effect on the patch loading resistance by changing different geometric parameters is examined, see Figure 32, the following conclusions are observed:

- With increased web thickness the patch loading resistance increases, which means that thicker webs give higher resistance.
- With increased width of the flanges the patch loading resistance increases slightly.

- With increased flange thickness the patch loading resistance increases.
- With increased number of unit cells, the patch loading resistance increases.
- Changing the corrugation angle is not as clear as the other parameters therefore it is difficult to conclude if it is beneficial to have small or large angle. The main trend is that larger angles yield higher patch loading resistance but with a more complex behavior and is dependent on other parameters.
- With increasing the corrugation depth, the patch loading resistance increases for most girders.

These observations correlate to the results from the preliminary studies in chapter 5 where some of these parameters are also considered.

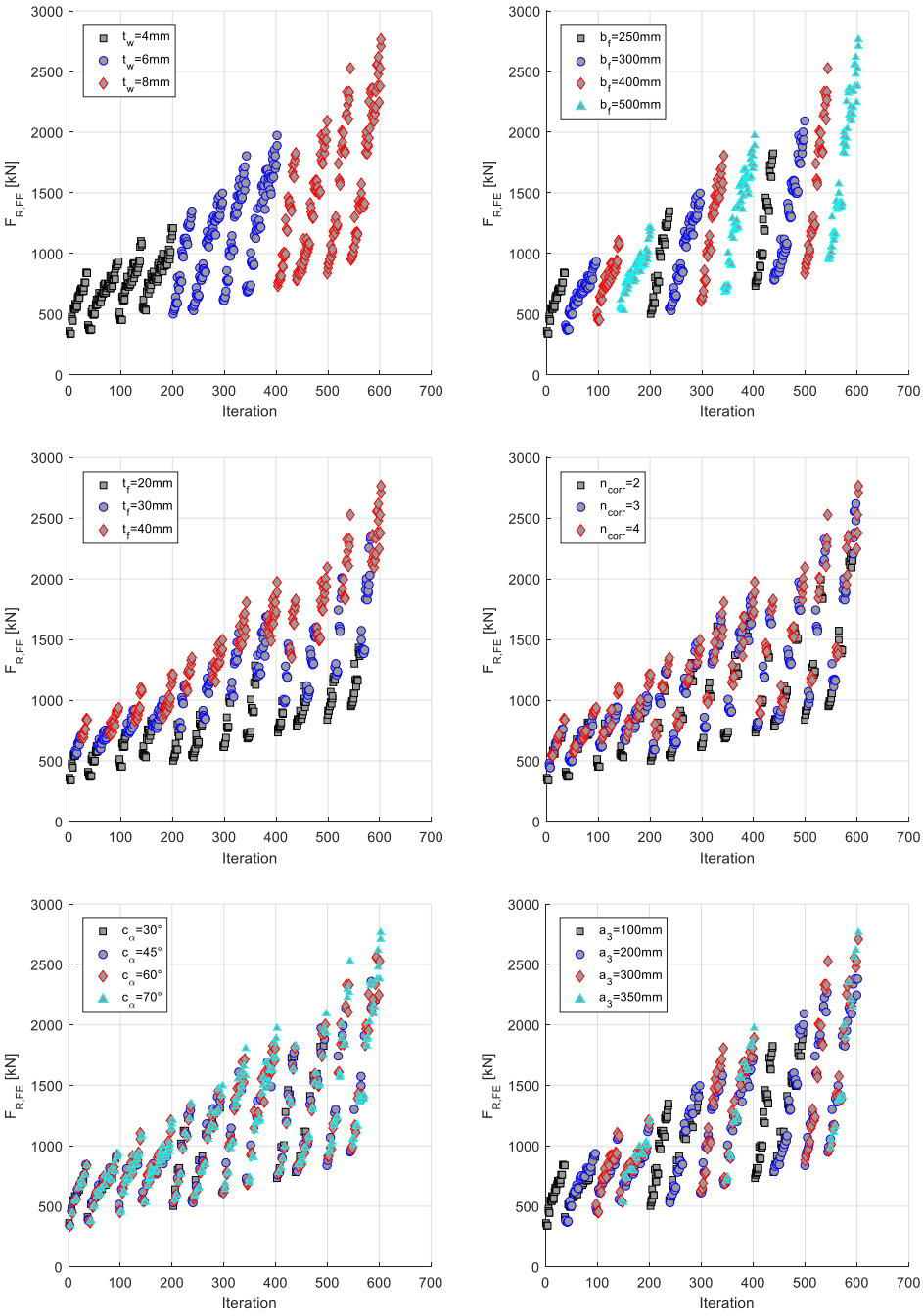

Figure 32. The patch loading resistance of a girder loaded at the longitudinal fold with respect to different geometrical parameters.

The ratio between the patch loading resistance and the weight of each girder is examined, see Figure 33, to find the optimal girders with respect to weight. This is done to see which girder has the most optimal resistance and material usage to minimize environmental and financial aspect. The figure shows that the girder with the highest patch loading resistance from Figure 31 is not the most optimized girder in terms of resistance and weight.

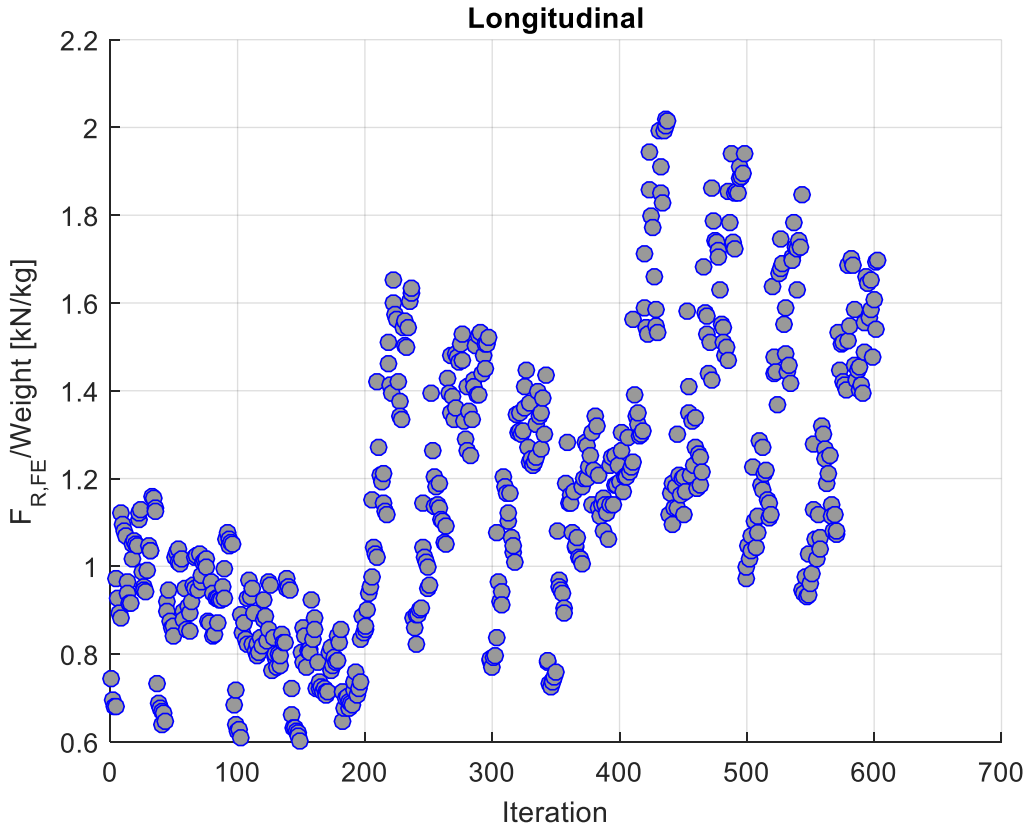

Figure 33. Ratio between patch loading resistance and weight of each girder for the longitudinal load case.

How changing different geometrical parameters affects the ratio between the patch loading resistance and the weight is presented in Figure 34, the following observations are deduced:

- With increased web thickness the ratio increases, which means that stockier webs give higher ratio between resistance and weight.
- With increased width of the flanges the ratio decreases. Wider flanges yield lower ratio this suggests that the increased weight from widening the flanges does not increase the patch loading capacity greatly.
- The trend of changing the flange thickness is not as clear but the main trend is that with increasing the thickness the ratio increases.
- With increased number of unit cells, the ratio increases.
- Changing the corrugation angle is not as clear as the other parameters therefore it is difficult to draw conclusions from this graph if the angle should be small or large for the optimized girder it seems to be highly influenced of the other geometrical parameters.
- With increasing the corrugation depth the ratio decreases, so the optimized girder has the smallest corrugation depth, this is directly related to the flange width.

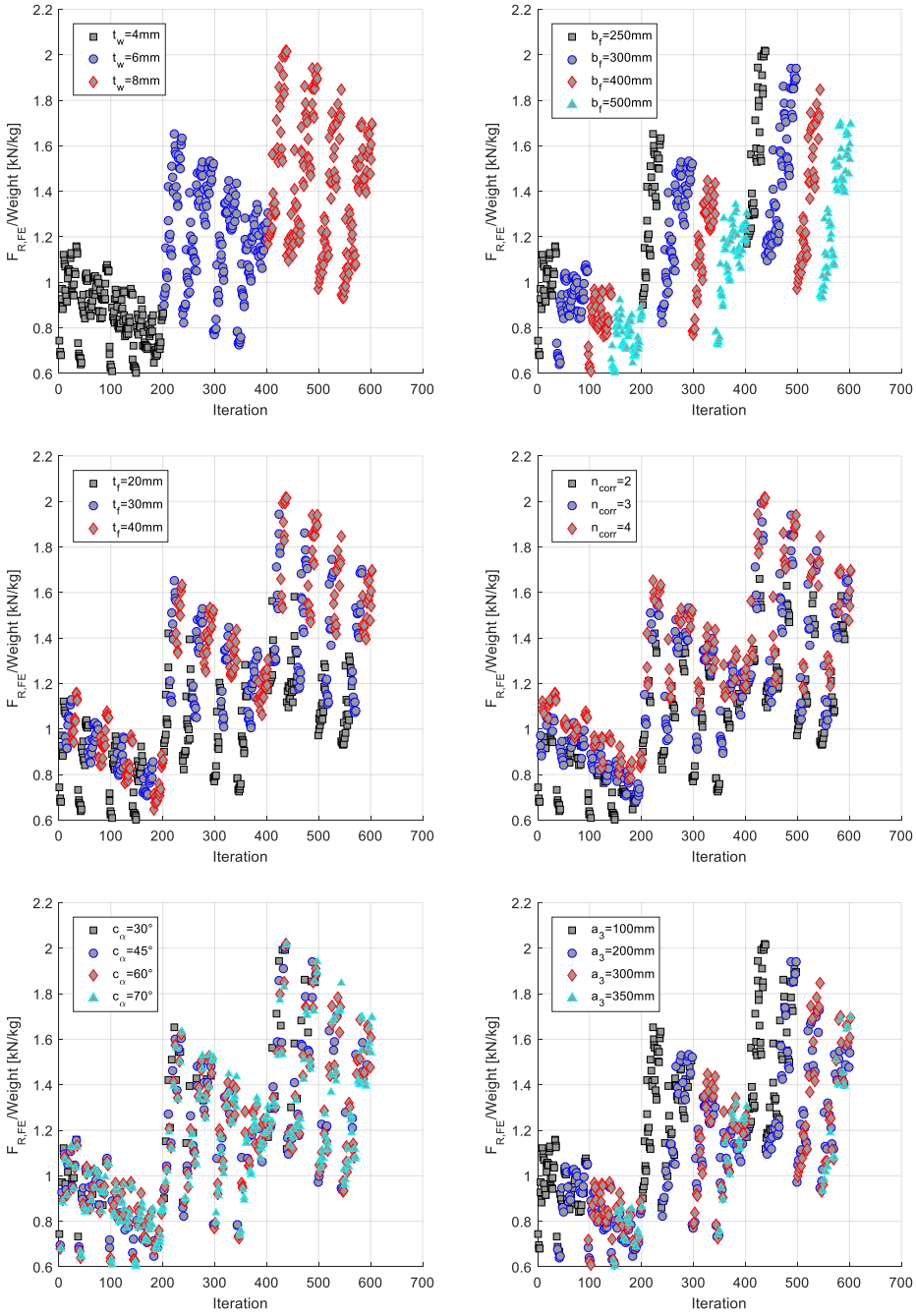

Figure 34. The effect of each varying parameter in the FE-analysis on the ratio between patch loading resistance and weight of the girder.

The top 10% most optimal girders with respect to resistance and weight have a few things in common. Most of the girders have a web thickness of 8 mm while some also have 6 mm web thickness, this suggests that thicker webs are more optimal. The girders have all different types of flange widths, however the narrowest flange of 250 mm is seen most often in the top 10% while the widest flange of 500 mm is seen the least, thus narrow flanges appear to be more optimal. A vast majority of the girders in the top 10% have a flange thickness of 40 or 30 mm, only a few have 20 mm, therefore thick flanges are more optimal. Most of the girders have either three or four number of unit cells for

the top 10% most optimal girders, only a few girders have two unit cells. Neither the corrugation angle nor the corrugation depth has a drastic influence for the most optimal girders.

The girder that has the optimized ratio between the resistance and the weight has the geometrical parameters presented in Table 18. The girder has the largest value for the corrugation angle, web – and flange thickness but the smallest value for the width of the flanges and the depth of the corrugation. Fewer number of unit cells are expected for the optimized girder, since those girders are lighter, here a number of unit cells equal to three is the most optimal. This result for the number of unit cells is not surprising since the longitudinal load case is sensitive to flange deformations and a higher number of unit cells helps to reduce flange deformations.

Table 18. Geometrical parameter of the girder with optimized load to weight ratio for the longitudinal load case.

Variable	Value
Thickness of web, t_w	8 mm
Width of flanges, b_f	250 mm
Thickness of flanges, t_f	40 mm
Corrugation angle, α	70°
Depth of the corrugation, a_3	100 mm
Number of unit cells, n_{corr}	3

6.2 Inclined fold

The results from the parametric study for when the load is applied at the inclined fold are shown in Figure 35. When the figure is compared to Figure 31 it is observed that there is not as clear division in this one, but the trend is the same that is with higher geometrical values the patch loading resistance increases. The stockiest girders result in the highest patch loading resistance and the least stocky girders have the lowest resistance. The effect of changing each parameter has the same trend as for the longitudinal load case but the figure for the inclined fold is found in Appendix B.2.1.

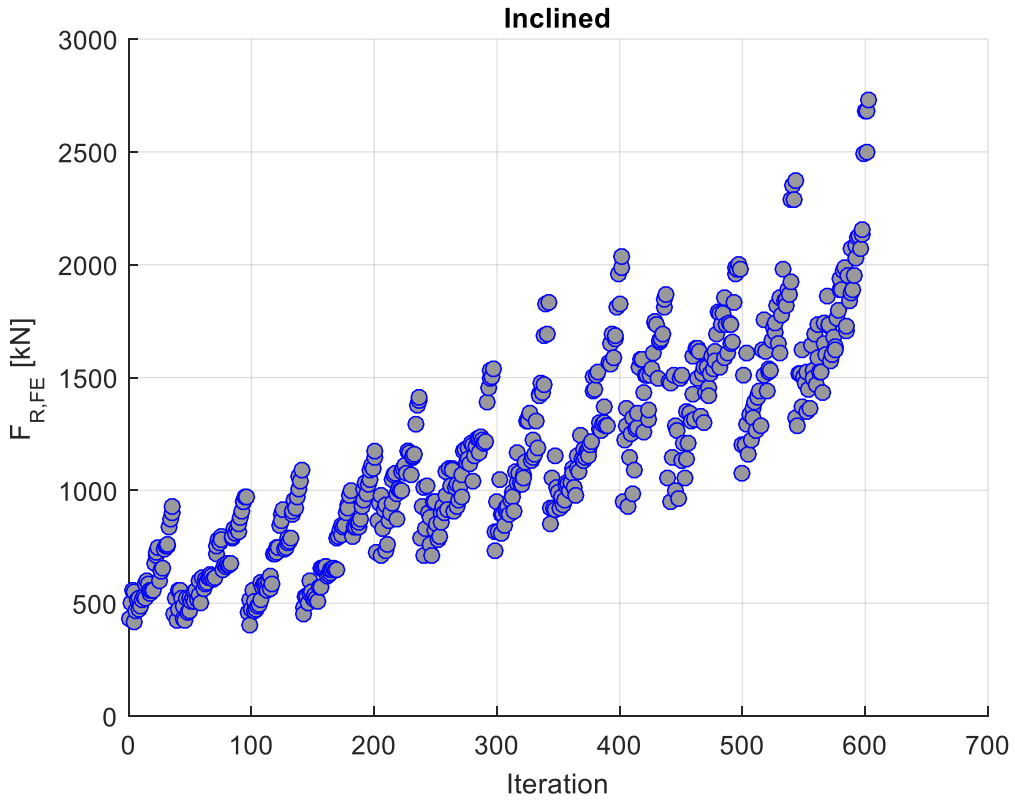

Figure 35. The patch loading resistance for each girder examined for the inclined load case.

The results from the parametric study for the ratio between the patch loading resistance and the weight when the load is applied at the inclined fold is shown in Figure 36. It has similar trends as Figure 33. The effect of changing each parameter has similar trends as in Figure 34 for the longitudinal load case but the figure for the inclined load case is found in Appendix B.2.2. A slight difference is observed when comparing the two load cases, for the inclined load case, increasing either the flange thickness or the number of unit cells does not universally increase the patch loading resistance.

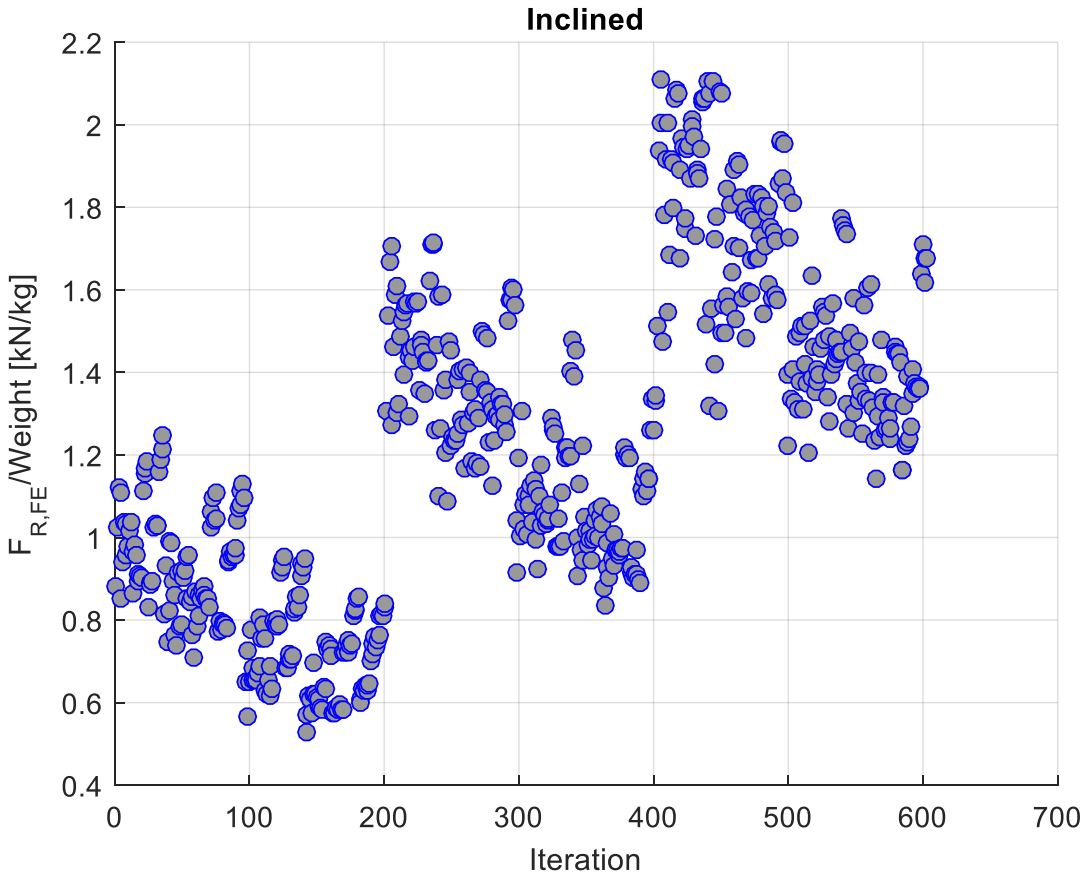

Figure 36. The ratio between patch loading resistance and weight of each girder for the inclined load case.

For the top 10% most optimal girders with respect to resistance and weight for the inclined load cas#e, not much differs from the longitudinal load case, however there are some differences. For the longitudinal load case, thick flanges are deemed optimal, for the inclined load case there is no distinct difference observed for thin or thick flanges. The number of unit cells for the longitudinal load case are optimal at either 3 or 4 unit cells, for the inclined load case, 2 unit cells are also observed in the top 10% most optimal girders. These observations can be visualized by comparing Figure 34 to the figure in Appendix B.2.2.

The girder that has the highest load to weight ratio for the inclined load case has the geometrical parameters presented in Table 19.

Table 19. Geometrical parameter of the girder with optimized load to weight ratio for the inclined load case.

Variable	Value
Thickness of web, t_w	8 mm
Width of flanges, b_f	250 mm
Thickness of flanges, t_f	20 mm
Corrugation angle, α	70°
Depth of the corrugation, a_3	100 mm
Number of unit cells, n_{corr}	2

The optimized girder has the highest value for corrugation angle, the thickness of the web but the lowest value for the number of unit cells, the depth of the corrugation, thickness of the flange and width of the flange.

6.3 Intersection

The results from the parametric study for the intersection load case are shown in Figure 37. Similar trends are observed for this load case and the other two load cases. The intersection load case correlates better to the inclined load case, but some similarities are seen when comparing this load case to the longitudinal load case as well. For the intersection load case, the load is applied at both the inclined fold and the longitudinal fold, so seeing a combination of trends for the other two load cases is not surprising.

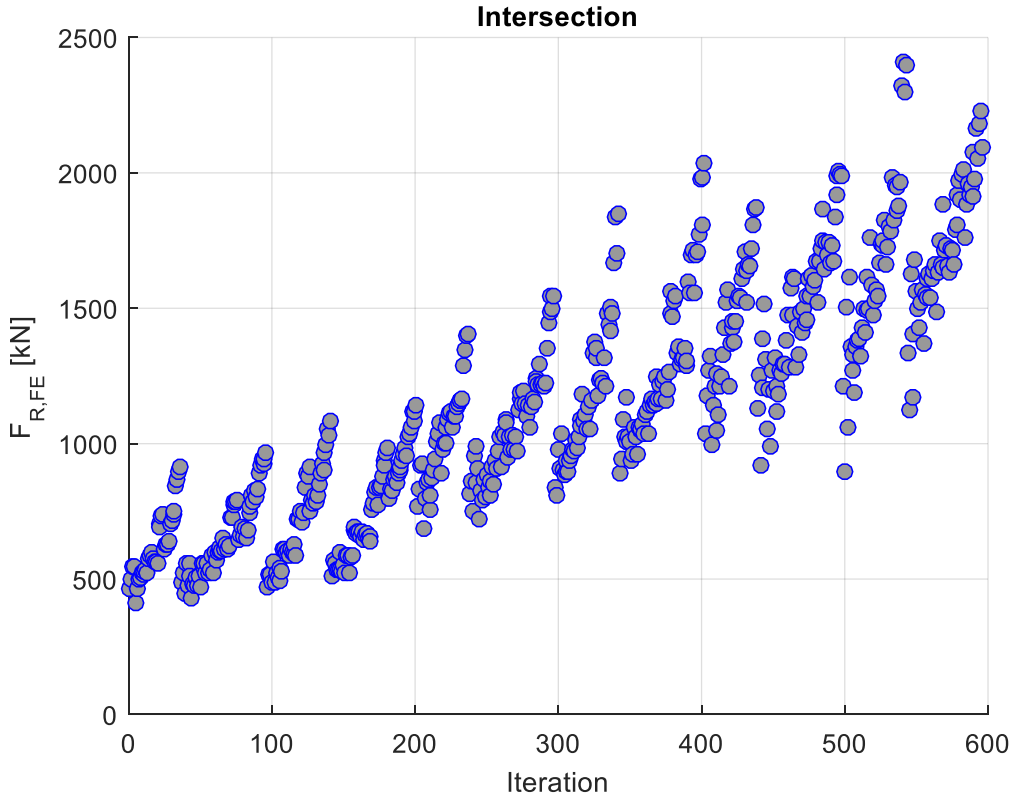

Figure 37. The patch loading resistance for each girder examined for the intersection load case.

The results from the parametric study for the ratio between the patch loading resistance and the weight when the load is applied at the intersection are shown in Figure 38. It has similar behavior as the other two load cases, see Figures 33 and 36. The effect of changing each parameter has similar trends for most parameters as in Figure 34 for the longitudinal load case, the figure for the intersection can be found in Appendix B.1.1. Similar behavior is detected for the intersection load case as the inclined load case, that is, increasing the flange thickness or the number of unit cells does not necessarily increase the patch loading resistance like is observed for the longitudinal case.

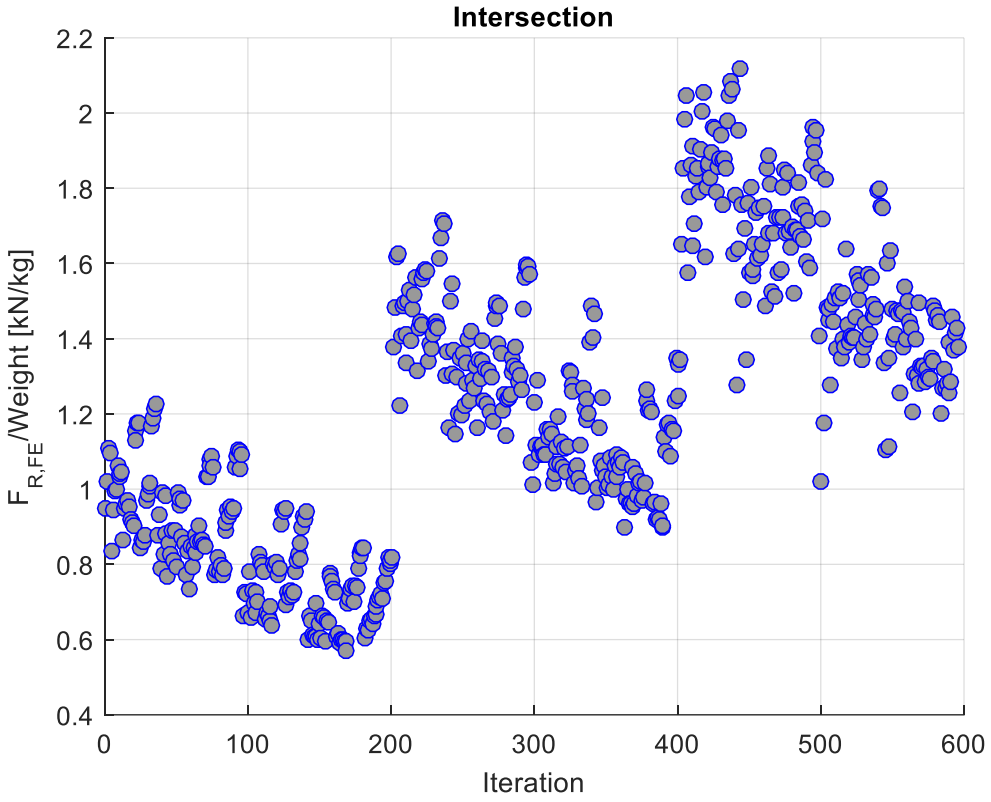

Figure 38. The ratio between patch loading resistance and weight of each girder for the intersection load case.

When analyzing the top 10% optimal girders with respect to resistance and weight loaded at the intersection, the parametrical trends appear very similar to the parametrical trends for the inclined load case. How each parameter effects the top 10% optimized girders loaded at the intersection can be visualized in the figures presented in Appendix B.1.2.

The girder with the highest ratio between the patch loading resistance and weight for the intersection load case has the geometrical parameters presented in Table 20. It is a girder with the highest value for corrugation angle and the thickness of the web, but the lowest value for the number of unit cells, the depth of the corrugation and the thickness of the flange, the width of flanges is 300 mm. It is worth to note that this girder is almost identical to the most optimal girder for the inclined load case, only the width of flanges is slightly wider.

Table 20. Geometrical parameter of the girder with optimized load to weight ratio for the intersection load case.

Variable	Value
Thickness of web, t_w	8 mm
Width of flanges, b_f	300 mm
Thickness of flanges, t_f	20 mm
Corrugation angle, α	70°
Depth of the corrugation, a_3	100 mm
Number of unit cells, n_{corr}	2

6.4 Comparison of the patch loading resistance between each load case

Here the patch loading resistance from the three load cases are compared to each other. First the resistance from when the load is applied at the longitudinal fold is compared to both when the load is applied at the inclined fold and the intersection, see Figure 39. In the figure the girders are split into two groups, the first group are girders with the ratio between the thickness of the flange and web lower than four, marked with blue in the scatter. The others have ratio equal or larger than four. The reason for the two groups is that each parameter was examined to see if there is any clear trend for girders that have higher resistance for the inclined and intersection load cases and girders that have higher resistance for the longitudinal load case. The thickness ratio is the combination of parameters that show the clearest trend for the difference in the figure. The main trend is that the girders with thickness ratio lower than 4 have higher resistance for the inclined and intersection load cases.

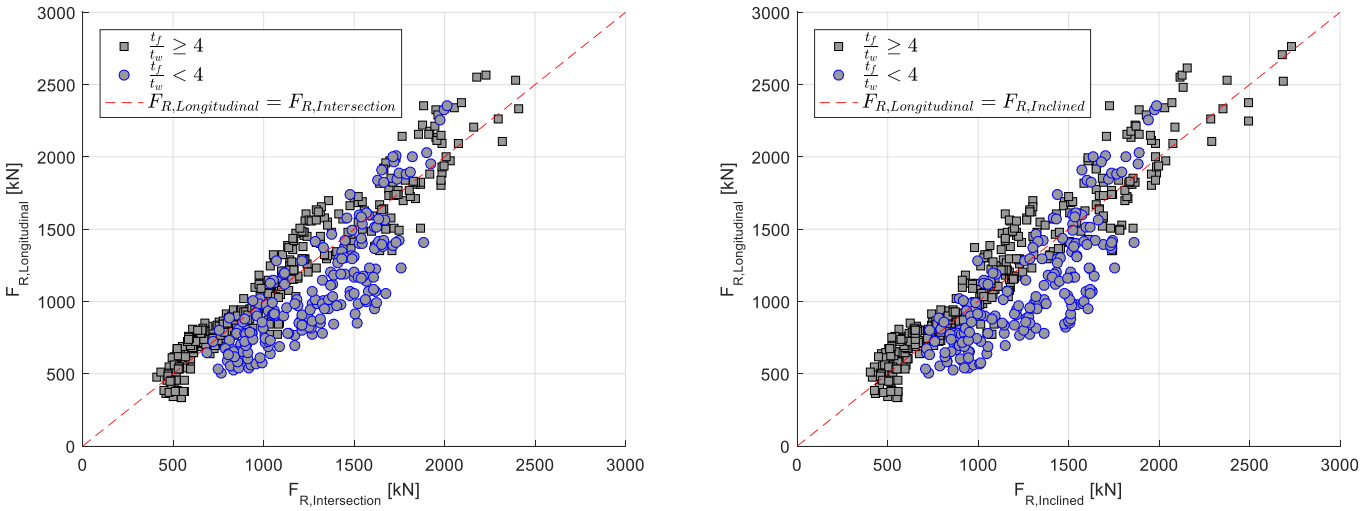

Figure 39. Comparison between the resistance of the longitudinal load case and the other two load cases.

The girders that yield 10% higher resistance for the longitudinal load case compared to the other two load cases all have a large flange thickness of 40 mm, large web thickness of 8 mm, wide flange width of 400 to 500 mm, number of unit cells around 2 to 3, all variation of the corrugation angle is present and corrugation depth of 200 to 350 mm is seen. This shows that for the longitudinal load case it is beneficial to have the thickness ratio higher than four and wide flanges.

The girders that yield 10% higher resistance for the inclined and intersection load cases compared to the longitudinal load case have a small flange thickness of 20 mm although in some cases 30 mm, large web thickness of 8 mm, all variations of the flange width, the number of unit cells is 2 but few girders have 3, all variation of the corrugation angle is present and corrugation depth of 100 to 350 mm is seen. This means that for the inclined and intersection load cases it is beneficial to have thickness ratio less than four but unlike before the flange is not as influential.

When the effect of flange width is further investigated when comparing the load cases, it is observed that larger flange widths are beneficial for the longitudinal load case and the patch loading resistance is closer to the two other load cases for larger flange widths.

The resistance from when the load is applied at the inclined fold is compared to when the load is applied at the intersection, see Figure 40. The resistance from both load cases correlate well to each other. When the girders that give 10% higher resistance for the inclined fold are examined and compared to the girders that have 10% higher resistance for the intersection then there is no clear trend in the parameters except for the web thickness. When the inclined load case gives 10% higher resistance then the web thickness is 8 mm but when the intersection is 10% higher the web thickness is always 4 or 6 mm.

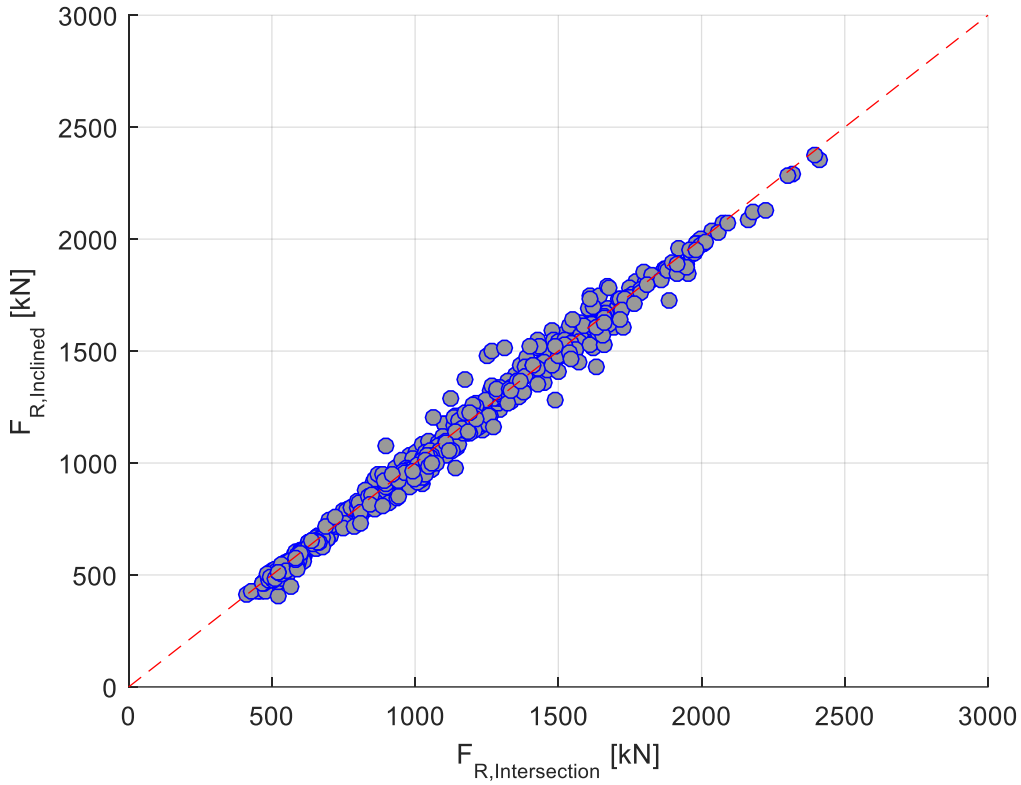

Figure 40. Comparison between the resistance from the inclined and the intersection load case.

6.5 Summary for the parametric study

Increasing the web thickness, flange thickness, flange width or number of unit cells increases the patch loading resistance for all load cases. Increasing corrugation angle and corrugation depth does not show increase in patch loading resistance in a clear way so these two parameters have more complex effect on the resistance and are dependent on other parameters.

When the optimized girders for all three load cases are compared, see Table 21, it is noted that for all three cases the optimized girder has the same thickness of the web, corrugation angle and corrugation depth. The width of the flanges is different for the intersection, but only 50 mm difference. The number of unit cells is highest for the longitudinal load case, that could be explained due to the fact that when the load is applied at the longitudinal fold it redistributes the load through the flanges over a shorter distance to the inclined folds since the length of the longitudinal fold is smaller. Out of the three optimized girders the highest ratio between patch loading resistance and weight is derived for the girder loaded at the intersection although the inclined load case yields similar value. The girder loaded at the longitudinal fold has the highest patch loading resistance but the stockiest girder and therefore yields in the lowest ratio.

Table 21. The optimized girder for each load case with respect to resistance and weight.

	Longitudinal	**Inclined**	**Intersection**
Thickness of web, t_w	8 mm	8 mm	8 mm
Width of flanges, b_f	250 mm	250 mm	300 mm
Thickness of flanges, t_f	40 mm	20 mm	20 mm
Corrugation angle, α	70°	70°	70°
Depth of the corrugation, a_3	100 mm	100 mm	100 mm
Number of unit cells, n_{corr}	3	2	2
Ratio between resistance and weight, F_R/W	2.02 kN/kg	2.11 kN/kg	2.12 kN/kg
Patch loading resistance, F_R	1632.1 kN	1363.4 kN	1515.3 kN
Total weight, W	895.9 kg	646.6 kg	716.0 kg

When the patch loading resistance from the three different load cases are compared to each other it is observed that the inclined and intersection load cases correlate well to each other. The longitudinal load case is different from the other two and a trend is observed in the patch loading resistance and that is that the ratio between the thickness of the flange and web influences if the longitudinal load case differs from the other two. If the ratio is equal or larger than four, the resistance of the girders yields higher resistance for the longitudinal load case compared to the other two load cases, but lower resistance when the ratio is less than 4 for most girders. Increase in flange width appears to cause increase in patch loading capacity for some girders loaded at the longitudinal fold.

7 Existing design models

Here the results from the FE-analysis are compared to four existing design models and the design model for corrugated webs from the newest draft of the Eurocode 3. The design models considered are from a wide range of years and the oldest one is from 1996.

7.1 Design model by Luo and Edlund (1996)

When the parametric study results are compared to the design model by Luo and Edlund (1996) it is clear that the model is on the unsafe side compared to the FE results, only a few models fall on the conservative side. The comparison for the longitudinal load case is shown in Figure 41, the figures for the other two load cases are presented in Appendix C.1. In the figure the 45 degree line represents when the patch loading resistance from the FE-analysis and the design model are equal, the red dashed line represents the mean value of both. Some abnormal behavior is observed where in three places, different girders from the parametric study yield the same patch loading resistance in the design model. This occurs when the condition in equation 8 is not fulfilled and for those girders only the yield strength of the web, loading length, flange thickness and web thickness control the patch loading resistance from the design model.

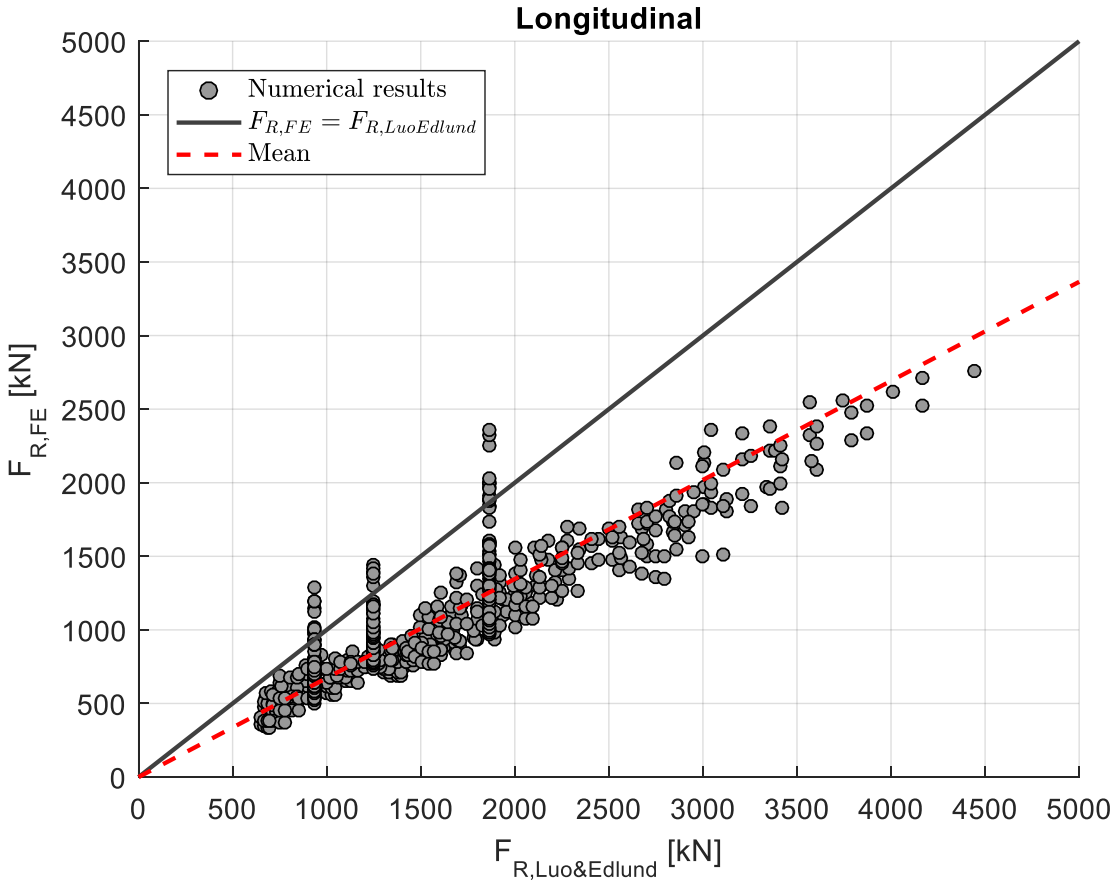

Figure 41. Patch loading resistance for applying the load on the longitudinal fold from FE-analysis compared to design model from Luo and Edlund (1996).

Luo and Edlund (1996) design model was developed after a parametric study where five different geometrical parameters were varied, that was the corrugation angle, height of the web, span length, flange and web thickness. This means that in their

parametric study the width of the flange was not examined and only one parameter of the corrugation was considered, that is the corrugation angle which although influences the other parameters of the corrugation. This reflects in the design model presented by Luo and Edlund (1996) which considers the yield stress of the web material, flange thickness, web thickness and a factor γ. This factor is influenced by the corrugation of the web and the distribution of the load. This shows that the model presented by Luo and Edlund (1996) is not sophisticated enough to determine the patch loading resistance of girders with corrugated web since it overestimates the resistance.

The mean value of the patch loading resistance for all three load cases is presented in Table 22. The difference in the average patch loading resistance for each load case is drastic, where the design model yields more than 45% higher average resistance compared to the FE analysis for all load cases. The design model by Luo and Edlund was developed around parameters different from this parametric study, that is likely the reason for why the results do not correlate well together.

Table 22. Mean value for all three load cases from the FE-analysis and the design model presented by Luo and Edlund (1996).

Average patch loading resistance	Longitudinal	Intersection	Inclined
FE-analysis [kN]	1119.6	1136.6	1145.6
Design model [kN]	1663.7	1663.7	1663.7
Difference [%]	48.6	46.4	45.2

7.2 Design model by Elgaaly and Seshadri (1997)

The design model from Elgaaly and Seshadri (1997) is compared to the results from the FE-analysis for the longitudinal load case, the results are presented in Figure 42. The results from the design model presented by Elgaaly and Seshadri (1997) show that the patch loading resistance matches quiet well to the results from the parametric study. This is easily seen from the mean value line which lies closely to the line, $F_{R,FE}=F_{R,Elgaaly,}$ which is when the results from the two are equal. However, a lot of the models are on the unsafe side of the line which means that the model is not conservative in estimating the patch loading resistance of all girders considered.

In the model they take into consideration two failure modes, web crippling and web yielding. The web crippling model considers contribution from both the web and the flange unlike the formula presented by Luo and Edlund (1996) which only considers parameters of the web and thickness of the flange. The formula presented by Elgaaly and Seshadri (1997) consider more parameters than the formula presented by Luo and Edlund (1996). The parameters considered are the plastic moment capacity of the flanges, the loading length, Youngs modulus, yield stress of the web and flange, thickness of the web, thickness of the flange, distance between the plastic hinges, width of the inclined fold and longitudinal fold. This shows that the formula is more complex and considers a broader variety of girders then the model presented by Luo and Edlund.

What is similar to the FE-analysis performed and the research done by Elgaaly and Seshadri (1997) is that there are the same load locations considered, excluding the intersection, and the loading length is rather narrow in both studies.

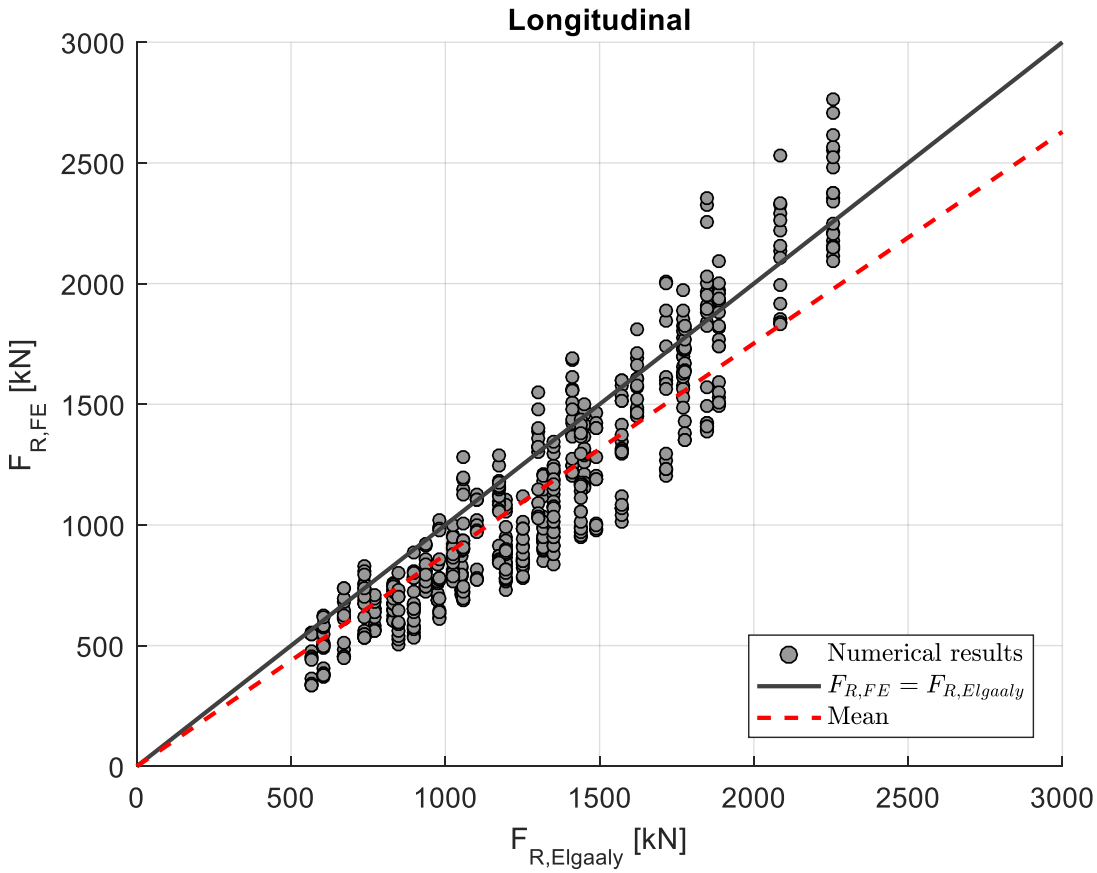

Figure 42. Patch loading resistance for the longitudinal load case from the FE-analysis compared to design model from Elgaaly and Seshadri (1997).

The mean value for the patch loading resistance for all three loading locations from the FE-analysis and the model is shown in Table 23. The mean value from the design model is 14% higher for the longitudinal load case compared to the resistance from the FE-analysis. For the other two cases it yields almost the same value or approximately 1-2% difference. This result underlines that the model is unconservative for the longitudinal load case compared to this FE-analysis and can overestimate the patch loading resistance of girders with corrugated web for that load case. For the other two the mean value correlate well together.

Table 23. Mean value for all three load cases from the FE-analysis and the design model presented by Elgaaly and Seshadri (1997).

Average patch loading resistance	Longitudinal	Intersection	Inclined
FE-analysis [kN]	1119.6	1136.6	1145.6
Design model [kN]	1277.8	1127.4	1127.4
Difference [%]	14.1	-0.8	-1.6

Since there was a good correlation between the intersection and inclined load case the design model from Elgaaly and Seshadri (1997) was compared to the results from the FE-analysis for the other two load cases, inclined and intersection, and can be seen in Figure 43. From the figure it is clear that for those two load cases the results from the model and the FE-analysis fit well together which matches the results from the mean

value comparison although there are still girders falling on the unconservative side. It is also observed that there are a few girders that yield much higher capacity in the FE-analysis than in the design model. For the inclined load case two outlaw girders yield in around 2600 kN from the FE-analysis but only yield in around 1400 kN from the design model.

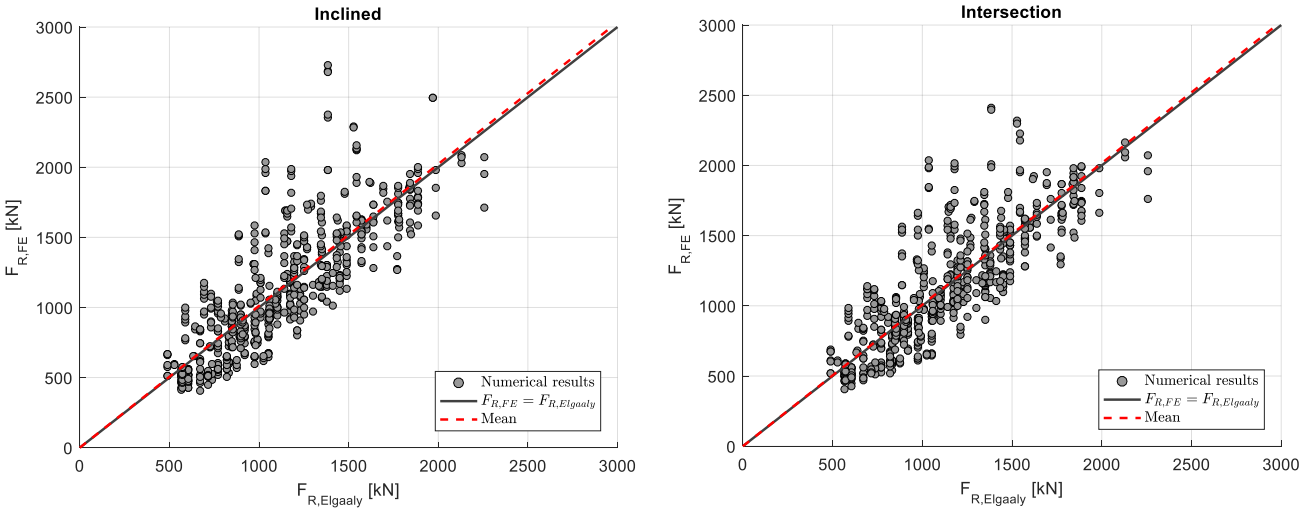

Figure 43. Patch loading resistance for the inclined and intersection load cases from FE-analysis compared to design model from Elgaaly and Seshadri (1997).

7.3 Design model by Kövesdi et al (2010)

The design model presented by Kövesdi et al (2010) is compared to the results from the FE-analysis for all three load cases. The comparison for the longitudinal load case is shown in Figure 44 but the other two load cases are found in Appendix C.2.1. In Figure 44 distinction is made for girders that fulfill the conditions set for the design model and girders that do not fulfill the conditions. There is one condition neglected, that is the criteria considering the ratio between the loading length and the height of the girder since none of the girders from this FE-analysis meets that criterion. The girders that do not fulfill the suggested conditions for the design model follow similar trend as the other ones although they are more unconservative compared to the ones that fulfill the conditions, which means that they yield higher resistance values.

The model from Kövesdi et al (2010) fits worse than the model presented by Elgaaly and Seshadri (1997), both models are on the unsafe side compared to the results from the FE-analysis. The formula developed by Kövesdi et al (2010) considers the contribution from the flanges and the web. The contribution from the flanges is influenced by the plastic moment capacity of the flanges, thickness of the web, yield stress of the web and the reduction factor. The contribution from the flanges is influenced by the same reduction factor and in addition the web thickness, yield stress of the web, loading length and modification factor due to the corrugation angle. In addition, the design model follows a non-dimensional slenderness curve. The same parameters are considered by Elgaaly and Seshadri (1997) but in addition they have a parameter which considers the distance between the plastic hinges which could explain why that formula gives better correlation to the FE-analysis.

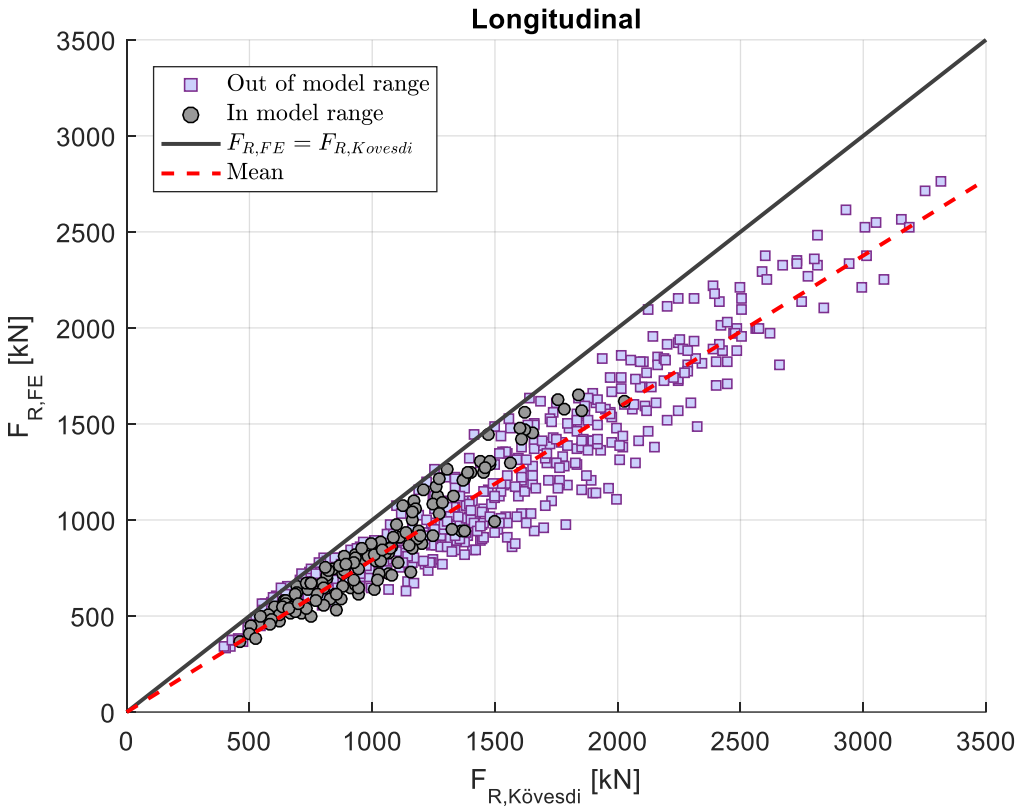

Figure 44. Patch loading resistance from FE-analysis compared to design model from Kövesdi et al (2010).

The mean value for the patch loading resistance for all three loading locations from the FE-analysis and the model is shown in Table 24. The mean value is lower for all three load locations from the FE-analysis compared to the mean value from the design model, the difference is around 15-26%.

Table 24. Mean value for all three load cases from the FE-analysis and the design model presented by Kövesdi et al.

Average patch loading resistance	Longitudinal	Intersection	Inclined
FE-analysis [kN]	1119.6	1136.6	1145.6
Design model [kN]	1413.4	1311.2	1349.6
Difference [%]	26.2	15.4	17.8

The girders that fulfill the criteria for the Kövesdi et al (2010) design model are further examined and compared to the results for those girders in the FE-analysis, see Figure 45 for the longitudinal load case. The results for the other two load cases can be found in Appendix C.2.2. The mean value for the design model gets closer to the mean value from the FE-analysis which means that those girders fit better together. This is expected since the model is developed based on girders that fulfill the condition set for the design model so girders outside of the condition could have different behavior and failure mechanism although the model should give a good estimate for those girders as well.

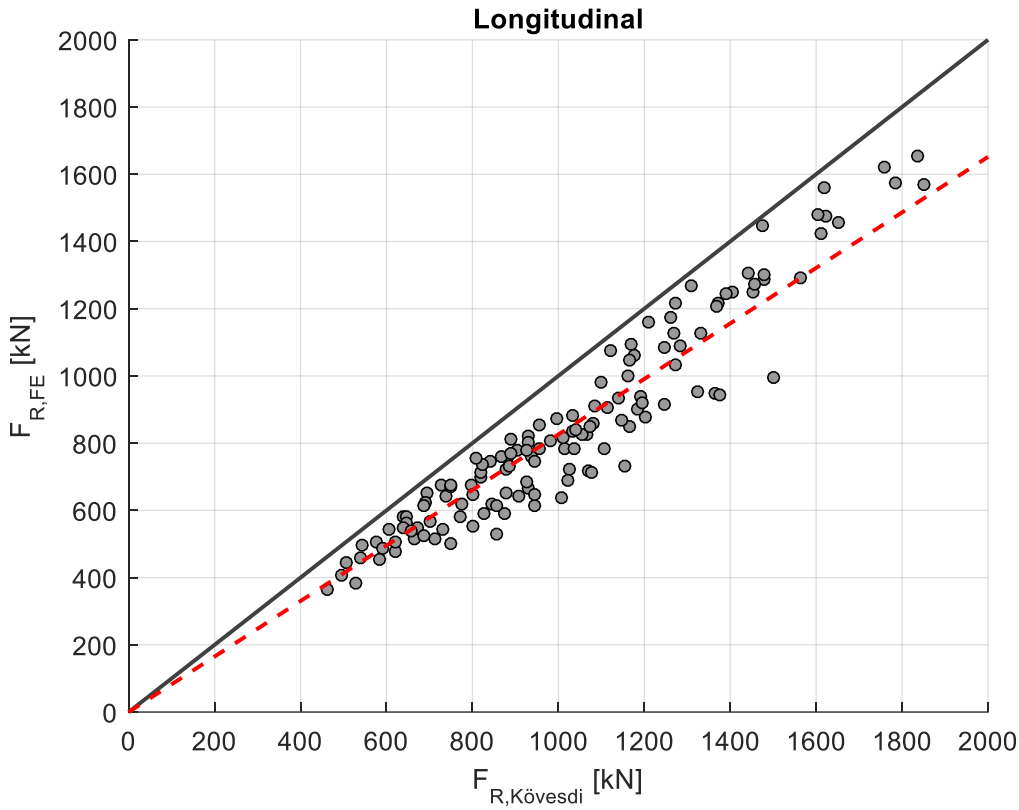

Figure 45. Patch loading resistance from FE-analysis compared to design model from Kövesdi et al (2010) for girders that fulfill the criteria of the model.

For girders that fulfil the criteria of the design model for all three loading locations, the mean value from the FE-analysis is compared to the mean value from the design model, see Table 25. The model gives around 18-22% higher resistance than the FE-analysis. The mean value for when the load is applied at longitudinal fold gets closer to the mean value from the design model compared to when all the girders are considered in Table 24, the difference decreases approximately 5%. The difference for the other two load cases increases approximately 3-5% compared to Table 24.

Table 25. Mean value for all three load cases from the FE-analysis and the design model presented by Kövesdi et al (2010) for girders that fulfill the criteria set by the design model.

Average patch loading resistance	Longitudinal	Intersection	Inclined
FE-analysis [kN]	851.5	910.2	920.4
Design model [kN]	1031.2	1080.2	1123.8
Difference [%]	21.1	18.7	22.1

7.4 Design model by Kövesdi (2010)

The design model presented by Kövesdi (2010) is compared to the results from the FE-analysis. The comparison for the longitudinal load case is presented in Figure 46, the results for the other two load cases can be found in Appendix C.3.1. In the figure the same distinction is made as before that is girders that fulfill the conditions set for the

design model and girders that do not fulfill the conditions, excluding the loading length. The only difference between this model by Kövesdi (2010) and the design model by Kövesdi et al (2010) is the reduction in flange capacity for girders where not all four plastic hinges can form. This reduction in flange capacity makes the design model and the FE-analysis fit closer together.

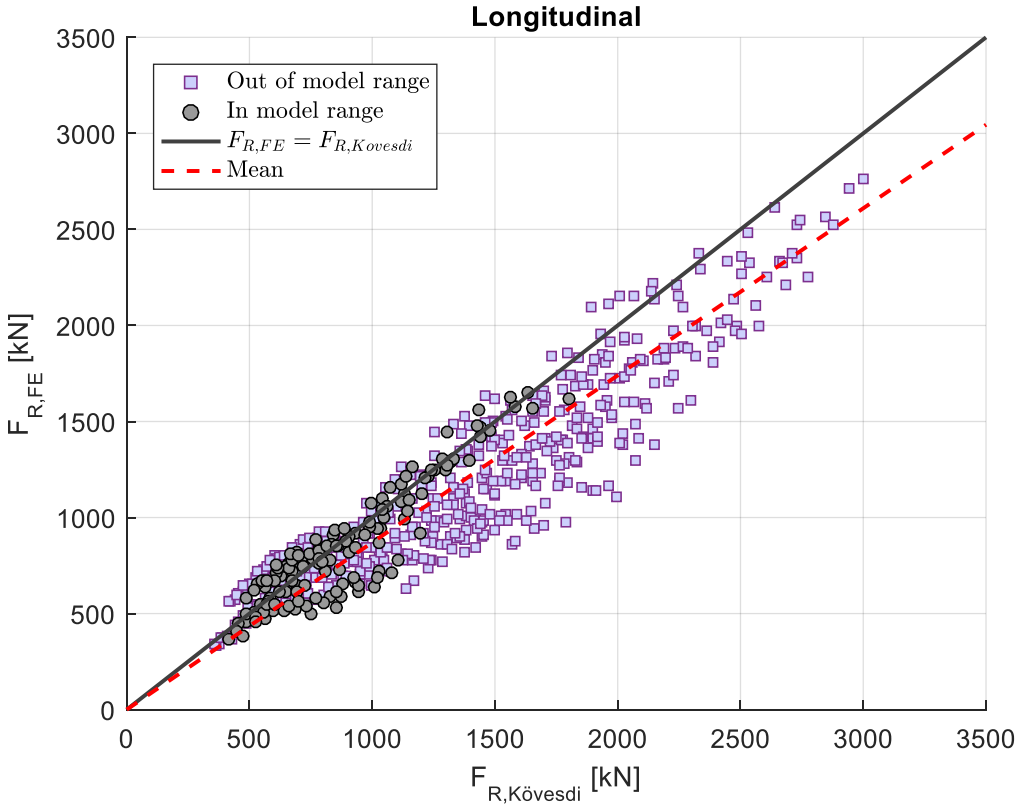

Figure 46. Patch loading resistance from FE-analysis compared to design model from Kövesdi (2010).

The mean value for the patch loading resistance for all three loading locations from the FE-analysis and the model is shown in Table 26. The difference between the three loading locations and the model are all similar or about 5-15%. The longitudinal load case has the highest difference from the model and the intersection the lowest.

Table 26. Mean value for all three load cases from the FE-analysis and the design model presented by Kövesdi (2010).

Average patch loading resistance	Longitudinal	Intersection	Inclined
FE-analysis [kN]	1119.6	1136.6	1145.6
Design model [kN]	1287.0	1193.5	1228.3
Difference [%]	15.0	5.0	7.2

The results for the girders that fulfill the conditions of Kövesdi (2010) design model were further studied. Comparison between the design model and the FE-analysis can be seen in Figure 47 for the longitudinal load case and the figures for the other two load cases can be found in Appendix C.3.2. When comparing Figure 47 to the results from

Kövesdi et al (2010) design model presented in Figure 45 it is observed that the results from the FE-analysis fit better to the current design model.

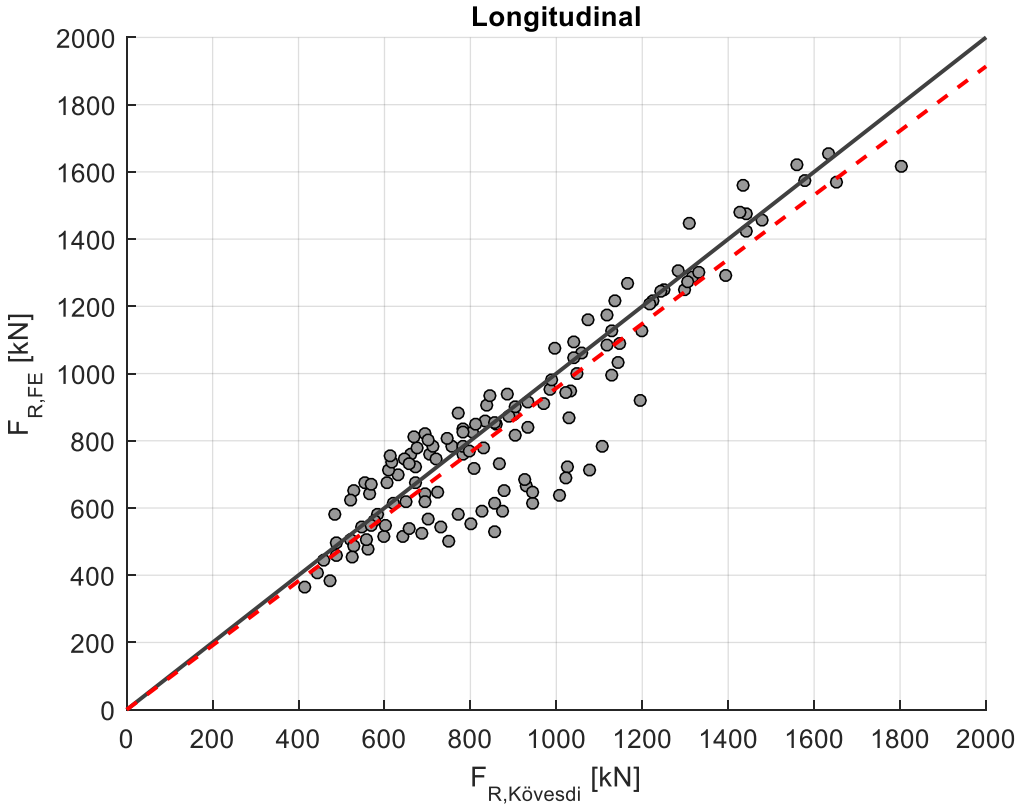

Figure 47. Patch loading resistance from FE-analysis compared to design model from Kövesdi (2010) which fulfill the criteria of the model.

The difference for the average patch loading resistance for each load case of the FE-analysis compared to the design model is less than 7% for all load cases, like can be seen in Table 27. The average patch loading resistance for all the load cases is on the unsafe side. The difference for the longitudinal load case has been reduced by approximately 10% when comparing Table 27 to Table 26, while the difference for the other two load cases has only reduced slightly.

Table 27. Mean value for all three load cases from the FE-analysis and the design model presented by Kövesdi (2010) for girders that fulfill the criteria set by the design model.

Average patch loading resistance	Longitudinal	Intersection	Inclined
FE-analysis [kN]	851.5	910.2	920.4
Design model [kN]	889.9	940.3	981.4
Difference [%]	4.5	3.3	6.6

If the girders that fulfil the criteria for Kövesdi (2010) design model are further analyzed with respect to flange and web thickness ratios, some interesting results can be observed for the longitudinal load case. The vast majority of girders with flange and web thickness ratio greater than 5 are on the conservative side compared to the FE-analysis, like can be seen in the figure in Appendix C.3.3. These results indicate that

the Kövesdi (2010) model could be used to estimate the patch loading resistance for a certain parametric range.

7.5 Design model in the latest draft of EN 1993-1-5 (2020)

The design model presented in the latest draft of Eurocode 3 is compared to the results from the FE-analysis. The results for the longitudinal load case are presented in Figure 48 and the results from the other two load cases are found in Appendix C.4. The figure shows that the model from Eurocode 3 is very conservative and thus on the safe side compared to the results from the FE-analysis. In the figure distinction is made between girders that fulfill the conditions in equation 19 for the design model and girders that do not fulfill the conditions.

If the model presented in Eurocode 3 is examined, see equation 35, it is clear that it only considers the web that means that the contribution from the flanges is neglected. Therefore, the Eurocode 3 model is expected to be on the safe side and that the results from the FE-analysis will yield higher resistance since it takes into account the resistance from the flanges.

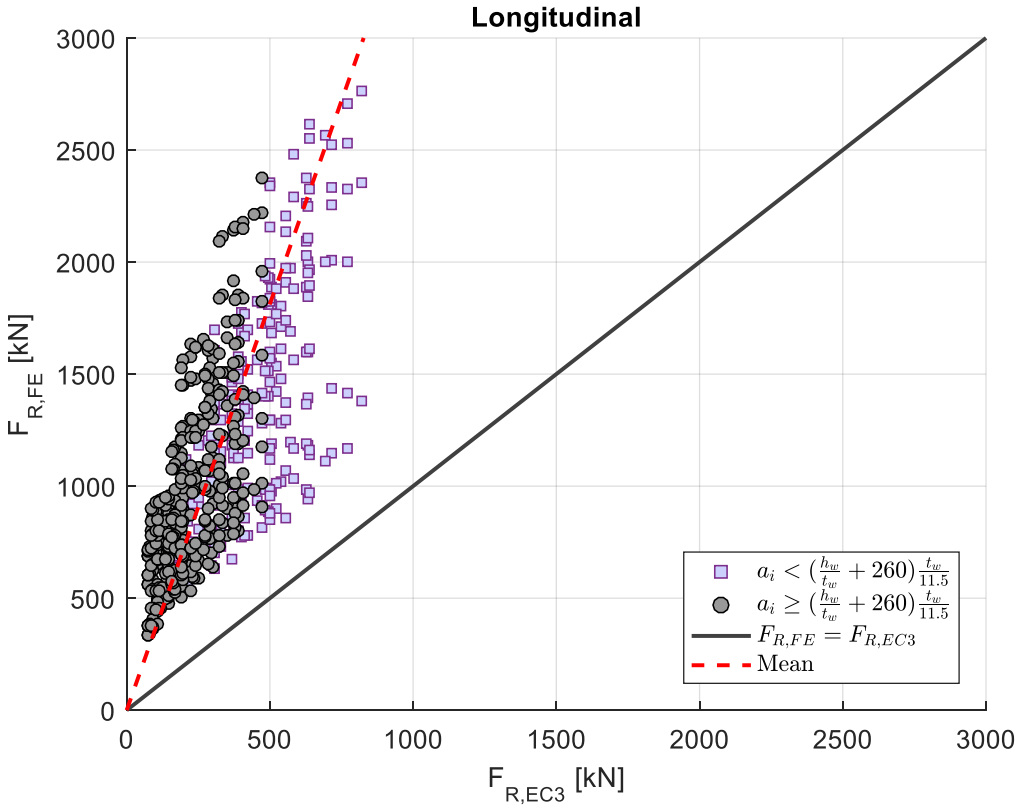

Figure 48. Patch loading resistance from FE-analysis compared to design model from the draft of EN 1993-1-5 (2020).

The mean patch loading resistance from the FE-analysis for all three load cases is compared to results obtained with the Eurocode model. The average resistance from the Eurocode 3 model is about 72-76% smaller than the results for the three load cases in the FE-analysis. This shows that if the model from the newest draft of Eurocode 3 is used in design it yields very conservative results for the patch loading resistance.

Table 28. Mean value for all three load cases from the FE-analysis and the design model presented in the draft of EN 1993-1-5 (2020).

Average patch loading resistance	Longitudinal	Intersection	Inclined
FE-analysis [kN]	1119.6	1136.6	1145.6
Design model [kN]	308.8	275.7	286.0
Difference [%]	-72.4	-75.7	-75.0

7.6 Summary and discussion

These results mean that the only model that can be deemed applicable and safe to use for the results from the parametric study is the model from Eurocode 3, since that is the only model which is conservative. The model although gives very conservative results and lacks contribution from the flanges. If the flange contribution would be added in the design model it could make the model unsafe if it is not done correctly. Therefore, it is important to be careful when deciding how to take into consideration the contribution from the flanges since that is a complex problem.

These results are not what was expected, that is that the existing design models show so unconservative results compared to the FE-analysis. Therefore, a reasoning for why the simulations gave lower resistance then the existing design model was further looked at. That is if any of the input parameters in the FE-analysis were too conservative for the model. The material model used was elastic-plastic material model that is the stress-strain relationship is assumed to follow an elastic-plastic material with strain hardening. According to Luo and Edlund (1996), using the Ramberg-Osgood strain-hardening model showed that the load capacity increased around 8-12% but that is not enough increase to reason this difference.

The design model from Luo and Edlund (1996) yielded unconservative results and largely overestimated the patch loading resistance compared to the FE-analysis, this supports the conclusion drawn by Kövesdi (2010). A possible reason for this is that the parametric range for the FE-analysis is different from the parametric range in their design model. From the comparison of the design model to the FE analysis it is concluded that the design model is not a good tool to use in practice

Elgaaly and Seshadri (1997) design model had the best fit with the FE-analysis in average patch loading, however many girders are on the unconservative for the patch loading resistance. The average value for the longitudinal load case from the FE-analysis has 14% difference from the model so for that load case the model overestimates the patch loading resistance, but the other two load cases had only 1-2% difference. Even if the inclined and intersection load cases correlate well for the average patch loading resistance there are girders that differ in resistance more than 1000kN between the FE-analysis and the design model. For all load cases, the standard deviation for this design model is quite large.

When comparing the two design models presented by Kövesdi et al (2010) and Kövesdi (2010) it is concluded that for the parametric ranges and combinations in the FE-analysis that the Kövesdi (2010) design model is more appropriate. The only difference of the design models is that the Kövesdi (2010) formula has a factor, *n*, instead of the

constant 4 which considers how many plastic hinges can develop in the flange and is dependent on the ratio between the thickness of the flange and web. The results show that with adding this factor the design model and the FE-analysis correlate better.

If the Kövesdi (2010) formula, see equation 31, is compared to the one given in the latest draft of the Eurocode 3 (2020), see equation 35, it is clear that the formulas are similar when looking at the contribution from the corrugated web, although the Kövesdi (2010) model lacks safety factors. If the contribution part of Kövesdi (2010) equation that considers the contribution from the flanges would be added to the formula from the EN 1993-1-5 (2020) it would show similar results as the Kövesdi (2010) design model. The results from the models show that the contribution from the flanges according to Kövesdi (2010) exaggerates the capacity compared to the FE-analysis. The reason for this overestimation could be the loading length.

The contribution from the flanges in Kövesdi (2010) formula is based on research where a wide loading length, s_s, was used but in this FE-analysis narrow loading length is considered. For a narrow loading length, loaded on the longitudinal fold, the distribution of the load to the corners of the corrugation is through bending of the flange and it depends on the bending stiffness of the flange. The torsional rigidity of the flanges distributes the load to the inclined part of the corrugations which means that if the longitudinal part, a_1, is long in relation to the loading length, s_s, then the flange will become flexible which means that there will be high bending and the concentrated force will be large on the web. This means that for narrow loading length the flange dimensions have a large influence. Then when the loading length is wide the influence of the flange dimensions is not as effective because the load will transfer directly to the corner of the corrugation. For example, if it is loaded over the whole corrugation then there are four rigid points, one in each corner which is much stiffer compared to when the loading length is narrow. This could explain that if the contribution from the flanges suggested by Kövesdi (2010) is added to EN 1993-1-5 (2020) formula it will give unconservative results for narrow loading lengths since the contribution from the flanges is made from cases where the loading was long.

The average patch loading resistance for all four design models and the formula from the Eurocode 3 are compared to results from the FE-analysis for all load cases in Figure 49. The resistance is higher for the design model presented by Luo and Edlund (1996), Kövesdi et al (2010) and Kövesdi (2010) than the average from the FE-analysis for all three load cases. However the resistance from the formula in EN 1993-1-5 (2020) draft yields much smaller average values then the FE-analysis. The mean value from Elgaaly and Seshadri (1997) is the closest to the mean value from the FE-analysis results although that has quite larger standard deviation compared to the Kövesdi (2010) design model.

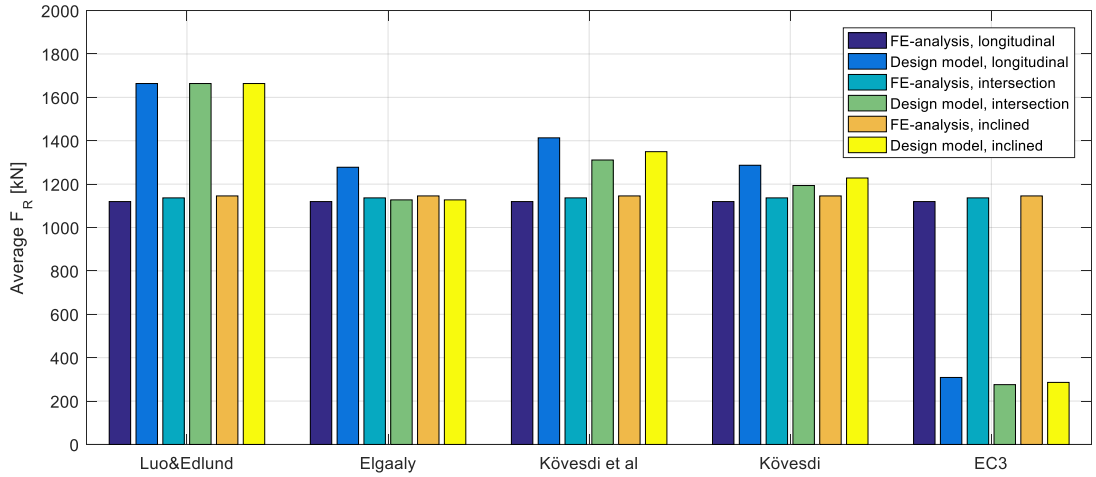

Figure 49. Mean resistance values for all three loading cases from the FE-analysis compared to results from each design model.

Note that none of these existing design models are sophisticated enough to capture the influence of every parameter that effects the patch loading resistance and therefore a further enhanced design model is still needed for the subject. All of the existing design models analyzed were developed considering carbonated steel. Therefore, it is not surprising that some of the design models were sensitive to the flange-web thickness ratio range for a FE-analysis developed for stainless steel girders.

8 Conclusion

8.1 Preliminary studies

The thickness parameters for the web and flange, t_w and t_f, have the largest influence on the patch loading resistance. Increasing the web thickness, flange thickness and flange width increases the patch loading resistance. Increasing the fold slenderness ratio decreases the patch loading resistance.

The influence of the corrugation angle and flange width are dependent on the thickness of the web. For girders with thin webs increasing the corrugation angle gives constant or slightly decrease in the patch loading resistance. Increasing the flange width increases the patch loading resistance slightly or nothing. For girders with thicker webs increasing the corrugation angle increases the patch loading resistance almost linearly. Increasing the flange width increases the patch loading resistance linearly for girders that fails with local patch. When the failure mechanism changes the patch loading resistance increases with less rate.

In the analyses the corrugation depth is varied less than the other parameters. Increasing the corrugation depth shows no clear trend in either increasing or decreasing the patch loading resistance, however there is a slight increase in the capacity for thin webs.

The patch loading resistance is for majority of the girders lower when the load is applied at the longitudinal fold than for the other two load cases. However, the longitudinal load case has slightly higher resistance for girders with high flange-web thickness ratios. Loading of the inclined fold is more sensitive to changing buckling mode from local patch buckling compared to the other two load cases.

8.2 Extensive parametric study

The extensive parametric study shows that the patch loading resistance increases with increased web thickness, flange thickness, flange width or number of unit cells. Increasing corrugation angle and corrugation depth has a more complex effect on the resistance and is highly dependent on other geometrical parameters.

The optimized girders have the same thickness of the web, corrugation angle and corrugation depth. The width of the flanges is slightly different for the intersection load case. The highest ratio between patch loading resistance and weight is derived for a girder loaded at the intersection although the inclined load case gives similar results. The girder loaded at the longitudinal fold has the highest patch loading resistance but the stockiest girder, so the ratio is lower than the other two.

The patch loading resistance for the inclined and intersection load cases correlate well to each other. The longitudinal load case is different from the other two. If the ratio between the thickness of the flange and web is equal or larger than four the resistance of the girders yields higher resistance for the longitudinal load case, but lower resistance when the ratio is less than four for most girders. This is the trend for most girders, but not all. Increase in flange width appears to cause increase in patch loading capacity for some girders loaded at the longitudinal fold.

8.3 Existing design model

The design model presented in the draft for the upcoming Eurocode 3 is conservative for all girders analyzed, however the model may be too conservative as it only accounts for the web contribution. None of the other existing design models are conservative enough to be applied in practice for the parametric range presented in this study. The design model by Luo and Edlund (1996) yields very unconservative results and is therefore not recommended to be used in practice.

The results from the design model developed by Elgaaly and Seshadri (1997) for the average patch loading resistance fits well with the FE-analysis especially for the inclined and intersection load case. Although it has larger standard deviation when compared to Kövesdi (2010) design model. Thus, the design model presented by Kövesdi (2010) could be deemed more promising for the parametric range in this study.

Two design models presented by Kövesdi, Kövesdi (2010) and Kövesdi et al (2010), are considered. The design model that accounts for the number of developed plastic hinges with the factor, *n*, has a closer fit to the FE-analysis and is deemed more appropriate for the parametric range in this study.

None of the existing design models that are investigated in this thesis are sophisticated enough to estimate the patch loading resistance for stainless steel girders. Adjustments are needed on the models and safety factors to be considered, so they yield conservative resistance. A better model is needed to consider this loading type so that future designers have a good design tool to predict the resistance of girders with corrugated web in an efficient way, so the resistance is not underestimated in a major extend.

8.4 Further research proposals

This study shows that the model from the newest draft of Eurocode 3 is very conservative since it only considers the contribution from the corrugated web. To get a better fit with the FE-analysis the contribution from the flanges is needed to be added although that contribution needs to be further studied so that it will not make the model unconservative.

This parametric study is aimed for girders with stainless steel and only one grade of stainless steel is considered. Further studies could compare two or more different grades of stainless steel and see if there is any other difference then increase in resistance proportion to the increase in yield stress.

In further study one could vary the geometrical parameters more and increase the range that was used in this thesis. In addition, there could be other parameters varied. In this study the same height and span length is used throughout the study since previous studies have shown that the height does not influence the patch loading resistance. This could be further examined.

For further research a parametric study could be performed, with variety of loading lengths, from very narrow patch loads to wide patch loads over one or more unit cells. In this thesis only a constant narrow loading length is considered. This could result in a design model that accounts for both narrow and wide loading lengths.

In this thesis, only one corrugation shape is considered and that was trapezoidal shape since that is the one that is most common in design. Same or similar work as was done in this thesis could be beneficial for other shapes as well, for example sinusoidal shape.

A similar parametric study with comparison to experimental results for stainless steel girders with large flange-web thickness ratios would be precious. This would verify if this FE-analysis correlates well to reality or not.

In addition to the pure patch load considered in this thesis, applying a moment around the longitudinal axis of the girder at the same location as the patch load could yield interesting results. In many cases the center of gravity for the patch load is eccentric to one side of the girder and thus can create out of plane bending.

9 References

al-Emrani, M. (2020): *Analysis of the load-carrying capacity of beams with corrugated web with respect to lateral-torsional buckling.* Chalmers University of Technology, Gothenburg, Sweden, 9 pp.

Baddoo, N. R., (2008): Stainless steel in construction: A review of research, applications, challenges and opportunities. *Journal of Constructional Steel Research,* vol 64, no. 11, pp. 1199-1206.

Bergfelt, A. and Lindgren, S. (1974*): Livintryckning under koncentrerad last vid balkar med slankt liv.* Division of Steel and Timber Structures, Chalmers University of Technology, Publication no. S 74:5, Gothenburg, Sweden.

Boutillion, L., Combault, J., Ikeda, S., Imberty, F., Mori, T., Nagamoto, N., Saito, K. (2015): *Corrugated-steel-web bridges*. Fédération internationale du béton.

Dahlén, A. and Krona, K.-M., (1984): *Lokal intryckning av veckat liv*. Division of Steel and Timber Structures, Chalmers University of Technology, Publication no. 84:5, Gothenburg, Sweden.

Dahlström, S. E. and Persson, J. (2018): *Implementation of Stainless Steel Reinforcement in Concrete Bridges - Redesign of Reinforcement using Stainless Steel to Increase Durability and Profitability in Bridge Design.* Department of Architecture and Civil Engineering, Chalmers University of Technology, Publication no. 01, Gothenburg, Sweden, 110 pp.

Den Uijl, N.J. and Carless, L.J. (2012): 3 - Advanced metal-forming technologies for automotive applications. *Advanced Materials in Automotive Engineering,* Vol. 1, No. 1, 2012, pp. 28-56.

Elgaaly, M., and Seshadri, A. (1997): Girders with corrugated webs under partial compressive edge loading. *Journal of Structural Engineering*, pp.783-791.

EN 1993-1-5, (2020): *Eurocode 3 - Design of steel structures, Part 1-5: Plated structural elements*. Brussels, Belgium: CEN, European Committee for standardization.

EN 1993-1-5, (2006): *Eurocode 3 - Design of steel structures, Part 1-5: Plated structural elements*. Brussels, Belgium: CEN, European Committee for standardization.

EN 1993-1-4, (2006): *Eurocode 3 - Design of steel structures, Part 1-4: General rules – Supplementary rules for stainless steels*. Brussels, Belgium: CEN, European Committee for standardization.

Górecki, M. and Śledziewski, K., (2020): Experimental Investigation of Impact Concrete Slab on the Bending Behavior of Composite Bridge Girders with Sinusoidal Steel Web. *Materials*, vol 13, no 2, pp. 273.

Hamada, M., Nakayama, K., Kakihara, M., Saloh, K. and Ohtake, F., (1984): Development of welded I beam with corrugated web. *The Sumitomo Search,* vol. 29, pp. 75-90.

Henrysson, A. and Yman, E., (2020): *Design of Composite Steel-Concrete Bridges using Stainless Steel Girders with Corrugated Webs.* Department of Architecture and Civil Engineering, Chalmers University of Technology, Publication no. 1, Gothenburg, Sweden, 114 pp.

Inaam, Q. and Upadhyay, A., (2020): Behavior of corrugated steel I-girder webs subjected to patch loading: Parametric study. *Journal of Constructional Steel Research,* vol 165, doi: 10.1016/j.jcsr.2019.105896

Karabulut, B., Ferraz, G., and Rossi, B. (2021): Lifecycle cost assessment of high strength carbon and stainless steel girder bridges. *Journal of Environmental Management,* vol 277, doi: 10.1016/j.jenvman.2020.111460.

Kähönen A. (1988): Zur Einleitung von Einzellasten in I-Träger mit trapezförmig profilierten Stegen. *Stahlbau,* vol 57, pp. 250-252.

Karlsson, E. (2018): *Stainless Steel Bridge Girders with Corrugated Webs Efficiency, stability and life-cycle cost analysis*. Department of Architecture and Civil Engineering, Chalmers University of Technology, Publication no. 1, Gothenburg, Sweden, 72 pp.

Kuchta, K.R., (2007): Design of corrugated webs under patch load. *Advanced Steel Construction,* vol 3, pp. 737-751.

Kuhlmann, U. and Braun, B. (2008): *Berechnungs- und Konstruktionsgrundlagen für sandwichähnliche Verbundträger mit Trapezstegen im Brückenbau*. Part of the Final Report, Project No. P 645, Forschungsvereinigung Stahlanwendung (FOSTA), Düsseldorf, Germany.

Kövesdi, B. (2010): *Patch loading resistance of girders with corrugated webs.* Budapest University of Technology and Economics, Publication no. 1, Budapest, Hungary, 109 pp.

Kövesdi, B., Braun, B., Kuhlmann, U., and Dunai, L. (2010): Patch loading resistance of girders with corrugated webs. *Journal of Constructional Steel Research,* vol 66, pp. 1445-1454.

Kövesdi, B. and Dunai, L., (2011): Determination of the patch loading resistance of girders with corrugated webs using nonlinear finite element analysis. *Computers and Structures,* vol 89, No. 21-22, pp. 2010-2019.

Leiva-Aravena, L., and Edlund, B., (1987); Buckling of Trapezoidally Corrugated Webs. *Colloquium on Stability of Plate and Shell Structures, ECCS*, Ghent University, pp. 107-116.

Ljungström, N. and Karlberg, O. (2010): *Girders with Trapezoidally Corrugated Webs under Patch Loading.* Department of Civil and Environmental Engineering, Chalmers University of Technology, Publication no. 1, Gothenburg, Sweden, 67 pp.

Luo, R., and Edlund, B. (1996): Ultimate strength of girders with trapezoidally corrugated webs under patch loading. *Thin-Walled Structures*, vol 24, No. 2, pp.135-156.

Raviraj, Dr. S., (2009): Design of Beams with Corrugated Web. *Construction Industry Reference Magazine Built Constructions*, available at http://www.builtconstructions.in/OnlineMagazine/Bangalore/Pages/Design-Of-Beams-With-Corrugated-Web-310.aspx (accessed April 2021).

Roberts, T.M. and Rockey, K.C., (1979): A mechanism solution for predicting the collapse loads of slender plate girders when subjected to in-plate patch loading. *Proceedings of the Institution of Civil Engineers*, Vol. 67, No. 2, pp. 155-175.

Appendix A – Results from reference model 1 compared to the FE-analysis

A.1 Analytical calculations

Geometry

$h_w := 300mm$ Height of web

$t_w := 6mm$ Thickness of web

$L_s := 4800mm$ Length of span

$b_f := 150mm$ Width of flanges

$t_f := 10mm$ Thickness of flanges

Corrugation profile

$a := 70mm$

$b := 47mm$

$d := 50mm$

Material properties

$$E := 210 \cdot 10^9 Pa \qquad f_y := 355 \frac{N}{mm^2}$$

$$G := \frac{E}{[2 \cdot (1 + 0.3)]} = 8.077 \times 10^{10} Pa$$

$$I_{tot} := 2 \cdot \left[b_f \cdot t_f \cdot \left(\frac{h_w + t_f}{2} \right)^2 + \frac{b_f \cdot t_f^3}{12} \right] = 7.21 \times 10^{-5} m^4$$

$$y_{na} := \frac{(h_w + 2 \cdot t_f)}{2} = 0.16 m$$

$$W_y := \frac{I_{tot}}{y_{na}} = 0.451 L$$

Loading

$$M_{ref} := 100 kN \cdot m$$

$$F_{ref} := \frac{M_{ref}}{b_f \cdot (h_w + t_f)} = 2.151 \times 10^6 \frac{kg}{s^2}$$

Linear buckling

$$I_z := \frac{b_f^3 \cdot t_f}{6} = 5.625 \times 10^{-6} m^4$$

$$I_t := \frac{1}{3} \left(t_w^3 \cdot h_w + b_f \cdot t_f^3 + b_f \cdot t_f^3 \right) = 1.216 \times 10^{-7} m^4$$ Torsion constant

$$I_w := \frac{I_z \cdot (h_w + 2 \cdot t_f - t_f)^2}{4} = 0.135 L^2$$ Warping constant

$$u\_x := \left[\left(\frac{h\_w}{2 \cdot G \cdot a \cdot t\_w}\right) + \left[\frac{h\_w^2 \cdot (a+b)^3}{25 \cdot a^2 \cdot E \cdot b\_f \cdot t\_f^3}\right]\right] = 4.178 \times 10^{-8} \frac{s^2}{kg}$$

$$c\_w := \frac{(2 \cdot d)^2 \cdot h\_w^2}{8 \cdot u\_x \cdot (a+b)} = 2.302 \times 10^4 \frac{kg \cdot m^3}{s^2}$$

$$M\_cr := \frac{\pi^2 \cdot E \cdot I\_z}{L\_s^2} \cdot \left[\frac{I\_w}{I\_z} + \frac{L\_s^2}{\pi^2 \cdot E \cdot I\_z} \cdot (G \cdot I\_t + c\_w)\right]^{0.5} = 1.509 \times 10^5 J$$

$$M\_cr\_abaqus := 162 \cdot 10^6 N \cdot mm$$

Difference between the two:

$$Mcr\_diff := \frac{M\_cr - M\_cr\_abaqus}{\frac{M\_cr + M\_cr\_abaqus}{2}} = -7.102 \cdot \%$$

Non-linear analysis

$$\lambda := \left(\frac{W\_y \cdot f\_y}{M\_cr}\right)^{\frac{1}{2}} = 1.03$$

curve b

$$\alpha\_b := 0.34$$

$$\phi\_b := 0.5 \cdot \left[1 + \alpha\_b \cdot (\lambda - 0.2) + \lambda^2\right] = 1.171$$

$$X\_LT\_b := \frac{1}{\left[\phi\_b + \left(\phi\_b^2 - \lambda^2\right)^{\frac{1}{2}}\right]} = 0.578$$

$$M\_ult\_b := X\_LT\_b \cdot W\_y \cdot f\_y = 9.251 \times 10^4 J$$

$$M\_ult\_b\_abaq := 110.94 \cdot 10^6 N \cdot mm$$

$$Mult\_b\_diff := \frac{M\_ult\_b - M\_ult\_b\_abaq}{\frac{M\_ult\_b + M\_ult\_b\_abaq}{2}} = -18.112 \cdot \%$$

curve c

$$\alpha\_c := 0.49$$

$$\phi\_c := 0.5\cdot\left[1 + \alpha\_c\cdot(\lambda - 0.2) + \lambda^2\right] = 1.233$$

$$X\_LT\_c := \frac{1}{\left[\phi\_c + \left(\phi\_c^2 - \lambda^2\right)^{\frac{1}{2}}\right]} = 0.523$$

$$M\_ult\_c := X\_LT\_c\cdot W\_y\cdot f\_y = 8.365 \times 10^4\,J$$

$$M\_ult\_c\_abaq := 105.38\cdot 10^6 N\cdot mm$$

$$Mult\_c\_diff := \frac{M\_ult\_c - M\_ult\_c\_abaq}{\frac{M\_ult\_c + M\_ult\_c\_abaq}{2}} = -22.987\cdot\%$$

curve d

$$\alpha\_d := 0.76$$

$$\phi\_d := 0.5\cdot\left[1 + \alpha\_d\cdot(\lambda - 0.2) + \lambda^2\right] = 1.345$$

$$X\_LT\_d := \frac{1}{\left[\phi\_d + \left(\phi\_d^2 - \lambda^2\right)^{\frac{1}{2}}\right]} = 0.452$$

$$M\_ult\_d := X\_LT\_d\cdot W\_y\cdot f\_y = 7.234 \times 10^4\,J$$

$$M\_ult\_d\_abaq := 96.73\cdot 10^6 N\cdot mm$$

$$Mult\_d\_diff := \frac{M\_ult\_d - M\_ult\_d\_abaq}{\frac{M\_ult\_d + M\_ult\_d\_abaq}{2}} = -28.847\cdot\%$$

A.2 Load-displacement curves

A.2.1 Curve C

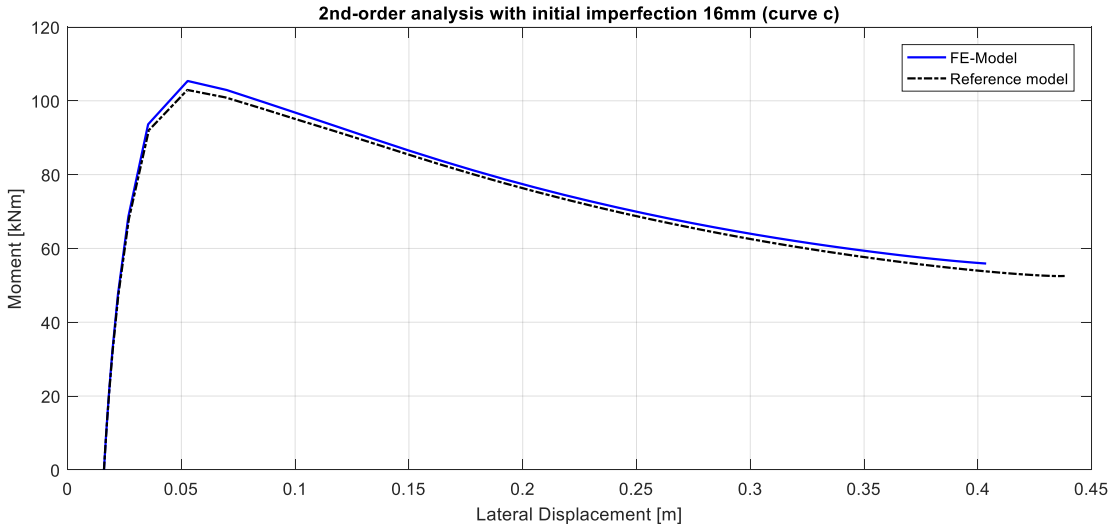

A.2.2 Curve D

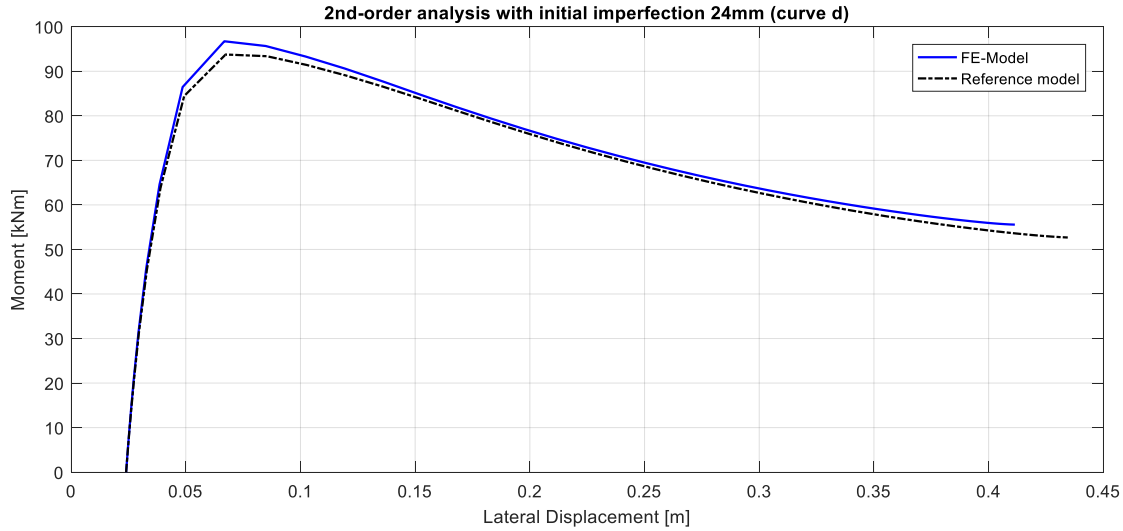

Appendix B – Parametric study

B.1 Intersection

B.1.1 Load vs iteration - Effect of changing each parameter

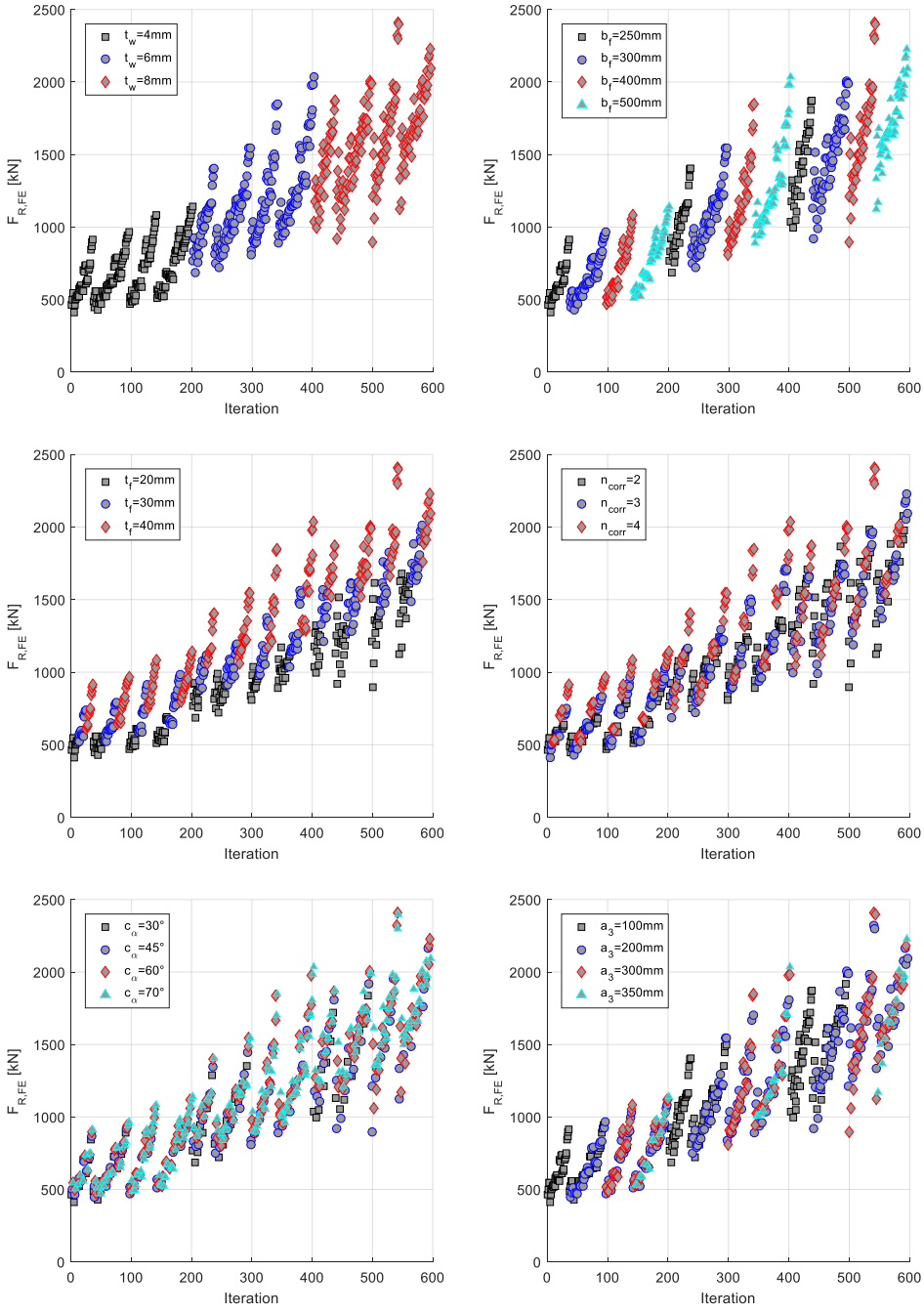

B.1.2 Load/Weight vs iteration - Effect of changing each parameter

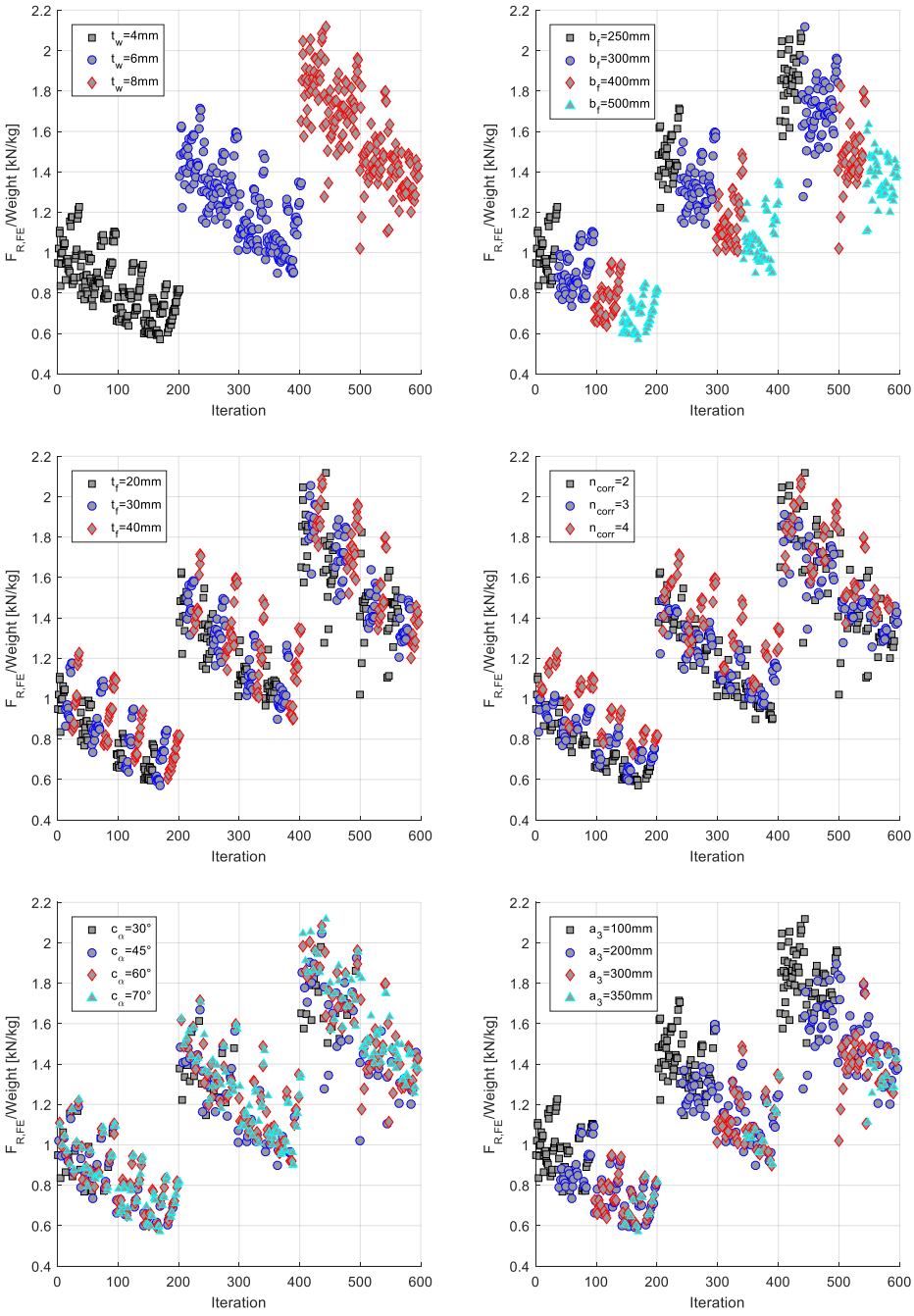

B.2 Inclined

B.2.1 Load vs iteration - Effect of changing each parameter

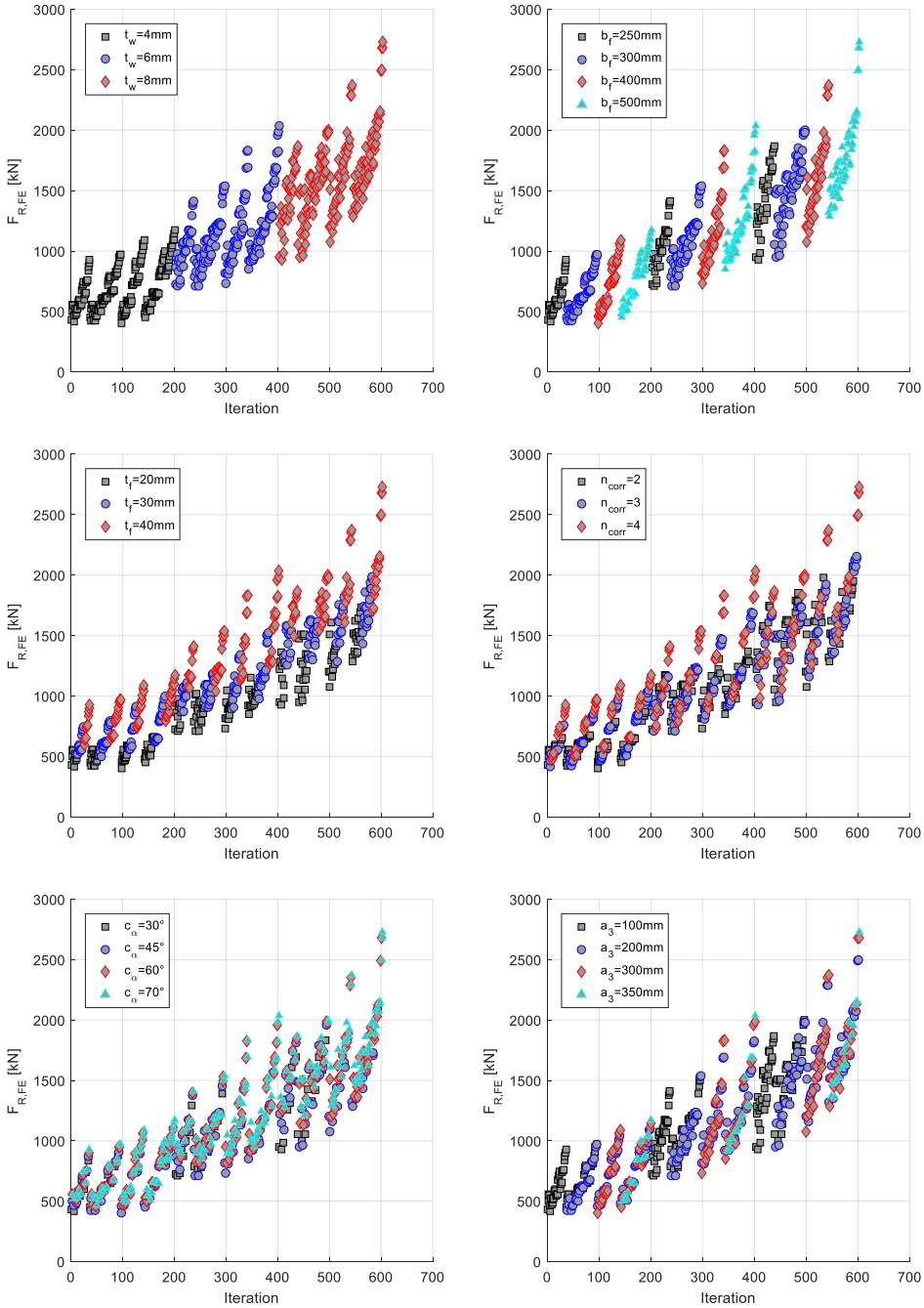

B.2.2 Load/Weight vs iteration - Effect of changing each parameter

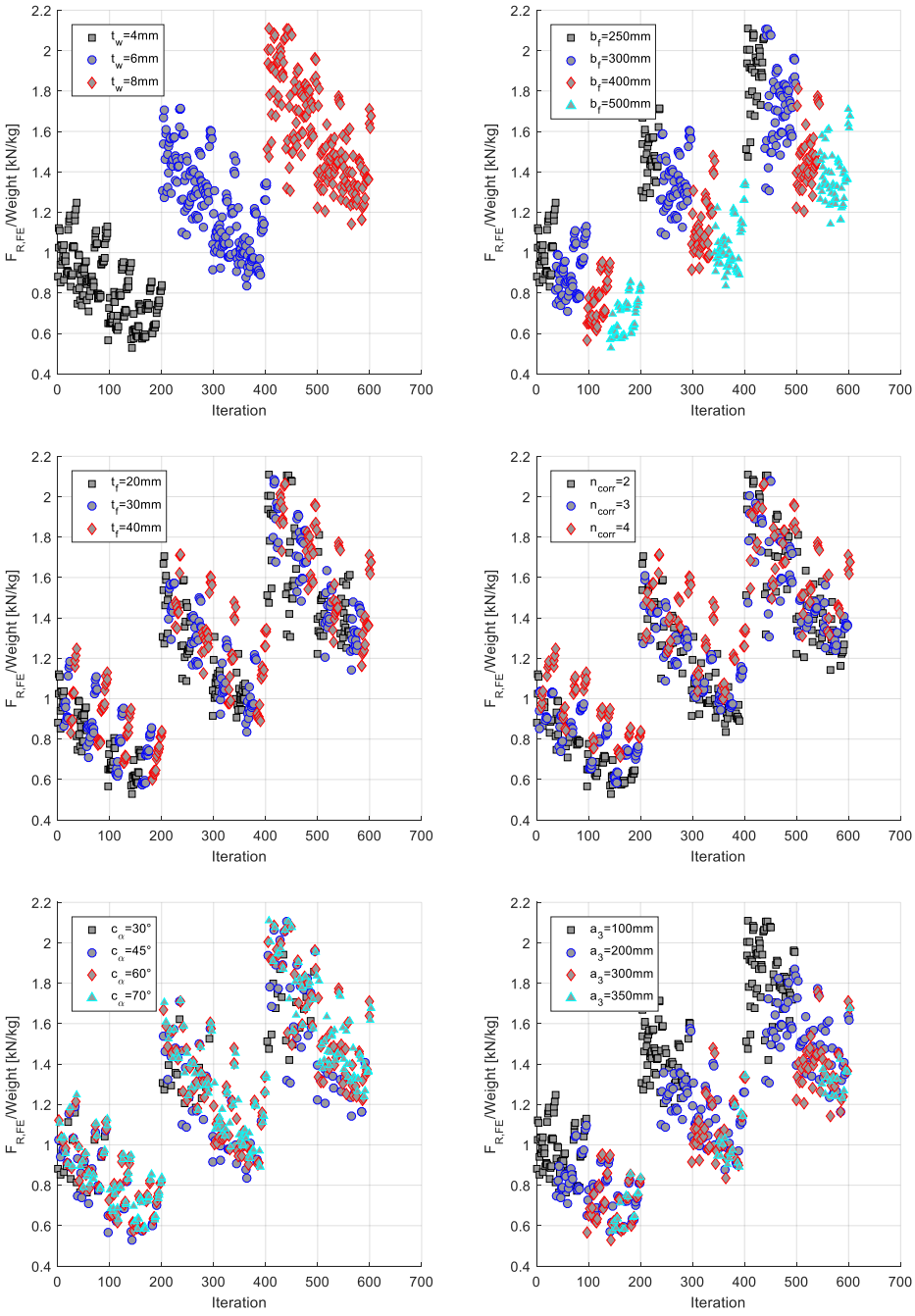

B.3 Flow chart for iterative algorithm

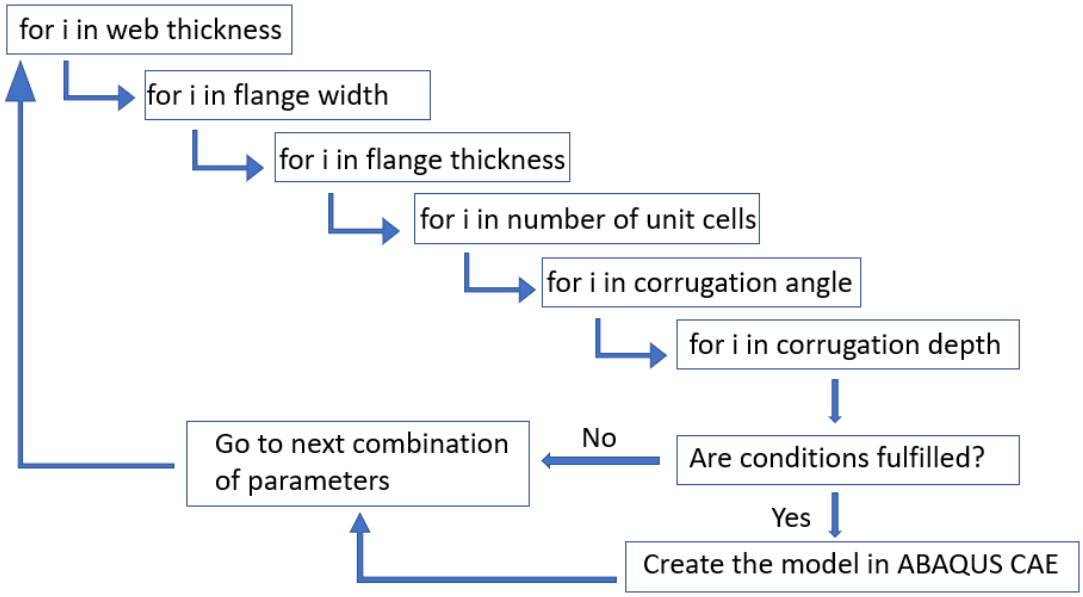

Appendix C – Existing design models

C.1 Luo and Edlund (1996) - Inclined fold and intersection load case for all girders

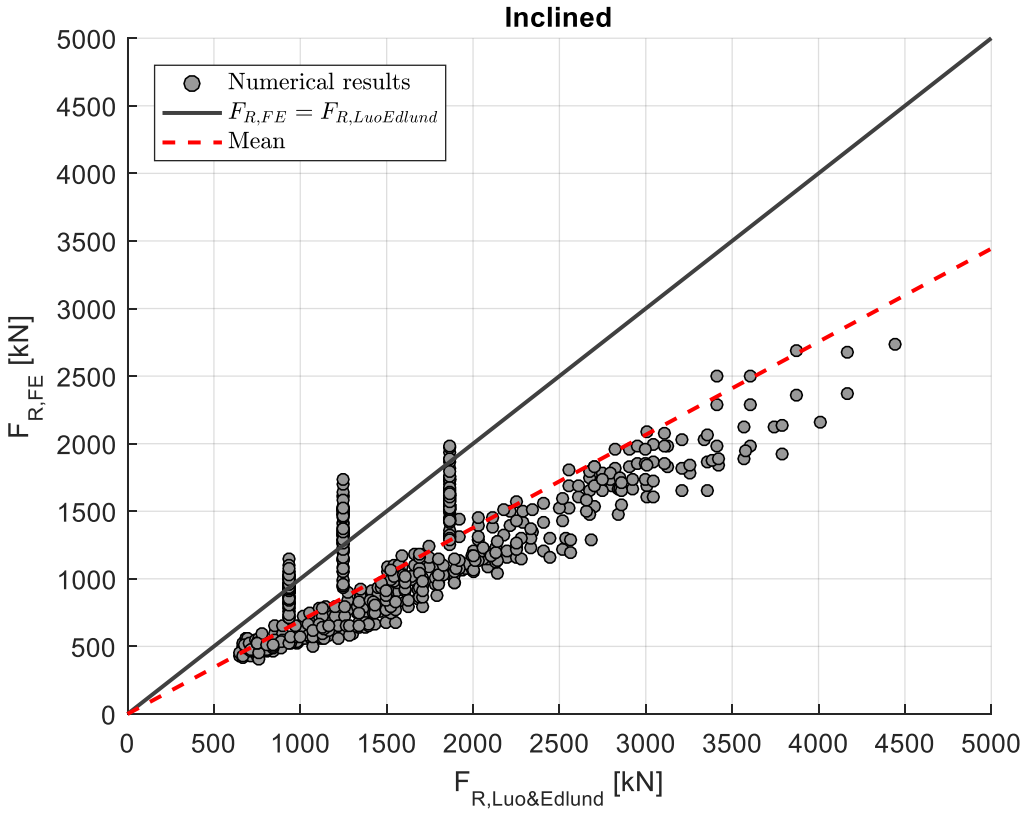

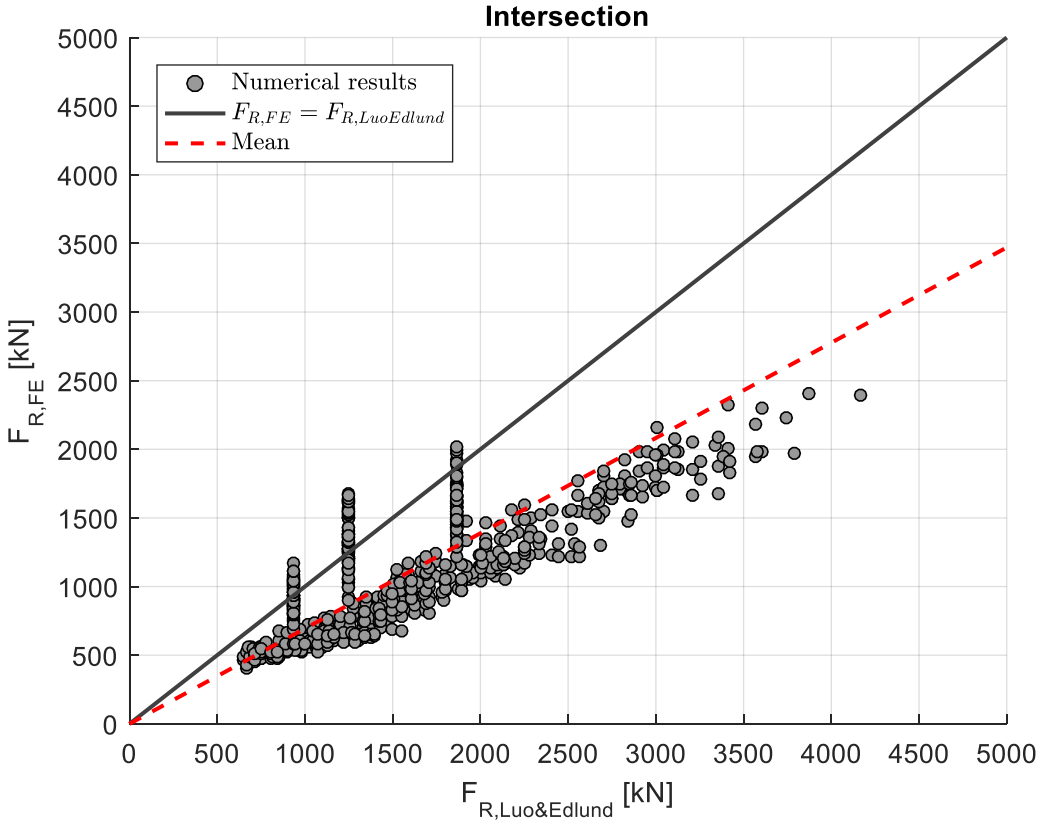

C.2 Kövesdi et al (2010)

C.2.1 Inclined and intersection load case for all girders

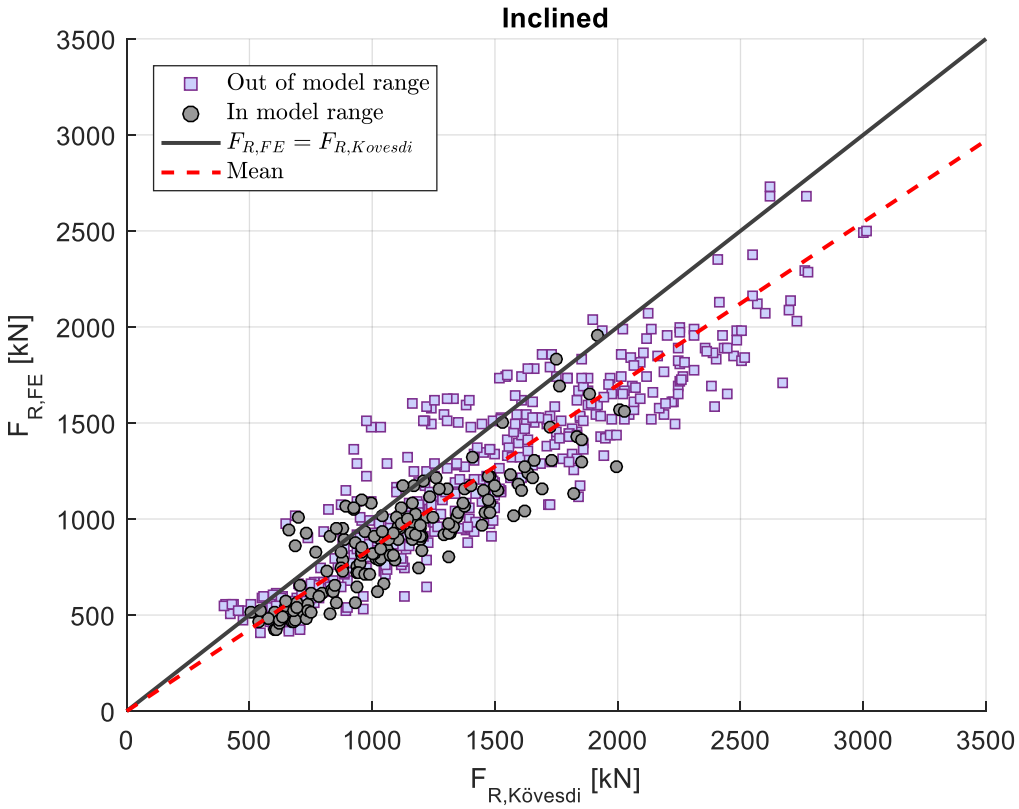

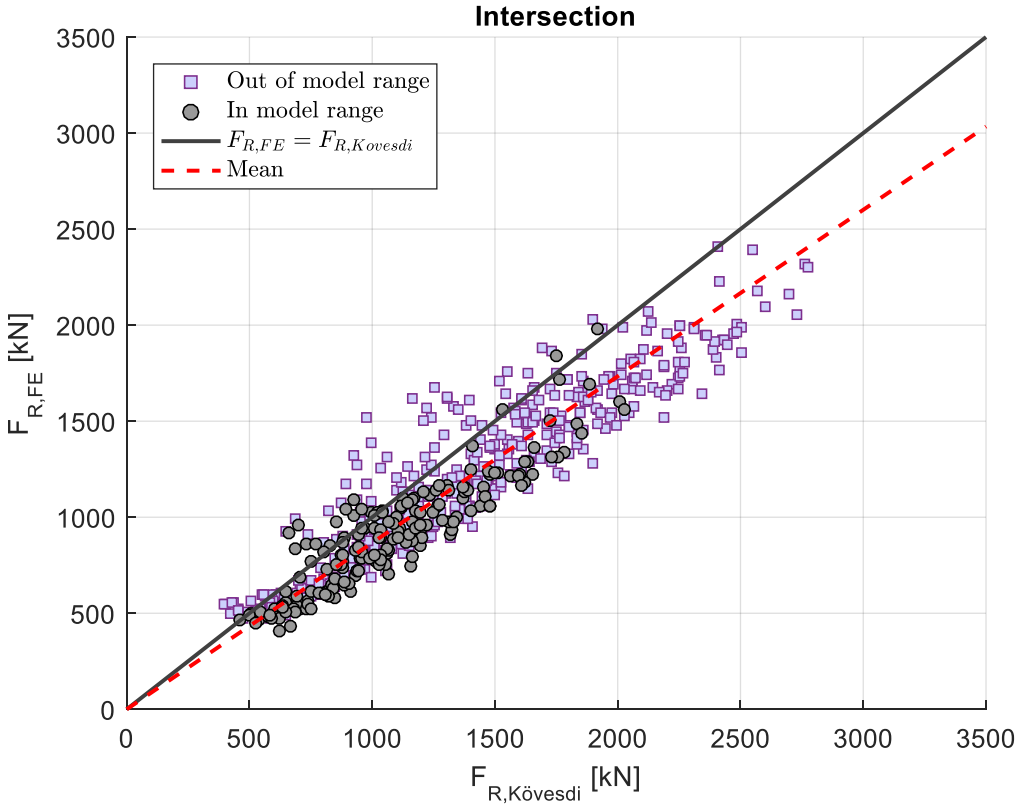

C.2.2 Inclined and intersection load case for girders that fulfil the criteria

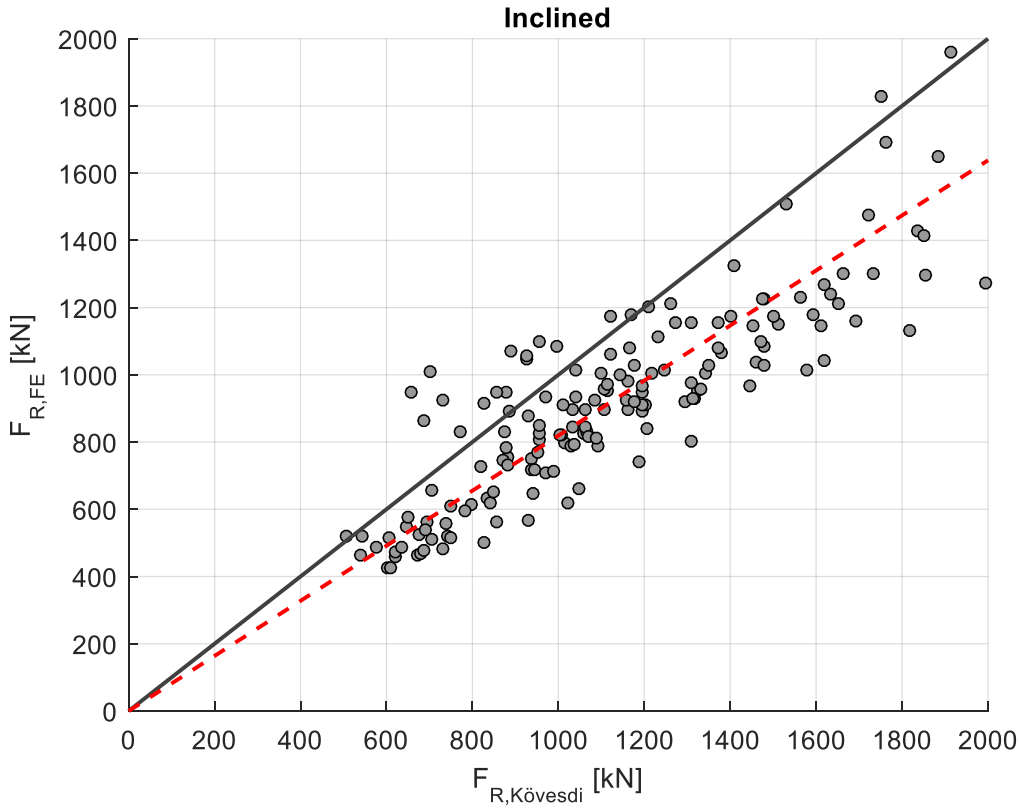

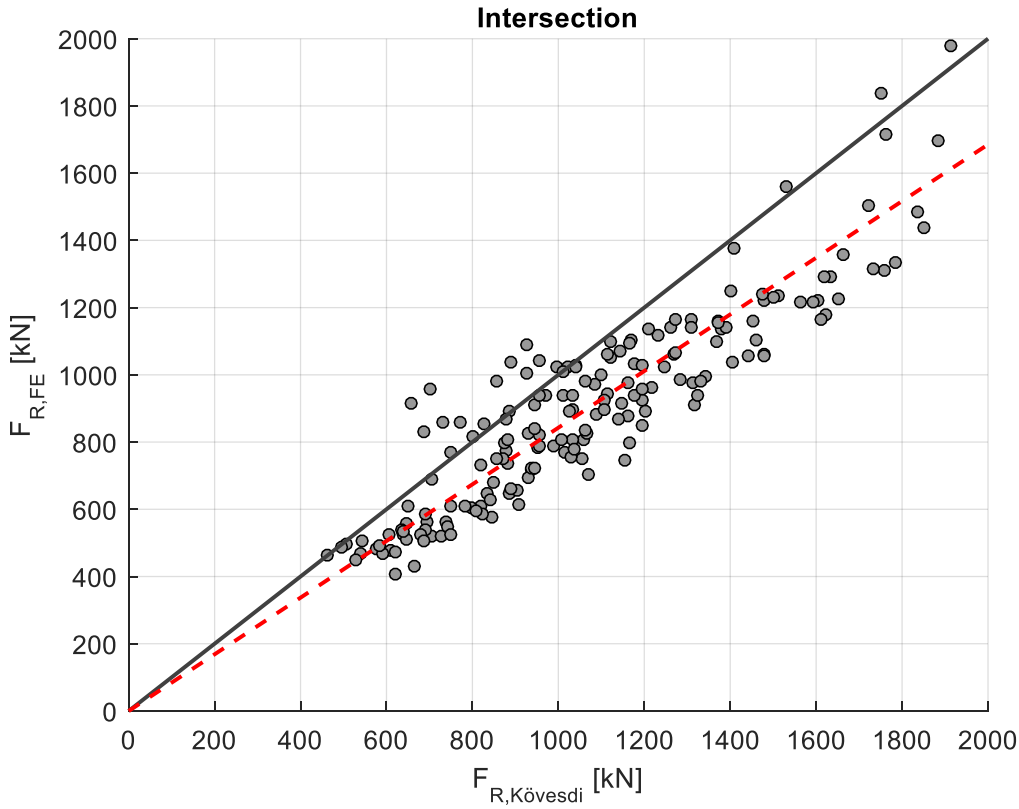

C.3 Kövesdi (2010)

C.3.1 Inclined and intersection load case for all girders

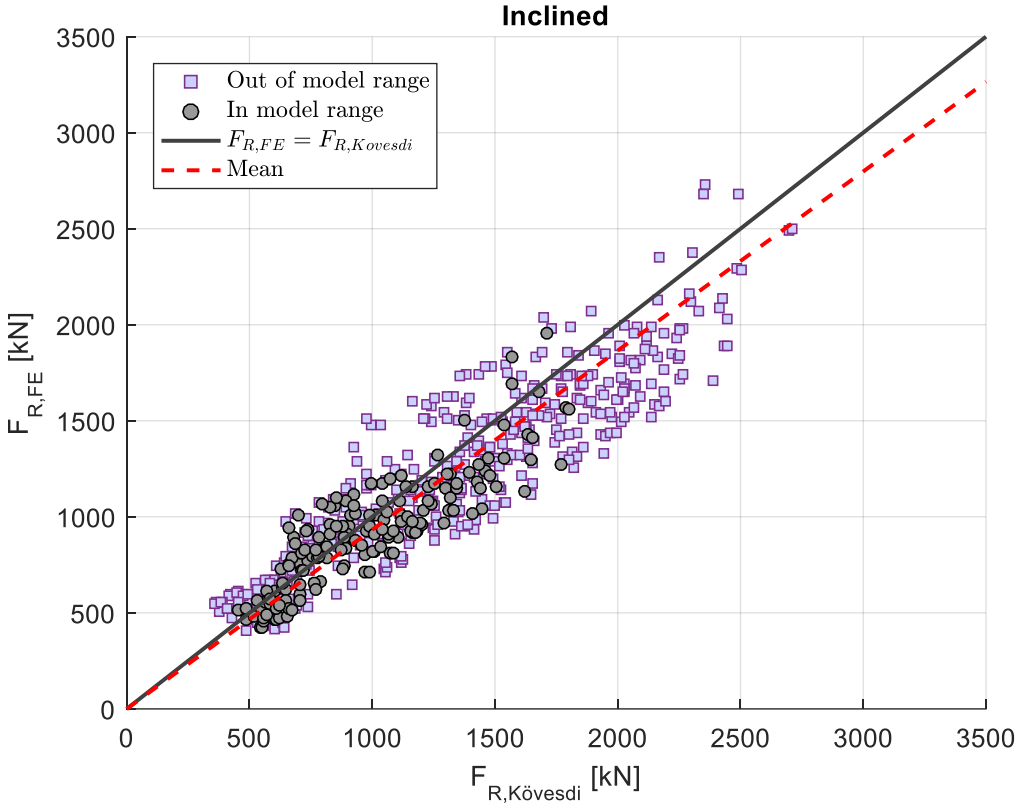

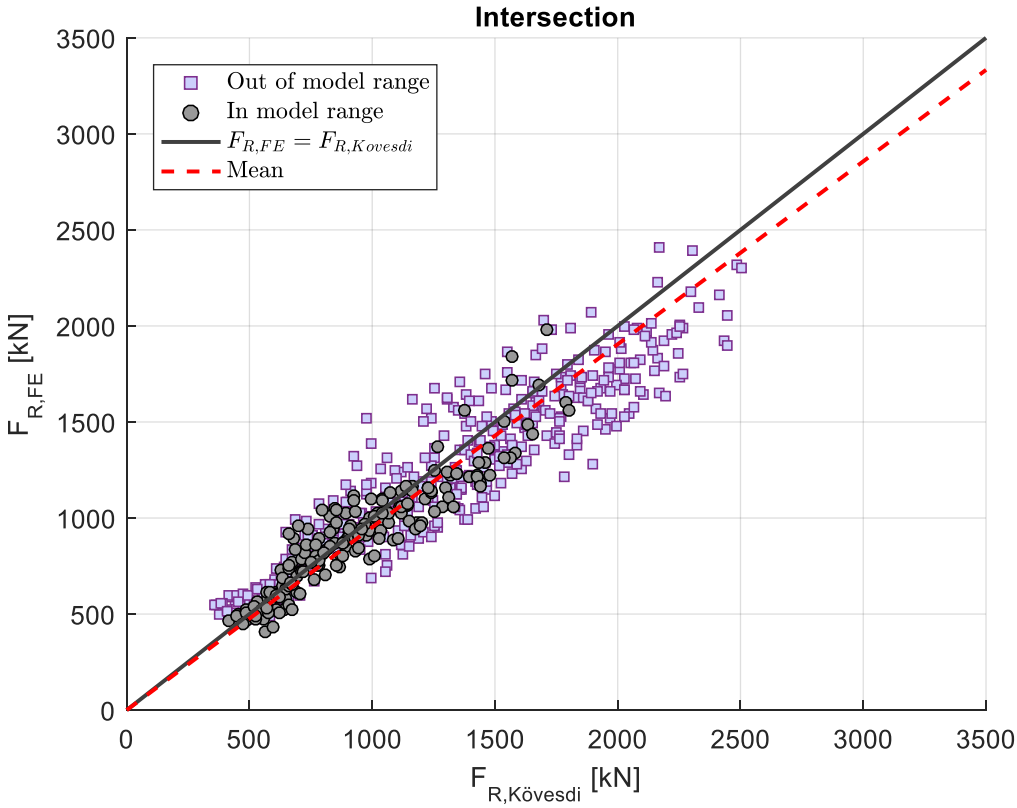

C.3.2 Inclined and intersection load case for girders that fulfill the criteria

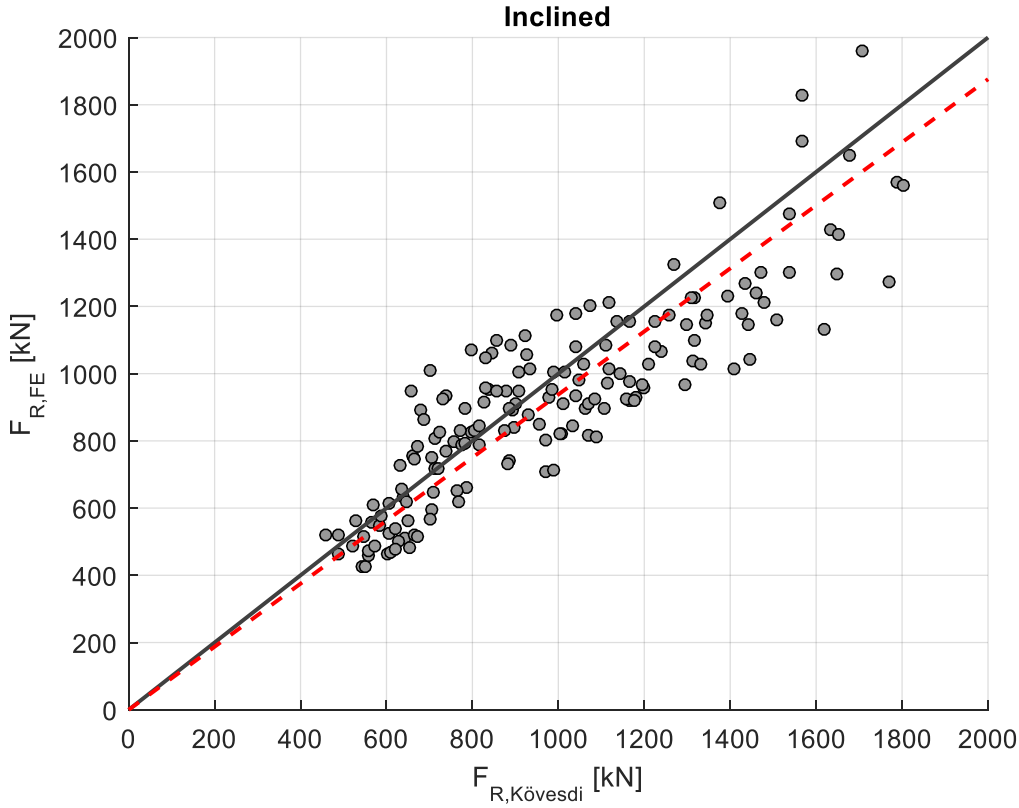

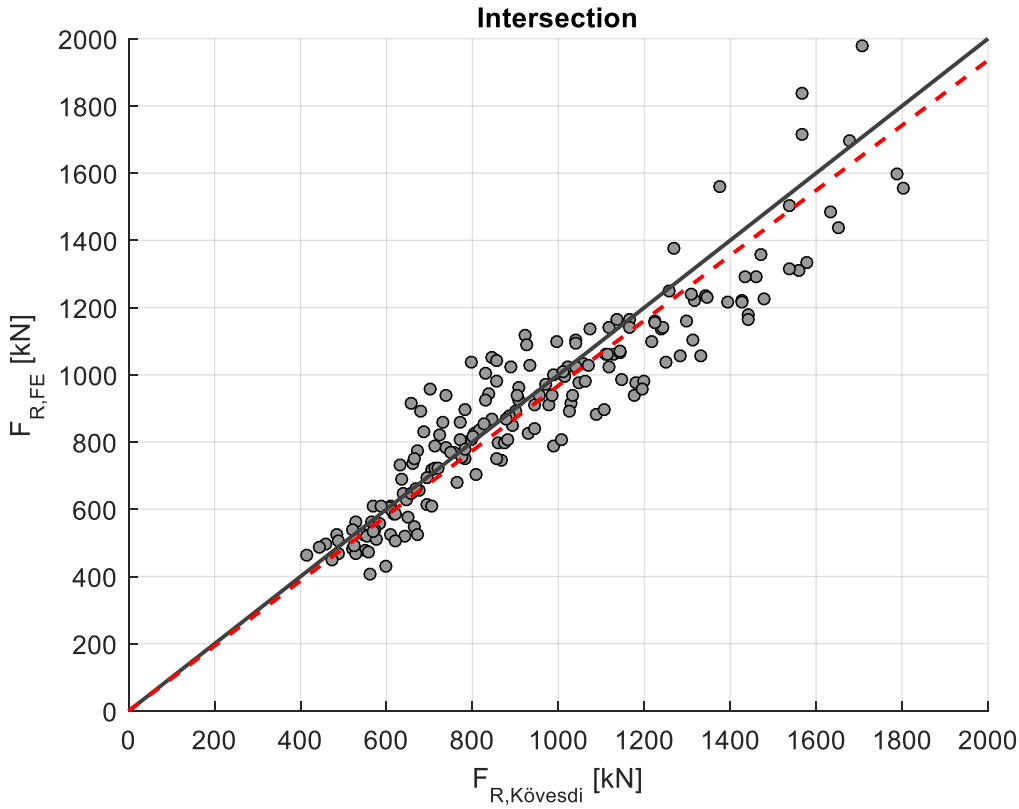

C.3.3 Flange-Web thickness ratio effect on the Kövesdi (2010) design model.

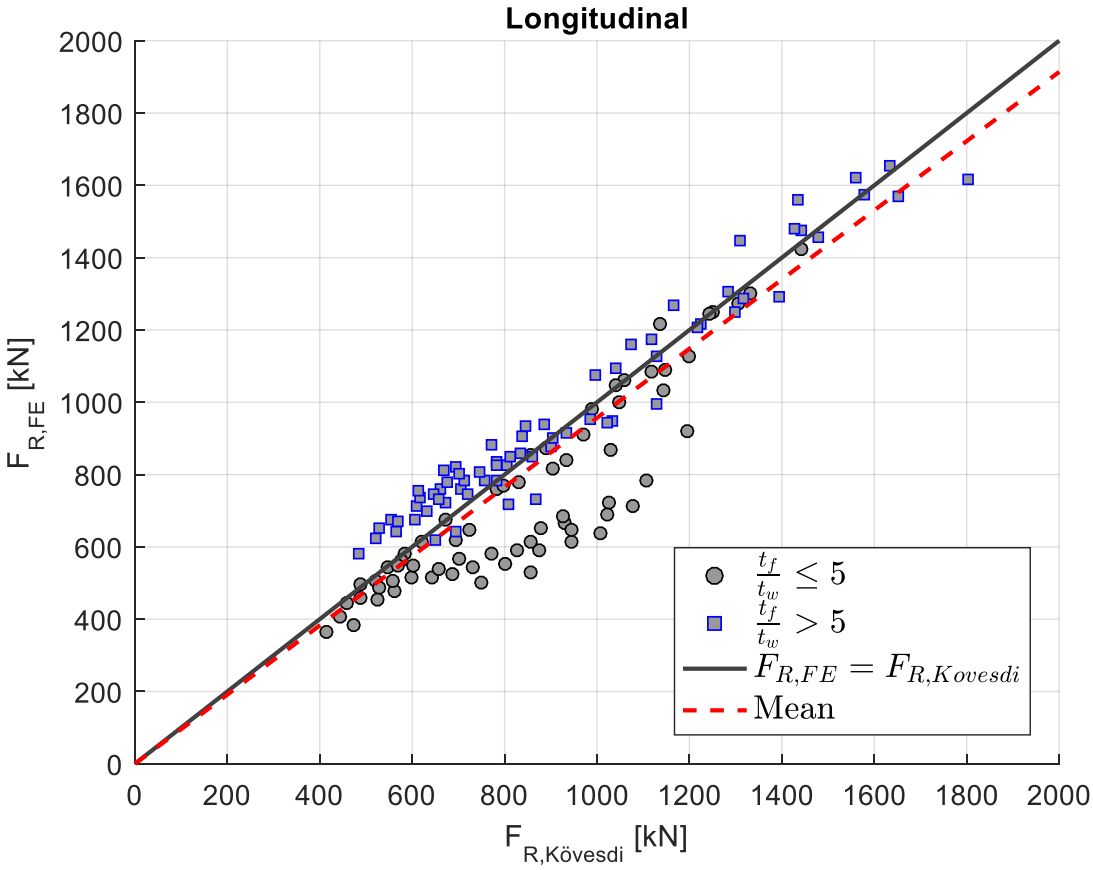

C.4 Eurocode - Inclined and intersection for all girders